CHAPTER 4

RESULTS AND DISCUSSION

In this chapter, the performance of direct alcohol fuel cell is discussed using laboratory synthesized (i) physical crosslinked alkaline membrane: **Part-I** and (ii) chemical crosslinked alkaline membrane: **Part-II**. In the first part, characterization of physical crosslinked alkaline membrane and CV studies of anode and cathode are discussed at the beginning. The effects of different parameters e.g., electrolyte concentration, alcohol concentration, electrocatalyst loading at anode and cathode, electrocatalyst type at anode, cell temperature, oxidant types, KOH doping in membranes and membrane types on the DAFC performance using physical crosslinked membrane are also discussed in detail in **Part I**. Similarly, characterization of chemical crosslinked alkaline membrane is discussed at the beginning of **Part II**. The effects of different parameters e.g., electrolyte concentration, alcohol concentration, electrocatalyst loading at anode and cathode, electrocatalyst type at anode, cell temperature, oxidant types, glutaraldehyde concentration, KOH doping in membranes and membrane types on the DAFC performance using chemical crosslinked membrane are also discussed in detail in **Part II**. It should be noted that pristine membrane characterization and performance evaluation are discussed in brief in both section **Part I** and **Part II** for comparison purpose. The CV studies for electrooxidation of methanol or ethanol or their mixture and oxygen reduction are presented in **Part I** only, as the parameters studied in CV are similar as that of single cell DAFC parameters tested using physical (**Part I**) and chemical (**Part II**) crosslinked membranes.

4.1 Performance of alkaline membrane synthesized by physical crosslinking: Part I

4.1.1 Membrane characterization

The homogenous and transparent physical crosslinked PVA membranes with a good mechanical flexibility were obtained at the end of the process, with a uniform thickness of approximately 180 ± 10 μm as described in the section 3.3.1 (page no.57). The important properties and indicators of the synthesized physical crosslinked PVA membrane like water uptake (W_U), KOH uptake (Q_U), ionic conductivity, high resolution scanning electron microscopy/energy dispersive X-ray spectroscopy (HR-SEM/EDX), fourier transform infrared spectroscopy (FTIR), X-ray diffraction (XRD) and mechanical testing are discussed below in detail.

4.1.1.1 Water uptake

Mechanical strength and ionic conductivity are strongly affected by the amount of membrane hydration. An optimum value of water uptake ensures the smooth functioning of the membrane. Too high water uptake results in loss of mechanical strength, membrane swelling, and reduction in ionic conductivity and durability. However, low levels of hydration may make the membrane brittle (Wu et al., 2010). Accordingly, water management is a vital issue for excellent membrane performance. The values for water uptake and KOH uptake of the membranes after immersing in 0 M KOH/water and KOH solution of different concentration are shown in Table (4.1). The pristine membrane shows a higher uptake of 131.8 wt % than the physical crosslinked PVA membrane (70 wt %) when immersed in 0 M KOH/water. The decrease in water uptake for the physical crosslinked membrane may be due to crosslinking (Zhou et al., 2010). The crosslinking in the polymer increases the interactions in the polymer matrix, disfavours chain mobility and

Table 4.1 Water uptake (W_U) and KOH uptake (Q_U) of pristine and physical crosslinked PVA membrane.

Membrane Types	**0 M KOH**		**4 M KOH**		**5 M KOH**		**6 M KOH**		**7 M KOH**		**8 M KOH**	
	W_U (wt %)	**Q_U (wt %)**	**W_U (wt %)**	**Q_U (wt %)**	**W_U (wt %)**	**Q_U (wt %)**	**W_U (wt %)**	**Q_U (wt %)**	**W_U (wt %)**	**Q_U (wt %)**	**W_U (wt %)**	**Q_U (wt %)**
Pristine PVA	131.8 ± 3.8	0	51.5 ± 2.1	23.1 ± 2.0	39.2 ± 2.3	29.1 ± 2.0	33.0 ± 2.1	37.8 ± 2.0	29.5 ± 1.9	33.7 ± 2.1	25.6 ± 1.9	31.6 ± 2.1
Physical Crosslinked PVA	70 ± 3.6	0	42.5 ± 2.2	23.6 ± 1.9	37.8 ± 2.4	29.8 ± 1.9	32.6 ± 2.1	**37.9** ± `2.2	26.3 ± 1.8	34.7 ± 2.0	22.3 ± 1.9	32.1 ± 2.0

reduces the void volume in the membrane (Merle et al., 2012, Zhou et al., 2010, Lewandowski et al., 2000, Yang 2007 and Li et al., 2010). It is also seen from the Table (4.1), the water uptake decreases with the increase in KOH concentration up to 8 M irrespective of membrane types. It may due to the increase in solution viscosity at higher concentration of KOH and decrease in water molecules in the solution at higher KOH concentration (Merle et al., 2012 and An et al., 2012).

4.1.1.2 KOH uptake

The values for KOH uptake as a function of KOH concentration is shown in Table (4.1). It is seen in Table (4.1) that the KOH uptake of pristine PVA membrane is lower in comparison to that of physical crosslinked PVA membrane for the all concentrations of KOH. The KOH uptake of both types of membranes increases with the increase in KOH concentration up to 6 M. However, further increase in KOH concentration beyond 6 M, the KOH uptake decreases. The highest KOH uptake of 37.9 wt % was observed for the physical crosslinked PVA membrane doped with 6 M KOH solution. Whereas, the KOH uptake of the physical crosslinked membrane decreased to 34.7 wt % with the further increase in KOH concentration to 7 M. The KOH uptake for the same membrane doped with 4 M and 5 M KOH concentrations were 23.6 wt % and 29.8 wt %, respectively. Similarly, the maximum KOH uptake of 37.8 % was obtained for pristine PVA membrane doped with 6 M KOH solution. Whereas, the KOH uptake values of 23.1 wt %, 29.1 wt %, and 33.7 wt % were found for the pristine membrane doped with KOH concentrations of 4 M, 5 M and 7 M, respectively. The reason for decrease in KOH uptake at 7 M KOH may be due to the increase in concentration of KOH solution, the solution viscosity increases which results in lesser adsorption and impregnation of KOH within the PVA membrane matrix (Merle et al., 2012 and An et al., 2012). Thus, the PVA

membrane gets saturated at a concentration of 6 M KOH giving a maximum amount of KOH uptake for both types of membranes. Although KOH uptake value of pristine membrane (37.8 wt %) is very close to the KOH uptake of physical crosslinked (37.9 wt %) membrane, the stability of pristine PVA is very poor as discussed earlier (page no. 8). Moreover, ionic conductivity of the membrane is one of the important property which control cell performance. This has been discussed in the next section.

4.1.1.3 Ionic conductivity

The membrane samples for ionic conductivity measurement were prepared in a similar way as that of adopted in KOH uptake. Fig (4.1a) and Fig (4.1b) show the typical electrochemical impedance spectra (EIS) for the pristine and physical crosslinked PVA membranes doped with various molar KOH solution. The ionic conductivity of the pristine and physical crosslinked PVA membrane doped with KOH are shown in Table (4.2). A good correlation is observed between ionic conductivity and KOH uptake of the PVA membrane as seen from Table (4.1) and Table (4.2). The ionic conductivity of pristine and physical crosslinked PVA membrane increases with the increase in KOH concentrations up to 6 M and further increase in KOH concentration, the ionic conductivity of membrane decreases. The ionic conductivity was always higher for physical crosslinked alkaline PVA membrane in comparison to alkaline PVA pristine membrane. The highest ionic conductivity of 5.6 x 10^{-3} S/cm was obtained for the physical crosslinked PVA membrane doped with 6 M KOH. Whereas, it was only 0.89 x 10^{-3} S/cm for pristine PVA doped with same KOH concentration of 6 M. However, the ionic conductivity of 4.1 x 10^{-3} S/cm and 0.58 x 10^{-3} S/cm were obtained for 7 M of KOH doping with physical crosslinked and pristine PVA membrane, respectively. The ionic conductivity of physical crosslinked membrane doped with 4 M and 5 M KOH were

3.6 x 10^{-3} S/cm and 4.5 x 10^{-3} S/cm, respectively. Some authors have reported similar type of observation i.e., the decrease in ionic conductivity for the doping with KOH solution beyond 6 M, it may be due to increased solution viscosity and consequent decrease in ionic mobility (An et al., 2012). Moreover, it is also seen in the published literature that many factors are responsible for the increase in ionic conductivity with the increase in KOH concentration in physical crosslinked membrane such as hydrogen bonding and induction forces between OH and C-O groups on KOH and PVA matrix. One more important reason may be inclusion of KOH molecules by water molecules of the PVA membrane. Although the KOH uptake of the pristine PVA membrane is high at optimum concentration of KOH doping (6 M), the ionic conductivity is very low (0.89 x 10^{-3}) than the physical crosslinked PVA membrane (5.6 x 10^{-3} S/cm). It may be due to the high crystallinity of pristine PVA membrane. The high crystalline nature increases the energy barrier for ion movement and thereby impedes the ion transport (Hema et al., 2009).

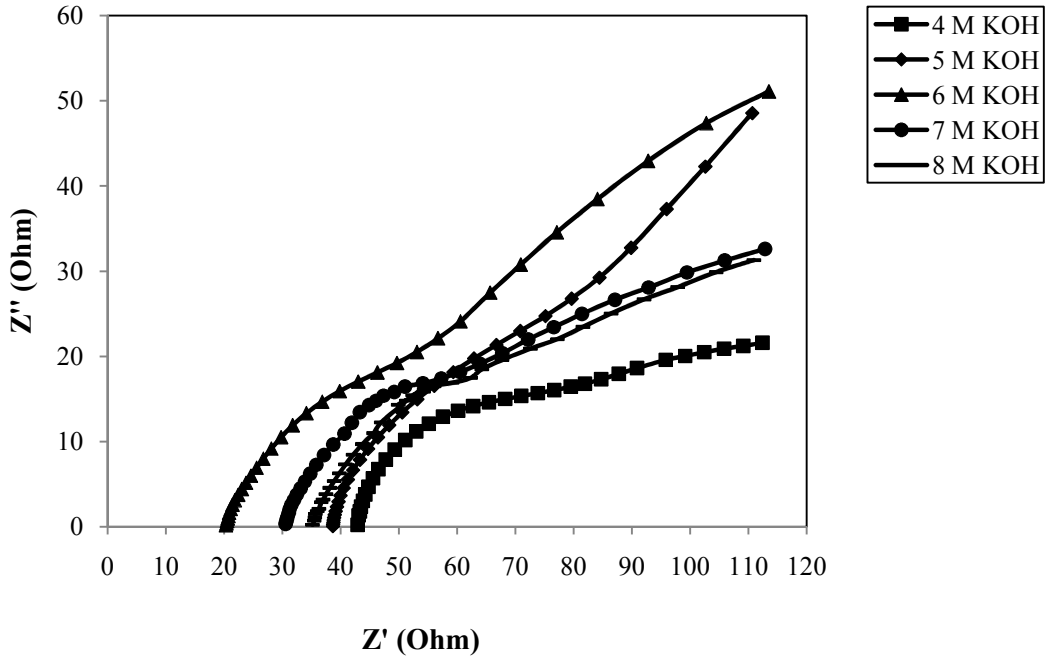

Figure 4.1a Electrochemical impedance spectra (EIS) for the pristine PVA membrane doped with various molar KOH solution at a temperature of 30 ^{o}C.

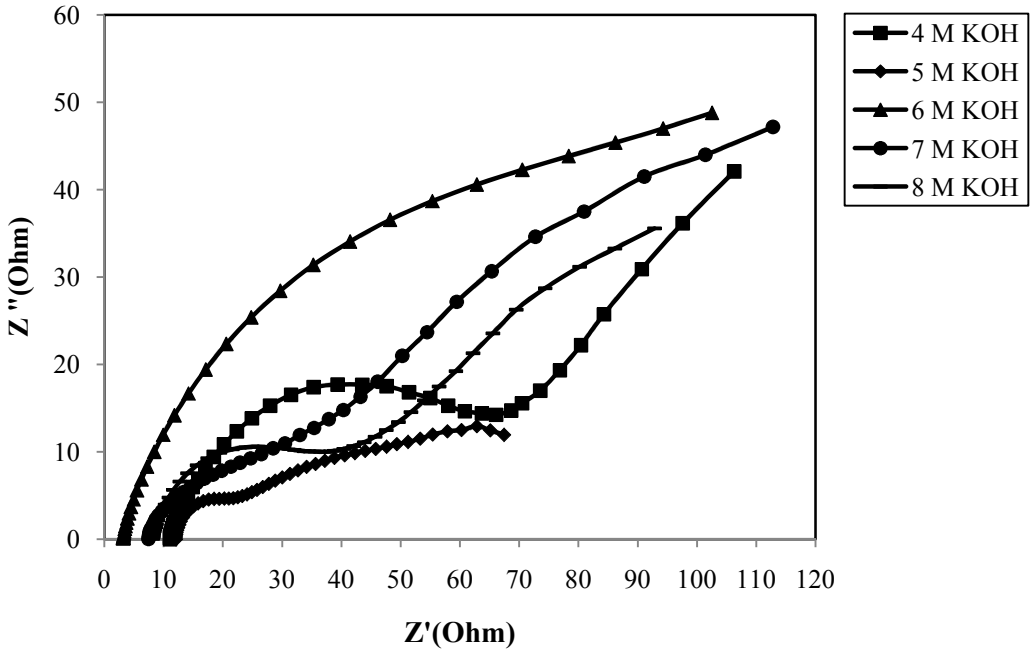

Figure 4.1b Electrochemical impedance spectra (EIS) for the physical crosslinked PVA membrane doped with various molar KOH solution at a temperature of 30 ^{o}C.

Table 4.2 Ionic conductivity of pristine and physical crosslinked PVA membrane impregnated at different concentration of KOH solution.

Membrane Types	**Ionic Conductivity (x 10^{-3} S/cm)**				
	4 M KOH	**5 M KOH**	**6 M KOH**	**7 M KOH**	**8 M KOH**
Pristine PVA	0.42 ± 0.02	0.46 ± 0.03	0.89 ± 0.04	0.58 ± 0.02	0.51 ± 0.02
Physical crosslinked PVA	3.6 ± 0.4	4.5 ± 0.5	**5.6** ± 0.5	4.1 ± 0.4	3.4 ± 0.3

4.1.1.4 Morphology

The surface morphology of three synthesized membranes viz. the pristine PVA membrane, physical crosslinked PVA membrane and physical crosslinked PVA membrane doped with optimum concentration of 6 M KOH at the uniform SEM resolution of 500 nm are shown in Fig (4.2a), Fig (4.2b) and Fig (4.2c), respectively. The cross sectional SEM morphology and EDX elemental composition of physical crosslinked PVA membrane (Fig 4.2d) and physical crosslinked PVA membrane doped with 6 M KOH (Fig 4.2e) were also investigated. It is seen from Fig (4.2a), pristine PVA membrane consisting of larger cracks which are uniformly distributed over the pristine membrane. Whereas, the cracks get reduced and membrane becomes compact with physical crosslinking (Fig 4.2b to Fig 4.2c). The SEM image of cross-sectional plane for physical crosslinked PVA membrane without KOH doping shows uniform pores distribution throughout the cross-sectional plane (Fig 4.2d). When the physical crosslinked PVA membrane is doped with 6 M KOH, cross-sectional plane of the same membrane shows spike like structures of adsorbed KOH within the membrane matrix (Fig 4.2e). It helps to keep the membrane conductivity consistent during DAFC operations.

The EDX analysis of physical crosslinked PVA membrane without KOH doping shows the peak of oxygen and carbon showing the characteristics constituents of PVA (Fig 4.2d). In the Fig (4.2e), additional peak of potassium (K) is observed indicating incorporation of KOH in the membrane matrix. The presence of Au peak in the EDX image is due to the sputtering of PVA membranes with Au particles.

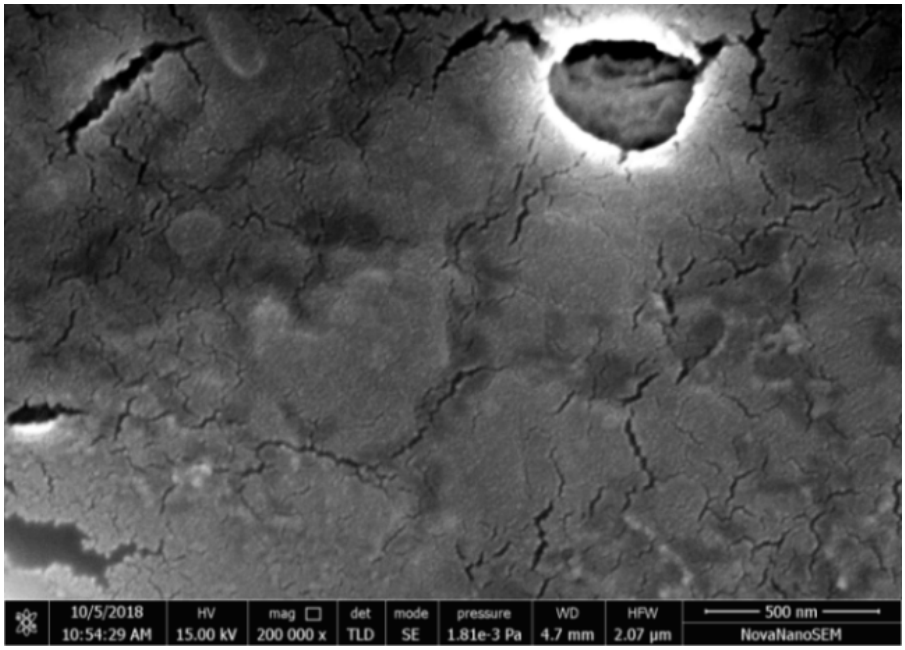

Figure 4.2a SEM image of the surface of pristine PVA membrane.

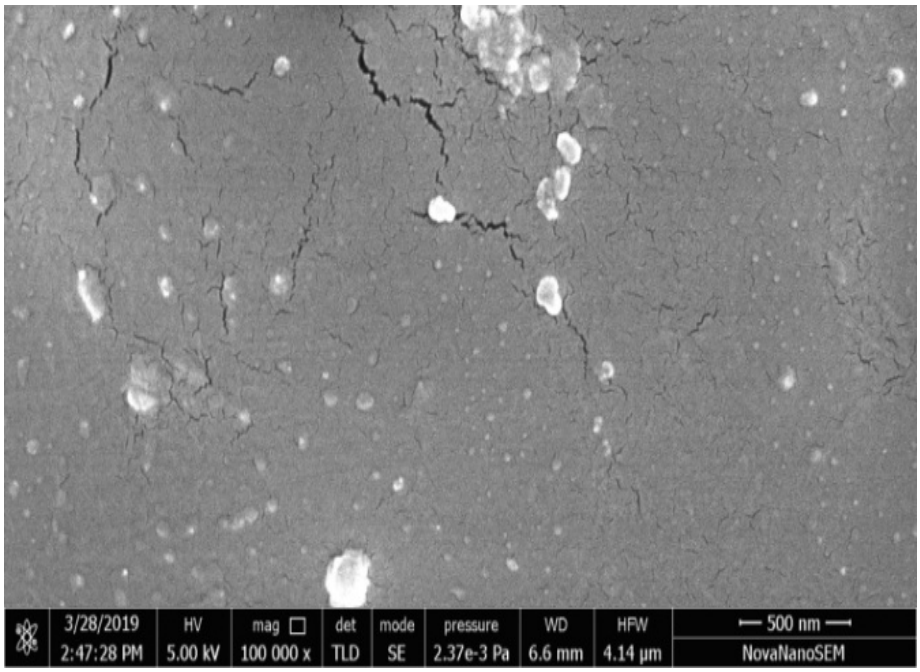

Figure 4.2b SEM image of the surface of physical crosslinked PVA membrane.

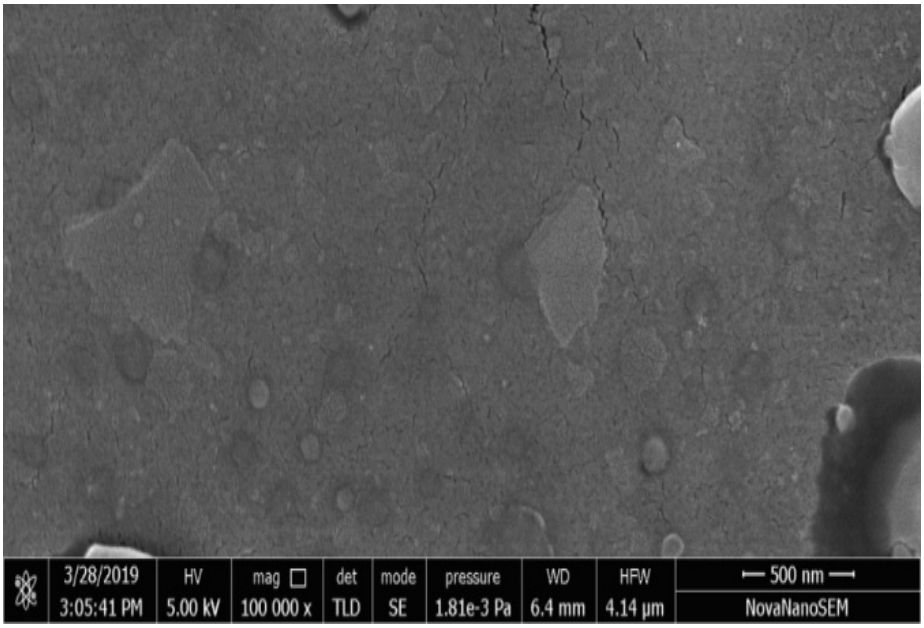

Figure 4.2c SEM image of the surface of physical crosslinked PVA membrane doped with 6 M KOH.

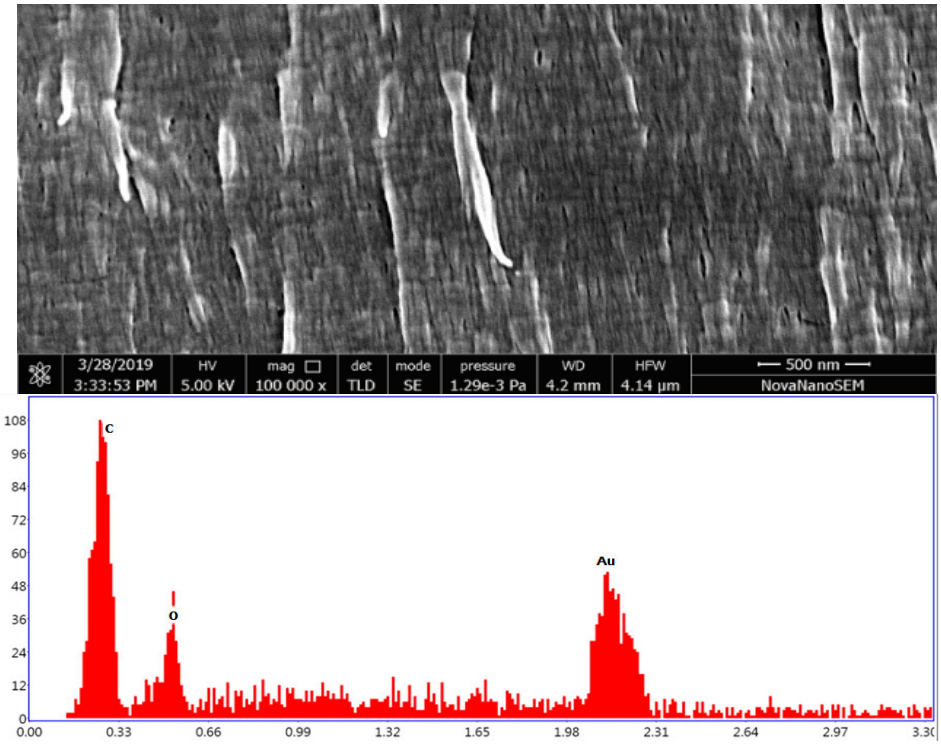

Figure 4.2d SEM-EDX image of cross section of physical crosslinked PVA membrane without KOH doping.

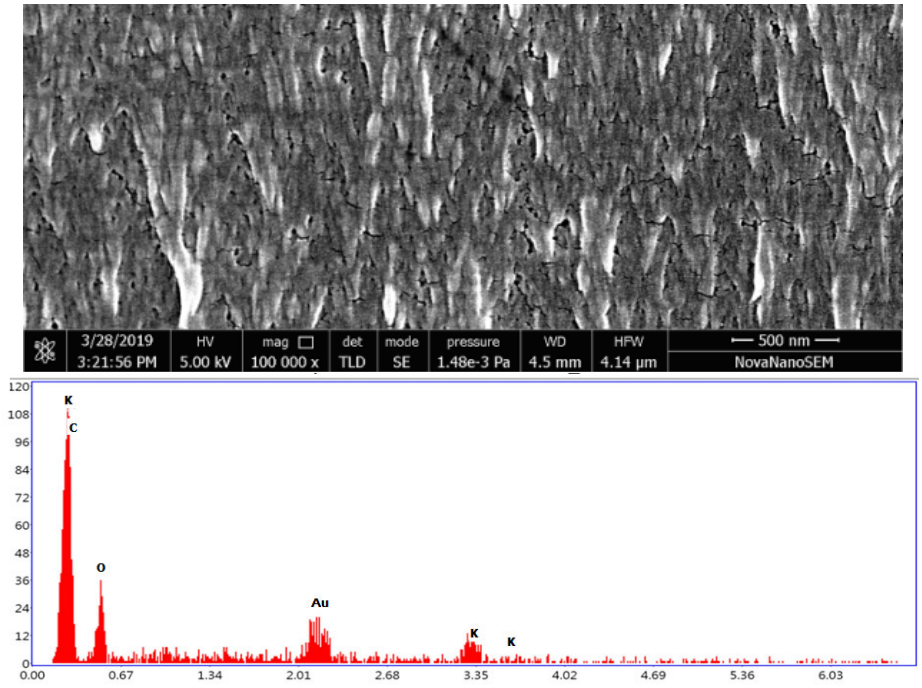

Figure 4.2e SEM-EDX image of cross section of physical crosslinked PVA membrane, doped with 6 M KOH.

4.1.1.5 Crystal structure

The X-ray diffraction (XRD) analysis was performed to examine the crystallinity of the physical crosslinked PVA membrane. Fig (4.3) shows the diffraction pattern of the pristine PVA membrane, physical crosslinked PVA membrane without any KOH doping and physical crosslinked PVA doped with optimum 6 M KOH. It is well known that the PVA polymer exhibits a semi-crystalline structure with a large peak at a 2θ angle of 19^{o}–20^{o} (101) and a small peak of 39^{o}– 40^{o} (111) (Wu et al., 2008, Herranz et al., 2018, Merle et al., 2012 and Fu et al., 2010). It is clearly seen in the Fig (4.3) that a large peak appears at 2θ of 20^{o} for the pristine PVA membrane. However, the peak intensity for the physical crosslinked PVA membrane reduced after crosslinking. It may be due to the decline in crystallinity. Moreover, the peak intensity at 2θ of 20^{o} for the physical crosslinked PVA membrane doped with 6 M KOH further reduced. It may be due to the

plasticizing effect of KOH molecules. The KOH molecules entangle the PVA polymer chains and thus reduce the crystalline domain (Hirankumar and Mehta 2018).

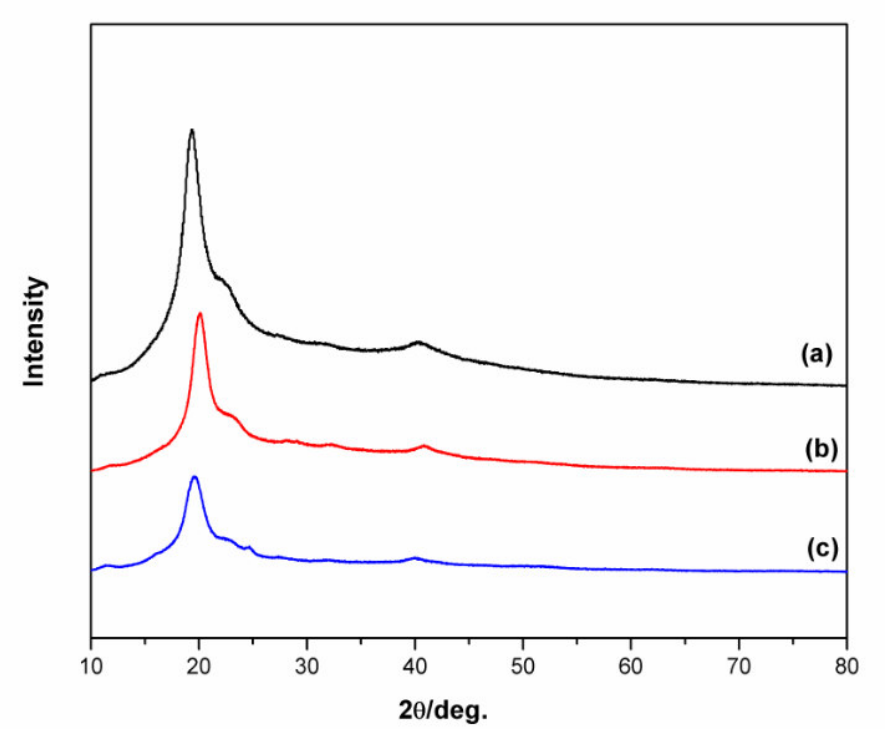

Figure 4.3 XRD spectra of the (a) pristine PVA membrane (b) physical crosslinked PVA membrane and (c) physical crosslinked PVA membrane, 6 M KOH doped.

4.1.1.6 Functional groups

Functional groups of the PVA based membranes were evaluated by FTIR analysis. Fig (4.4) shows the FTIR of the pristine PVA membrane, physical crosslinked PVA membranes without any KOH doping and physical crosslinked PVA membrane doped with optimum KOH concentration of 6 M. In the Fig (4.4), the absorption peaks of different PVA membranes are observed at different wave length spectra like –OH stretching of the bound water at about 3228-3431 cm^{-1} (region-i), CH stretching at about 2858- 2984 cm^{-1} (region-ii) and at about 1659-1665 cm^{-1} (region-iii) and

1433-1445 cm^{-1} (region-iv) for the –C–O group. The band at 1096-1105 cm^{-1} (region-v) is due to deformation vibration of the absorbed water molecules.

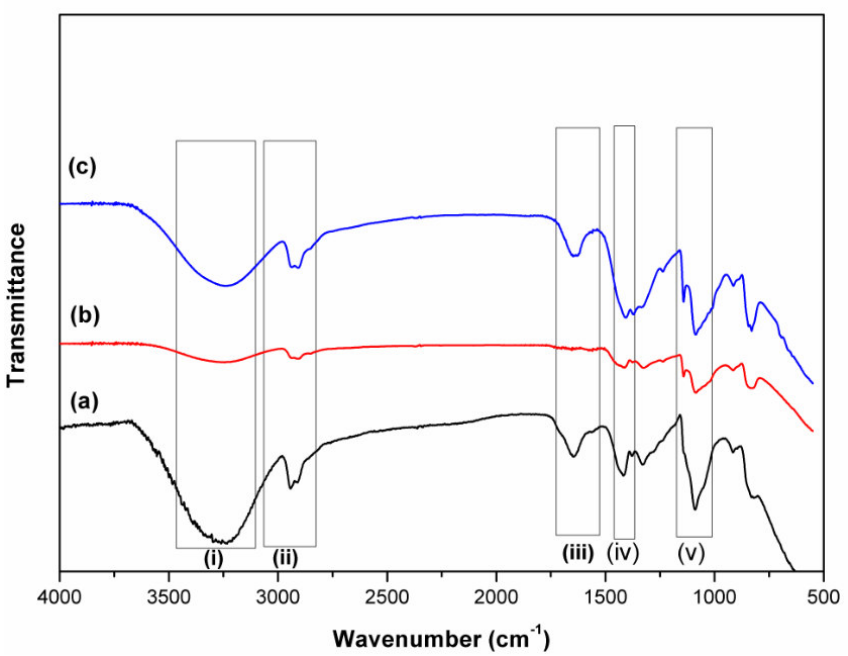

Figure 4.4 FTIR spectrum of the (a) pristine PVA membrane (b) physical crosslinked PVA membrane and (c) physical crosslinked PVA membrane, 6 M KOH doped.

4.1.1.7 Mechanical property

To study the effect of crosslinking on the mechanical behavior of PVA membrane, the mechanical stability of the pristine PVA membrane and physical crosslinked PVA membrane were tested and compared. The stress-strain curve of pristine and physical crosslinked PVA membranes are shown in Fig (4.5). The stress-strain curves demonstrate that the physical crosslinking of PVA enhances the tensile strength of the membrane. The crosslinked PVA membrane exhibits a tensile stress of 40 MPa which is higher than that of pristine PVA membrane (37 MPa). It may be due to the more ordered structure of the physical crosslinked membrane (Gupta and Pramanik 2019b).

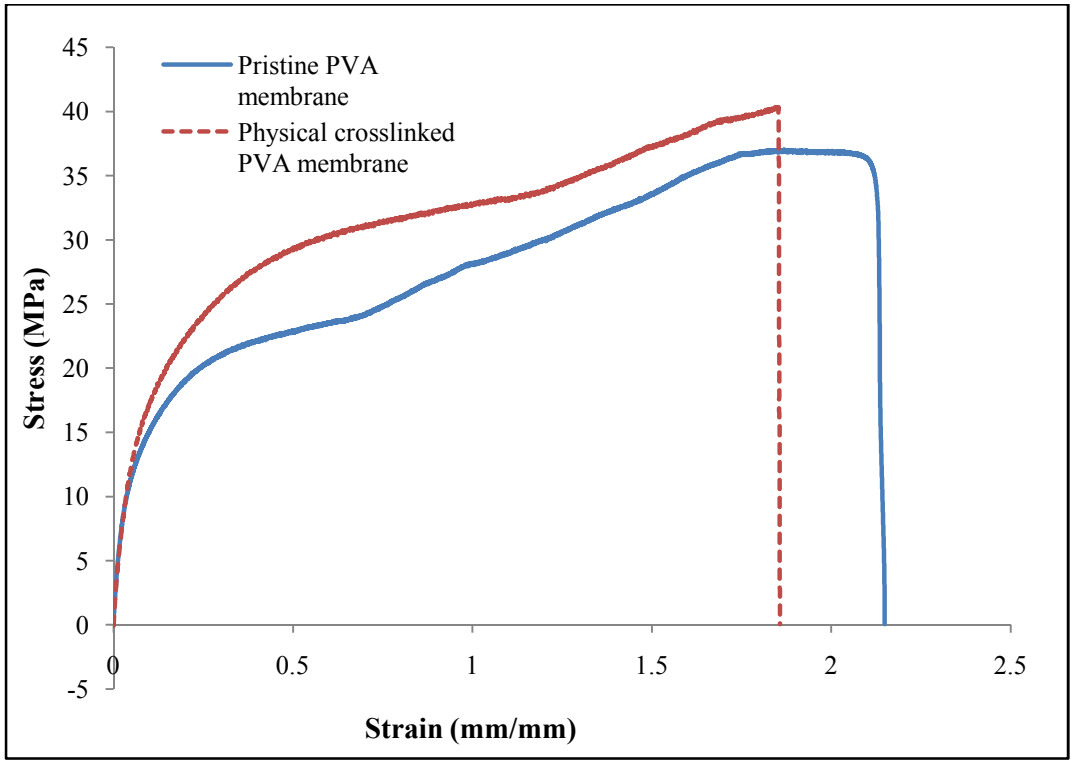

Figure 4.5 The stress-strain curves of pristine PVA membrane and the physical crosslinked PVA membrane.

4.1.2 SEM of electrodes

4.1.2.1 SEM of anode

The SEM of blank GDL is shown in Fig (4.6a) and that for anode of various loading ranging from 0.5 mg/cm^2 to 1.5 mg/cm^2 are shown in Fig (4.6b) to Fig (4.6d), respectively. Magnifications (20.00 X 10^3) were kept uniform for all SEM images for consistency in comparison (Fig 4.6a to Fig 4.6d). It is seen in Fig (4.6a), that the little larger carbon particles are uniformly distributed over GDL surface. Fig (4.6c) shows the porous structure of the anode of 1 mg/cm^2 Pt-Ru/C. The porous structure ensures smooth and continuous supply of the fuel and electrolyte system at the anode electrocatalyst layer and allows access of the active electrocatalyst sites which may be present at the inner side

of the electrocatalyst layer. Whereas, higher loading of 1.5 mg/cm^2 Pt-Ru/C shows the compacted and agglomerated mass of electrocatalyst over the GDL (Fig 4.6d).

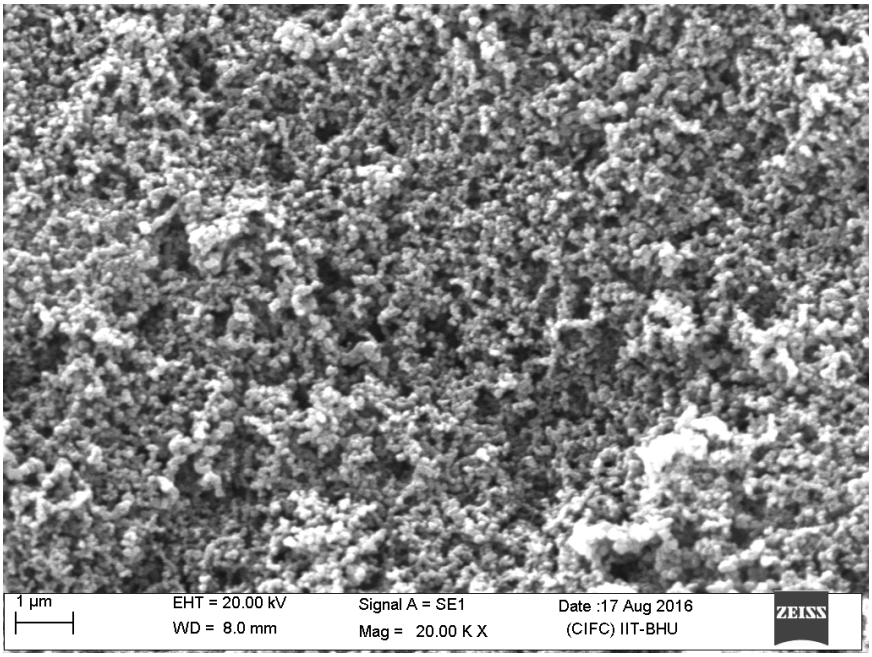

Figure 4.6a SEM of the blank GDL.

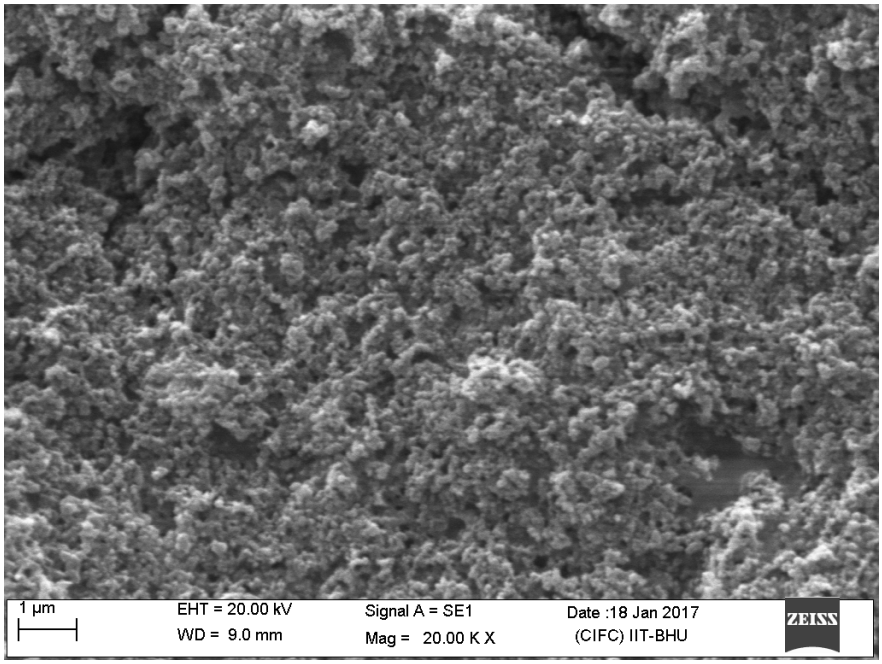

Figure 4.6b SEM of 0.5 mg/cm^2 Pt-Ru/C anode.

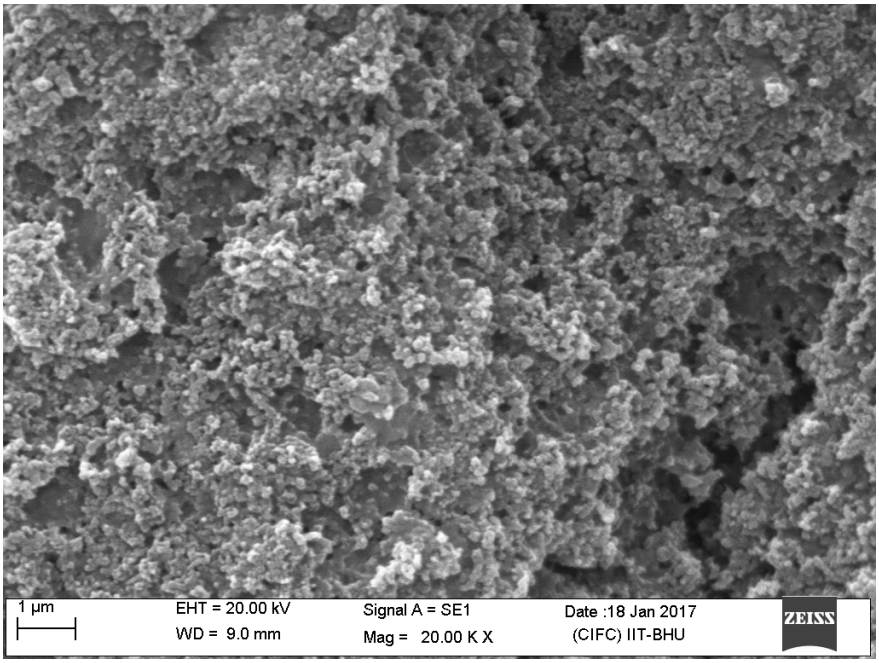

Figure 4.6c SEM of 1 mg/cm^2 Pt-Ru/C anode.

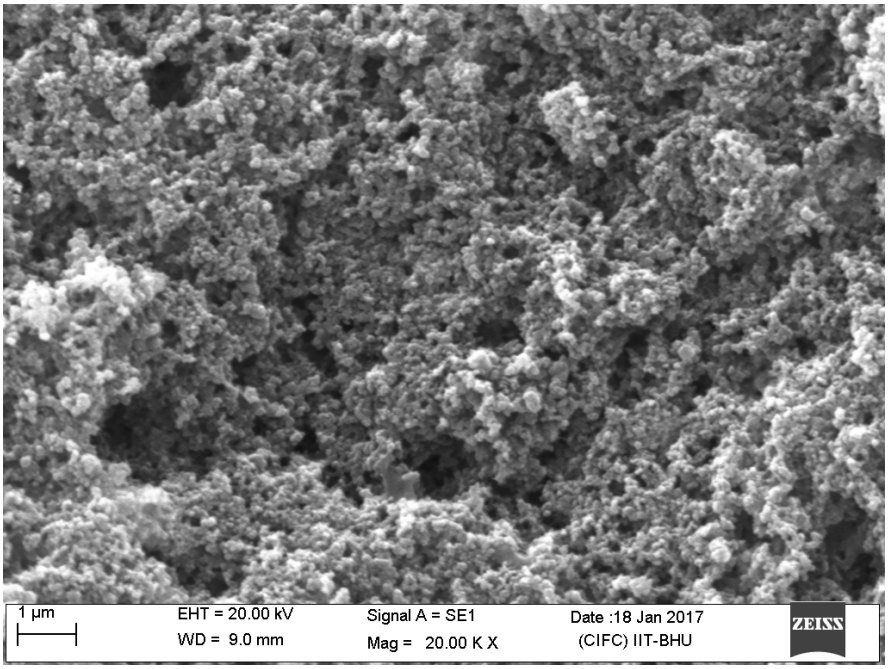

Figure 4.6d SEM of 1.5 mg/cm^2 Pt-Ru/C anode.

4.1.2.2 SEM of cathode

Fig (4.7a) to Fig (4.7c) show the SEM of cathode electrodes of varying electrocatalyst loading ranging from 0.5 mg/cm^2 to 1.5 mg/cm^2 of Pt (40 % by wt.)/C_{HSA}. Fig (4.7b) shows the even distribution of Pt/C_{HSA} electrocatalyst over the GDL surface along with pores for the loading of 1 mg/cm^2 in comparison to that of loading 0.5 mg/cm^2 (Fig 4.7a). As discussed in the section 4.1.2.1 (page no. 80) the porous structure ensures smooth and continuous supply of the oxidant at the cathode electrocatalyst layer and allows access of the active electrocatalyst sites which may be present at the inner side of the electrocatalyst layer.

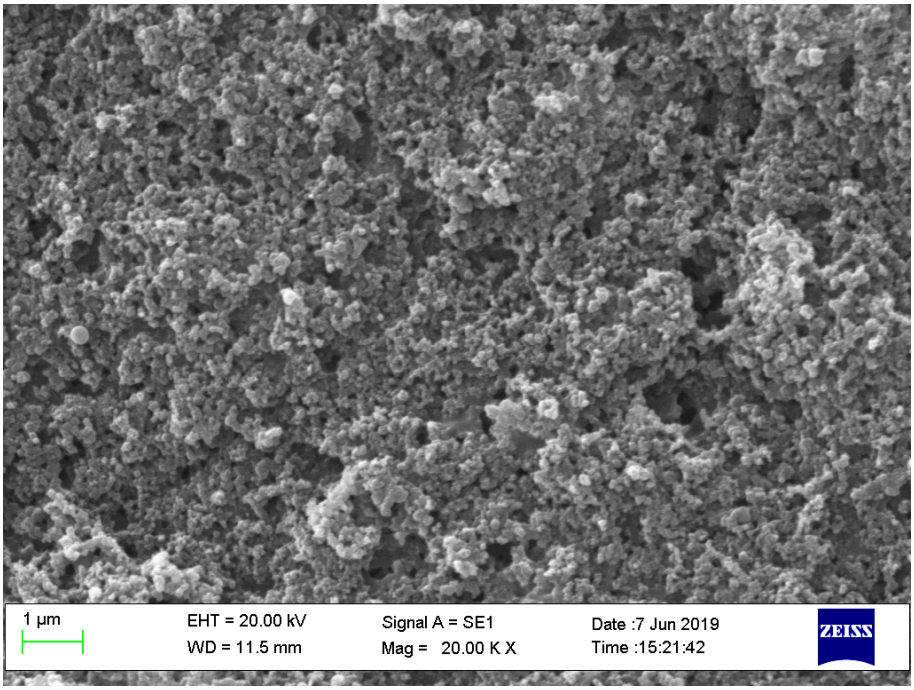

Figure 4.7a SEM of 0.5 mg/cm^2 Pt/C_{HSA} cathode.

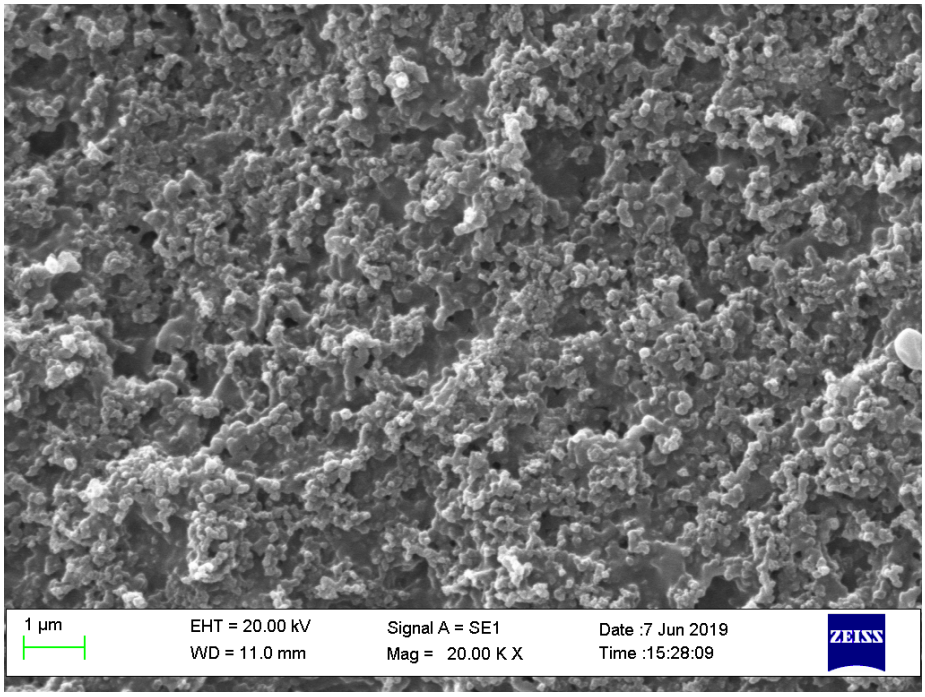

Figure 4.7b SEM of 1 mg/cm^2 Pt/C_{HSA} cathode.

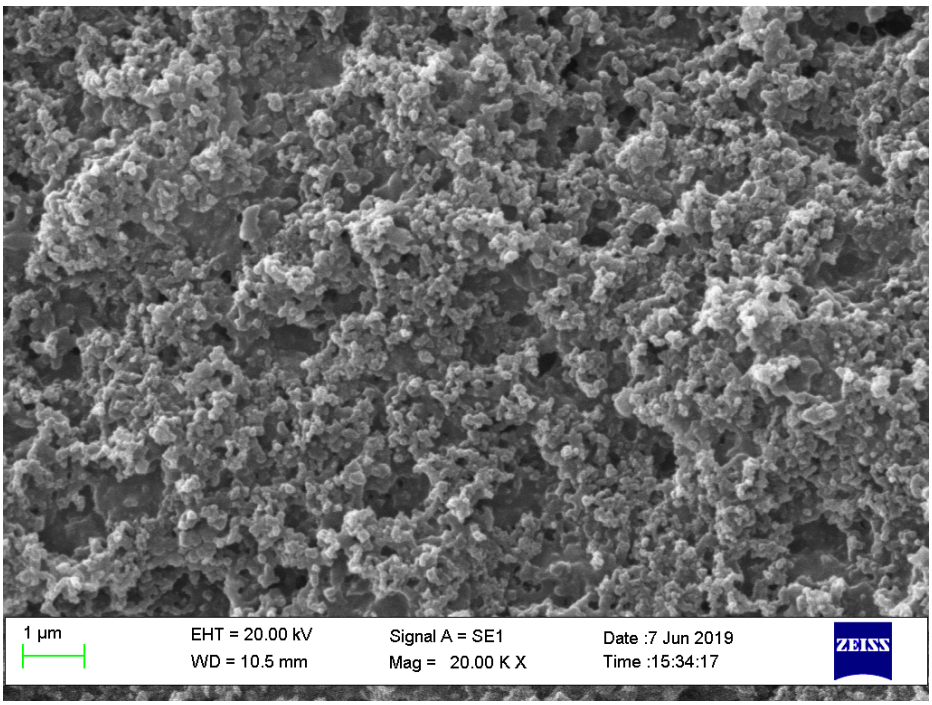

Figure 4.7c SEM of 1.5 mg/cm^2 Pt/C_{HSA} cathode.

4.1.3 Half cell study

4.1.3.1 Anode

The cyclic voltammetry (CV) experiments for methanol or ethanol of various concentration ranging from 0.5 M to 4 M mixed with varying concentration of KOH were investigated on Pt-Ru/C anode using different loading of electrocatalyst ranging from 0.5 mg/cm^2 to 1.5 mg/cm^2. In another CV experiment different ratios of methanol to ethanol in KOH solution were also studied to show the effect of ethanol in the mixture. The scan rates were varied from 5 mV/s to100 mV/s. The electrooxidation of methanol or ethanol takes place in the forward and reverse scan with well defined current peak. In the forward scan, the electrooxidation of alcohols produced a prominent anodic peak due to the electrooxidation of freshly chemisorbed species. The incomplete electrooxidation of carbonaceous species which are formed in the forward scan are removed by further electrooxidation in the reverse scan, thereby producing an anodic peak in the reverse scan (Manoharan and Goodenough 1992 and Morin et al., 1990). The activity of electrocatalysts for alcohol electrooxidation is indicated by the peak current density in forward scan and reverse scan as well.

4.1.3.1.1 Effect of scan rate

Fig (4.8a) and Fig (4.8b) show the effect of different scan rates on the response of cyclic voltammogram for the fuel of 1 M methanol (Fig 4.8a) and 1 M ethanol (Fig 4.8b), respectively. The electrolyte of 0.5 M KOH was mixed with both the fuels separately. The anode loading of 1mg/cm^2 Pt-Ru/C was maintained for methanol and ethanol electrooxidation both. It is seen from Fig (4.8a) and Fig (4.8b) that the peak current densities for forward and reverse scan increase with the increase in scan rate for both methanol and ethanol, respectively. This can be explained in the light of the general

electrochemical reaction mechanism reported by Tripkovic et.al (Tripkovic et.al., 2001) using the following Equations (4.1) to (4.4):

$$R - COH + OH^- \leftrightarrow R - CO_{ad} + H_2O + e^- \quad (4.1)$$

$$OH^- \leftrightarrow OH_{ad} + e^- \quad (4.2)$$

$$R - CO_{ad} + OH_{ad} \rightarrow R - COOH \quad (4.3)$$

$$R - COOH + OH_{ad} \rightarrow R - COO^- + H_2O \quad (4.4)$$

The electron transfer reactions (Equations (4.1) and (4.2)) increases with the increase in the scan rates from 5 mV/s to 100 mV/s while at the same time the chemical reactions (Equations (4.3) and (4.4)) have less time to occur thus, there is less time for the electrocatalyst surface to poison at higher scan rates.

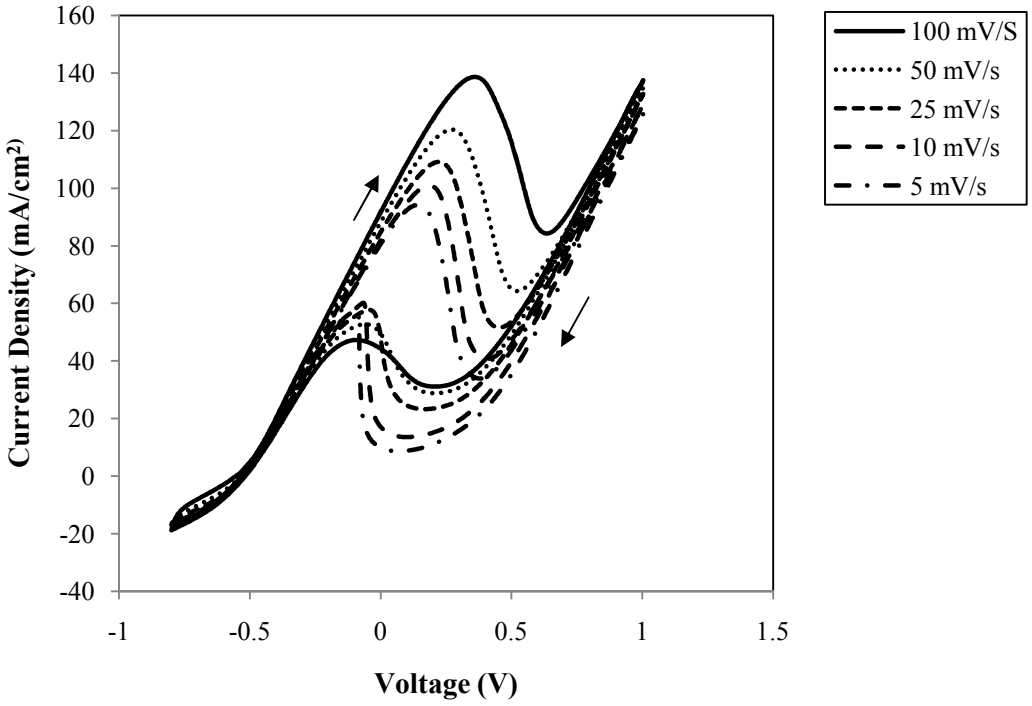

Figure 4.8a Cyclic voltammetry for Pt-Ru/C anode at different scan rates using 1 M methanol solution mixed with 0.5 M KOH solution; Temperature: 30 ^oC.

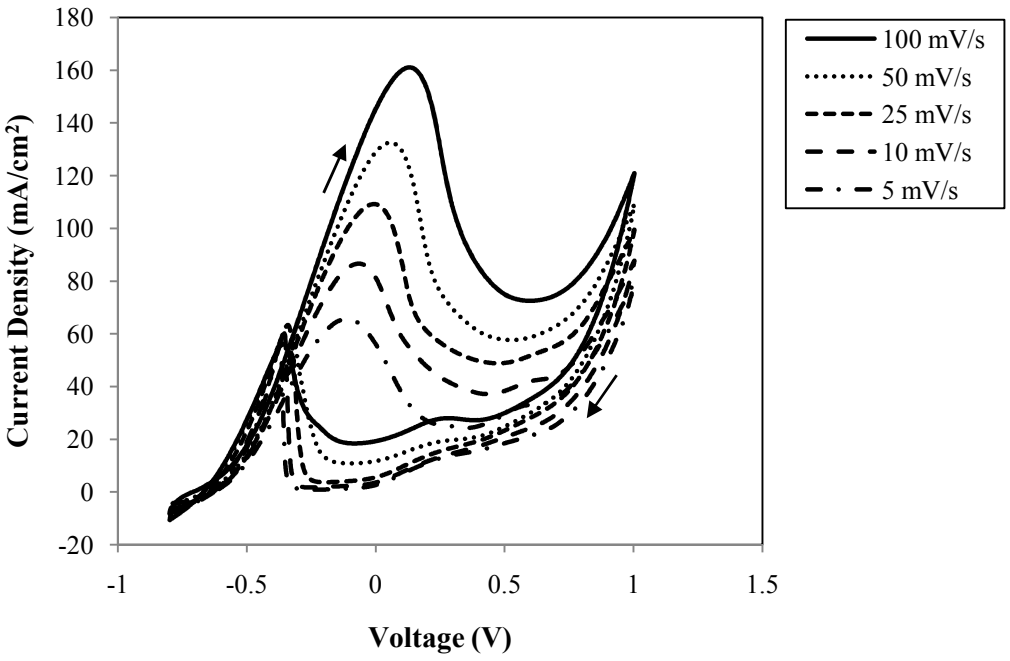

Figure 4.8b Cyclic voltammetry for Pt-Ru/C anode at different scan rates using 1 M ethanol solution mixed with 0.5 M KOH solution; Temperature: 30 ^{o}C.

Fig (4.8a) shows that the maximum peak current density of 138 mA/cm^2 at potential of 0.36 V obtained for 1 M methanol fuel mixed with 0.5 M KOH at scan rate 100 mV/s. However, the scan rate of 5 mV/s produced peak current density of 94 mA/cm^2 at a potential of 0.15 V. Similar, observation was noted for ethanol electrooxidation using the same condition where the maximum peak current density of 160 mA/cm^2 was found at a potential of 0.12 V at 100 mV/s (Fig 4.8b). However, the scan rate of 5 mV/s produced lower peak current density of 62 mA/cm^2 at a potential of -0.05 V. It is clearly seen that the ethanol electrooxidation potential shifted towards negative potential by 0.17 V at low scan rate of 5 mV/s. The electrooxidation of ethanol at more negative potential in comparison to methanol indicates that the Pt-Ru/C favours the electrooxidation of ethanol at low overpotential. Moreover, the scan rate of 100 mV/s gives prominent and highest electrooxidation peak current density for methanol and ethanol both fuels thus, the scan

rate of 100 mV/s was selected here as suitable scan rate to show the effects of other parameters in the next section.

4.1.3.1.2 Effect of electrocatalyst loading

Fig (4.9a) and Fig (4.9b) show the cyclic voltammograms for different anode loadings varying from 0.5 mg/cm^2 to 1.5 mg/cm^2 of Pt–Ru/C, in presence of methanol or ethanol concentration of 1 M mixed with electrolyte concentration of 0.5 M KOH at scan rate of 100 mV/s. It is seen in the Fig (4.9a) that the methanol electrooxidation peak current density increases with the increase in Pt-Ru/C loading from 0.5 mg/cm^2 to 1 mg/cm^2 and then further increase in electrocatalyst loading to 1.5 mg/cm^2, the peak current density decreases. The maximum peak current density of 138 mA/cm^2 at a potential of 0.36 V was obtained for electrocatalyst loading of 1 mg/cm^2 Pt–Ru/C using methanol as fuel. There was a significant increase in peak current density of 118 mA/cm^2 electrocatalyst loading was increased from 0.5 mg/cm^2 to 1 mg/cm^2. The higher loading of Pt-Ru/C i.e., 1.5 mg/cm^2 produced relatively lower peak current density of 115 mA/cm^2. It may be due to agglomeration of Pt-Ru/C electrocatalyst at higher loading of 1.5 mg/cm^2 , which was already observed in SEM images of electrode (Fig 4.6d) as discussed in section 4.1.2.1 (page no. 80) (Basu et al., 2008).

The similar trend was also found for the electrooxidation of ethanol using various Pt-Ru/C loading ranging from 0.5 mg/cm^2 to 1.5 mg/cm^2 (Fig 4.9b). It is seen in the Fig (4.9b) that the maximum peak current density of current density of 160 mA/cm^2 at a potential of 0.12 V was obtained for the electrocatalyst loading of 1mg/cm^2 Pt-Ru/C using ethanol fuel. The peak current density decreased to 147 mA/cm^2 when the electrocatalyst loading was increased from 1 mg/cm^2 to 1.5 mg/cm^2.

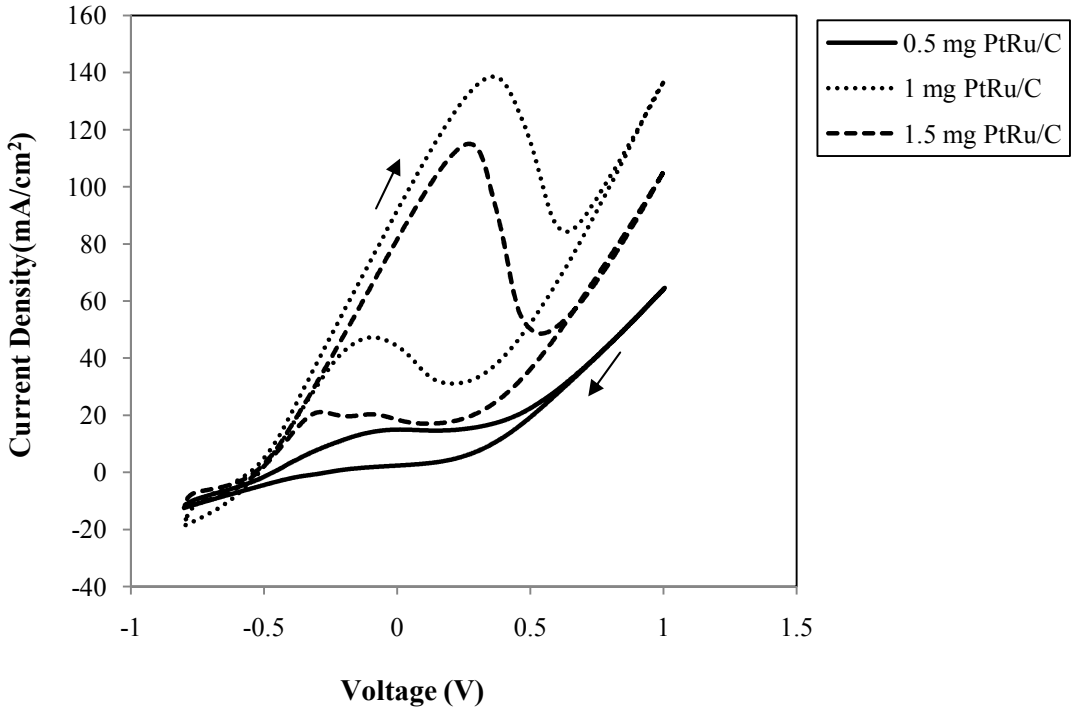

Figure 4.9a Cyclic voltammetry for different loading of Pt-Ru/C anode electrocatalyst using 1 M methanol solution mixed with 0.5 M KOH solution at scan rate of 100 mV/s; Temperature: 30 ^{o}C.

The electrocatalyst loading of 0.5 mg/cm^2 Pt-Ru/C produced very low peak current density of 21 mA/cm^2 at a potential of -0.12 V. Higher loading of electrocatalyst (1 mg/cm^2) provides more active sites of electrocatalyst, resulting in increased reaction rates and current. However, too high loading (1.5 mg/cm^2) of electrocatalyst resulting in electrocatalyst agglomeration followed by decrease in porosity of the electrocatalyst layer leading to increased diffusional resistance to mass transport of fuel from bulk phase to electrocatalyst sites (Basu et al., 2008 and Pramanik et al., 2008) The electrocatalyst loading of 1 mg/cm^2 Pt–Ru/C was found to be the optimum for both methanol and ethanol electrooxidation since, this results in the highest electrode performance in terms of current density. This optimum loading (1 mg/cm^2) was further used to study the effect of fuel and electrolyte concentration.

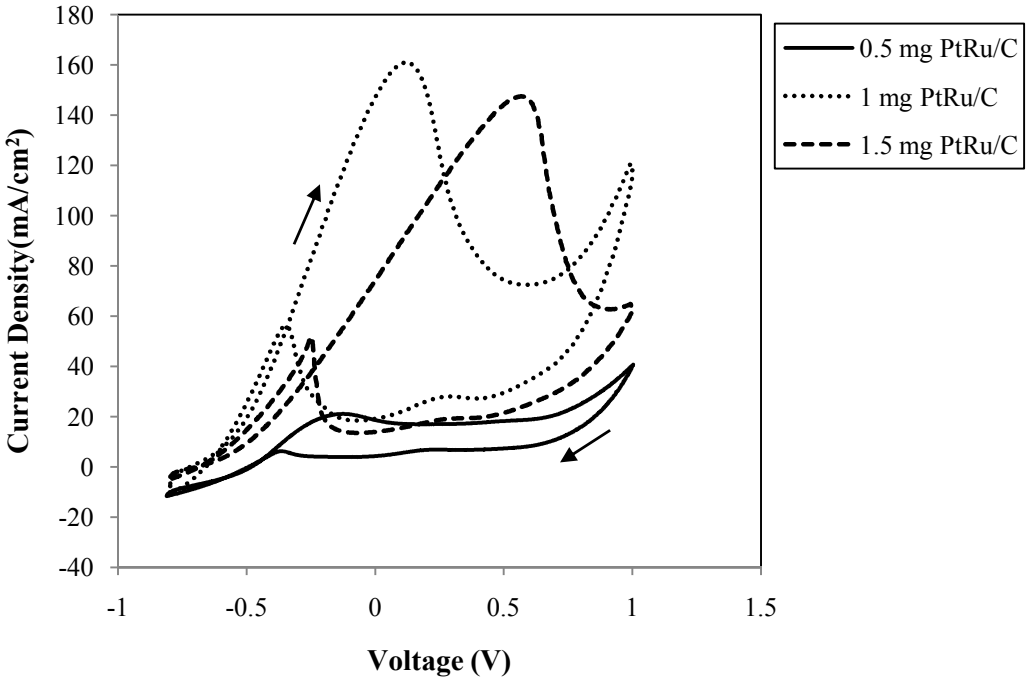

Figure 4.9b Cyclic voltammetry for different loading of Pt-Ru/C anode electrocatalysts using 1 M ethanol solution mixed with 0.5 M KOH solution at scan rate of 100 mV/s; Temperature: 30 ^{o}C.

4.1.3.1.3 Effect of fuel concentration

Fig (4.10a) and Fig (4.10b) show the CVs of different concentration of fuel methanol or ethanol mixed with fixed KOH of 0.5 M at the optimum loading of 1 mg/cm^2 Pt-Ru/C anode. It is observed in the Fig (4.10a) that the peak current density increases with gradual increase in methanol concentration from 0.5 M to 3 M and falls slightly on further increase in concentration of methanol to 4 M. The maximum peak current density of 188.141 mA/cm^2 at a potential of 0.60 V was obtained for 3 M of methanol. Whereas, methanol of 4 M produced peak current density of 180.44 mA/cm^2 at a potential of 0.41 V. The lower concentration of methanol (2 M) produced peak current density of 167.60 mA/cm^2 at a potential of 0.454 V. Thus the optimum concentration for methanol fuel was found to be 3 M in CV studies.

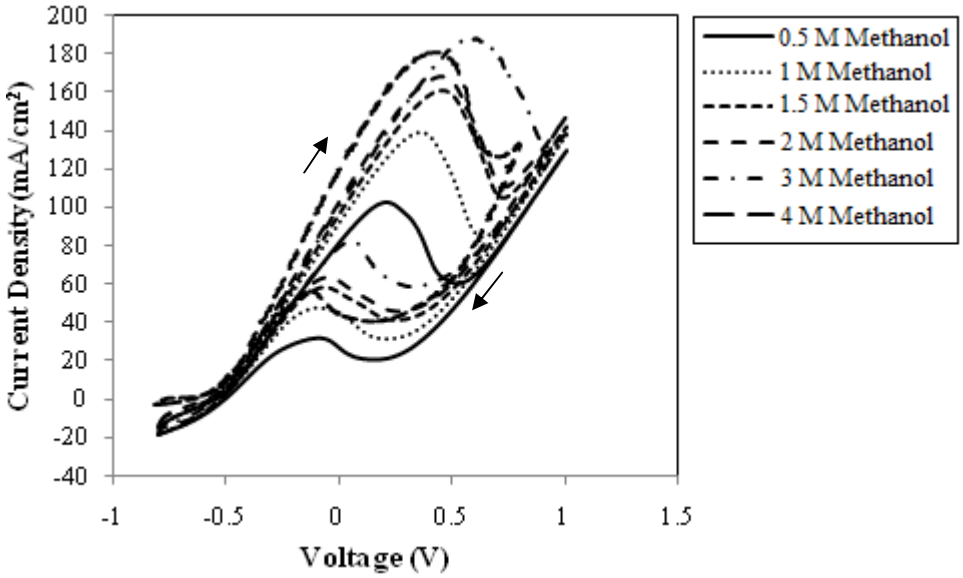

Figure 4.10a Cyclic voltammetry for Pt-Ru/C anode using different concentration of methanol mixed with 0.5 M KOH solution at scan rate of 100 mV/s; Temperature: 30 ^{o}C.

Similar trend was also observed in CV studies for ethanol fuel of varying concentration from 0.5 M to 3 M. It is seen in Fig (4.10b) that the maximum peak current density of 221 mA/cm^2 at a potential of 0.28 V was obtained for the ethanol concentration of 2 M. Whereas, ethanol fuel of 3 M produced lower peak current density of 212 mA/cm^2 at a potential of 0.30 V. The lower concentration of ethanol i.e., 0.5 M, 1 M, and 1.5 M gives the peak current density of 102 mA/cm^2 at -0.03 V, 161 mA/cm^2 at 0.13 V and 199.46 mA/cm^2 at 0.26 V, respectively. Thus, the optimum concentration of ethanol was recorded to be 2 M of ethanol in CV studies.

As observed in the CV studies of methanol (Fig 4.10a), similar trend of shifting the electrooxidation peak potential of ethanol towards positive value was also noticed when the concentration of ethanol is increased. This indicates difficulty in electrooxidation of ethanol at higher concentration.

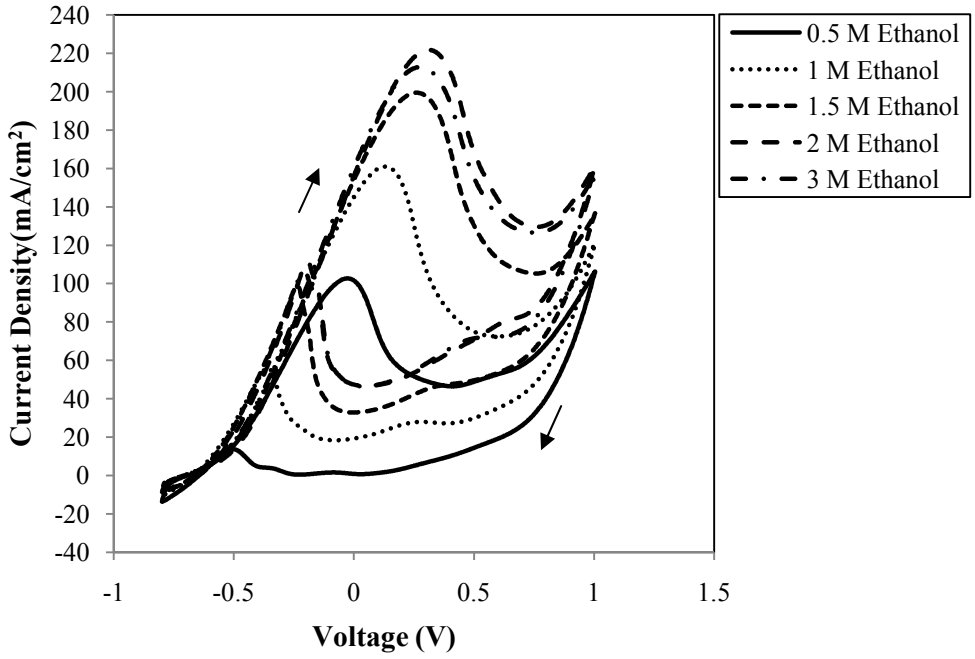

Figure 4.10b Cyclic voltammetry for Pt-Ru/C anode using different concentration of ethanol mixed with 0.5 M KOH solution at scan rate of 100 mV/s; Temperature: 30 ^{o}C.

Initial increase in peak current density may be because of the increase in alcohol concentration more molecules splits and give increased current density. However, the availability of OH^- ion at electrocatalyst site decreases with the further increase in alcohol concentration and excess unreacted alcohol crossover may take place to the cathode which creates mixed potential problem due to unwanted electrooxidation reaction ((Manoharan and Prabhuram 1992). As a result of reduced availability of adsorbed OH^- on the anode electrocatalyst sites and mixed potential at the cathode voltage and current density both decreases. The peak current density of ethanol at optimum concentration (2 M) is higher compared to that of optimum methanol (3 M) and the electrode potential of ethanol is less positive (0.28 V) compared to that of methanol (0.6 V). This indicates that ethanol electrooxidation is more favourable on Pt-Ru/C than methanol (Manoharan and Goodenough 1992 and Santasalo-Aarnio et al., 2013). It may be due to more poisoning of Pt-Ru/C by methanolic intermediates species (CO) reaction might stop at intermediate steps (Morin et al., 1990 and Seiler et al., 2004).

4.1.3.1.4 Effect of electrolyte concentration

Fig (4.11a) and Fig (4.11b) show the CVs for different concentration of KOH solutions mixed with optimum concentration of methanol (3 M) and ethanol (2 M) fuel, respectively. The electrolyte KOH plays a dual role in alcohol electrooxidation process in the form of OH_{ad} species like (i) as an active intermediate in alcohol electrooxidation and (ii) it helps in the formation of oxide species, which is responsible for the inhibition of the fuel electrooxidation (Rathoure and Pramanik 2016). It is observed that the peak current density increases with the increase in KOH concentration up to a certain value for both the fuels. The increase in peak current density may be because of the increase in KOH concentration, it enhances the OH_{ad} species on the electrode, which in turn increases the electrooxidation and the current density. However, the peak current density decreases with further increase in KOH concentration beyond the optimum value. The probable reason may be the higher adsorption of OH^- ion on electrocatalyst site compared to that of fuel molecules and formation of Pt-O layer (Rathoure and Pramanik, 2016).

It is seen in the Fig (4.11a) that the maximum peak current density of 453 mA/cm^2 at a potential of 0.87 V was observed for methanol mixed with 6 M KOH concentration. However, the peak current density for 2 M, 4 M and 8 M of KOH were 295 mA/cm^2, 443 mA/cm^2 and 437 mA/cm^2 at a potential of 0.62 V, 0.73 V and 0.64 V, respectively. This shows that the optimum KOH concentration for methanol electrooxidaton is 6 M.

Similarly, it is seen in the Fig (4.11b) that the maximum peak current density of 287 mA/cm^2 at a potential of 0.34 V was observed for ethanol mixed with 1 M KOH concentration. Whereas, the peak current density for 0.5 M, 1.5 M and 2 M of KOH were 212 mA/cm^2, 194 mA/cm^2 and 134 mA/cm^2 at a potential of 0.28 V, 0.49 V and 0.20 V, respectively.

This shows that the optimum KOH concentration for ethanol electrooxidation is 1 M. These CV show that the shift in peak potential for 1 M KOH is very less compared to 0.5 M KOH, however the peak current density is high (Fig 4.11b). The peak current density of ethanol (Fig 4.11b) is higher compared to that of methanol (Fig 4.11a) and the peak potential of ethanol is more negative compared to that of methanol (Fig 4.11a) at lower range of electrolyte concentration.

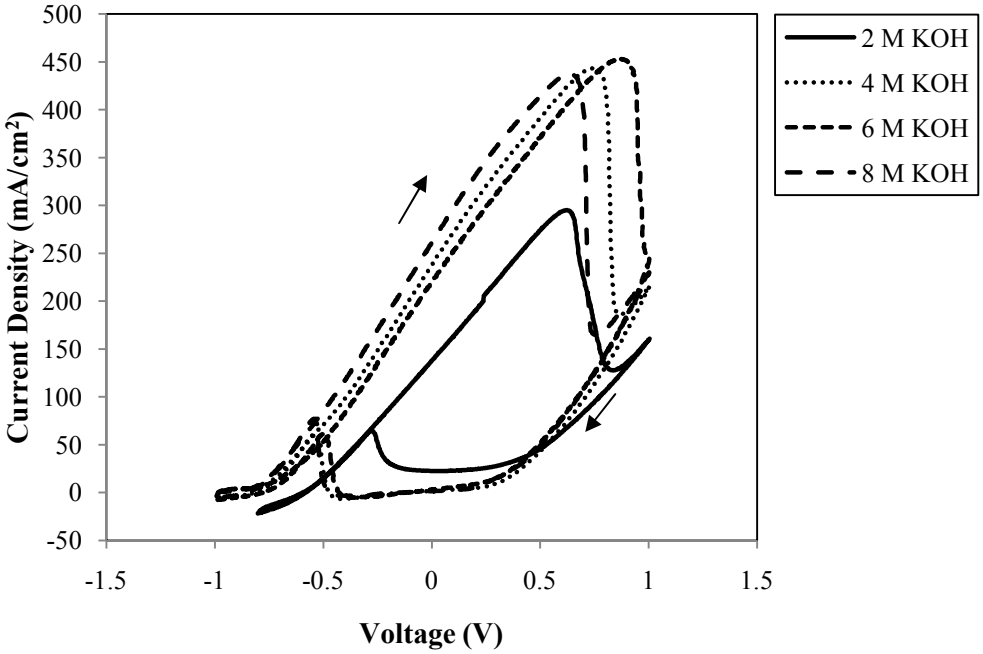

Figure 4.11a Cyclic voltammetry for Pt-Ru/C anode using different concentration of KOH mixed with 3 M methanol solution at scan rate of 100 mV/s; Temperature: 30 ^{o}C.

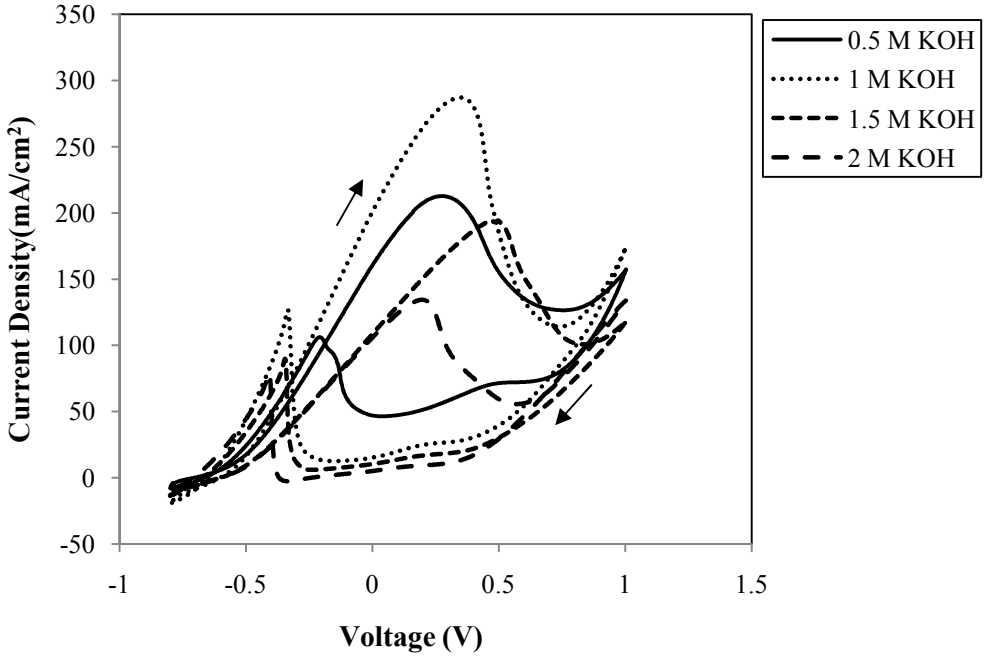

Figure 4.11b Cyclic voltammetry for Pt-Ru/C anode using different concentration of KOH mixed with 2 M ethanol solution at scan rate of 100 mV/s; Temperature: 30 ^{o}C.

4.1.3.5 Electrooxidation of methanol and ethanol mixture as fuel

It is seen from the CV studies that the optimum loading of electrocatalyst (Pt-Ru/C) for both methanol and ethanol is 1 mg/cm^2. Thus, methanol and ethanol mixture with molar ratios of 1:1, 1:2, 1:3 and 1:4 mixed with fixed KOH concentration of 0.5 M and electrocatalyst loading of 1 mg/cm^2 Pt-Ru/C were studied for electrooxidation of fuel mixture at a temperature of 30 ^{o}C (Fig 4.12). Literature suggests that the electrooxidation of methanol fuel on Pt-Ru/C is quiet easier than ethanol fuel. However, methanol is not primary fuel and is toxic, on the other side, ethanol is renewable in nature. Thus, to find out the activity of Pt-Ru/C electrocatalyst for ethanol in a mixture of fuel, the molar concentration of ethanol was increased. Fig (4.12) shows that the peak current density increases with the increase in methanol to ethanol molar ratio for 1:1 to 1:3. However, further increase in molar ratio to 1:4 the peak current density decreases. The peak current density of 141.09 mA/cm^2 at potential of 0.7 V was obtained for fuel mixture of methanol to ethanol 1:3 molar ratio. The peak current density was decreased to 130 mA/cm^2 at

potential of 0.74 V for methanol to ethanol molar ratio of 1:4. It is obvious that the peak current density of the mixture is lower than the pure solutions of methanol and ethanol as discussed earlier (Fig 4.8a to Fig 4.8b). As explained by Morin et.al, the molecular structure of electroactive species has a great influence on its electro activity particularly on a platinum based electrode (Morin et al., 1990). As per anode reaction (Equation (2.5) (page no. 21)), the presence of OH^- ions are very much essential for completion of anode reactions and release of electrons. The increase in ethanol concentration in the mixture beyond the optimum ratio of methanol to ethanol (1:3), the electrocatalyst occupied by the OH^- ions is replaced by the ethanol molecules. Thus, the electrooxidation reaction of ethanol molecule gets inhibited due to lack of OH^- ions at the electrocatalyst sites, which resulting in lower peak current density (Gupta and Pramanik 2019a, Wongyao et al., 2011 and Leo et al., 2013)." Thus, the peak current density for the fuel mixture beyond (1: 3) decreases.

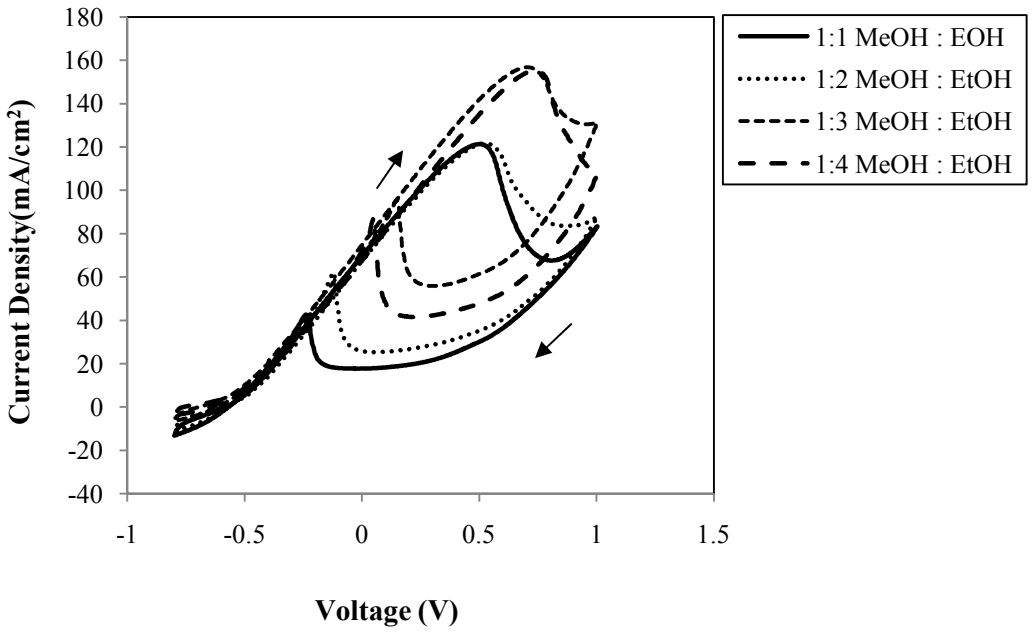

Figure 4.12 Cyclic voltammetry for Pt-Ru/C anode at fixed electrocatalyst loading of 1 mg/cm^2 using fixed KOH concentration of 0.5 M at different molar ratios of methanol to ethanol at scan rate of 100 mV/s; Temperature: 30 ^oC. MeOH-Methanol, EtOH-Ethanol.

4.1.3.2 Cathode

It has already been discussed in literature review (page no. 23) that the oxygen reduction reaction (ORR) kinetics is excellent in alkaline medium in comparison to acidic medium. The reduction reaction generally proceeds either by one step 4 electron or two step 4 electron pathways in alkaline medium (Ortiz and Gautier 2003). The single step 4 electron pathway (Equation (4.5)) for direct oxygen reduction reaction is given below:

$$O_2 + 2H_2O + 4e^- \longrightarrow 4OH^- \quad (4.5)$$

The alternative two steps 4 electron pathway also called as 2+2 electron pathway (Equation (4.6) and (4.7)) is shown below:

$$O_2 + H_2O + 2e^- \longrightarrow HO_2^- + OH^- \quad (4.6)$$

$$HO_2^- + H_2O + 2e^- \longrightarrow 3OH^- \quad (4.7)$$

Where, Equation (4.6) shows the oxygen reduction to peroxide (HO_2^-) ions followed by reduction of HO_2^- to OH^- ions (Equation (4.7)).

Fig 4.13a and Fig 4.13b show the CVs of cathode (Pt/C_{HSA}) at scan rate of 100 mV/s for 1 M KOH purged with nitrogen and 1 M KOH oxygen saturated solution, respectively. The electrodes were fabricated using electrocatalyst Pt/C_{HSA} of loading 1 mg/cm^2. It is seen in the Fig (4.13a) that no reduction peak is observed during the reverse scan since the KOH solution is purged with nitrogen and thus, no dissolved oxidant is present in the solution. However, in Fig (4.13b) two reduction peaks in the reverse scan are observed at -0.48 V and -0.58 V when the electrolyte (KOH) is purged with oxygen. The peak current density of -0.08 mA/cm^2 at potential of -0.48 V and -0.07 mA/cm^2 at potential of -0.58 V were obtained due to oxygen reduction reaction at Pt/C_{HSA} cathode immersed in oxygen saturated KOH electrolyte solution. The occurrence of two peaks indicates two steps 2+2 electron pathway mechanisms for oxygen reduction (Equations (4.6) and (4.7)).

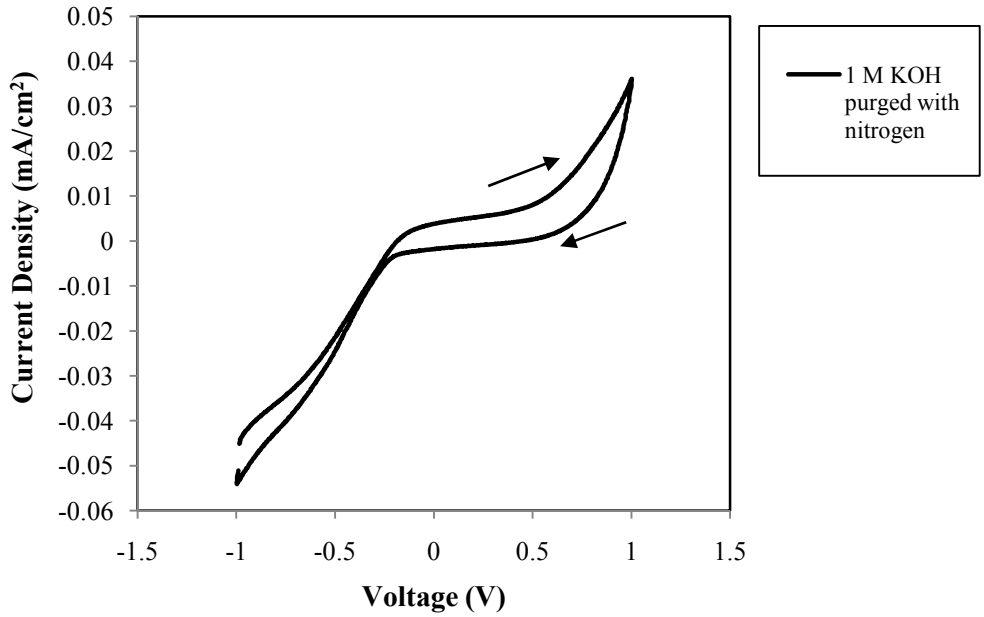

Figure 4.13a Cyclic voltammetry for Pt/C_{HSA} cathode loading of 1 mg/cm^2 and 100 mV/s scan rate using 1 M KOH purged with nitrogen; Temperature: 30 ^oC

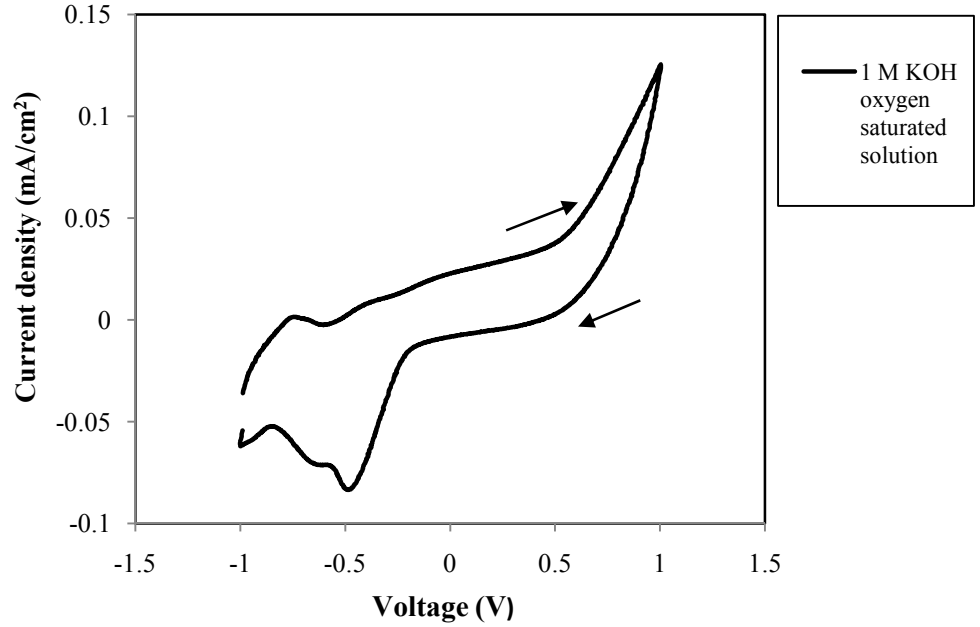

Figure 4.13b Cyclic voltammetry for Pt/C_{HSA} cathode loading of 1 mg/cm^2 and 100 mV/s scan rate using 1 M KOH oxygen saturated solution; Temperature: 30 ^oC.

4.1.4 Single cell studies

The performance of direct alcohol fuel cell (DAFC) using KOH doped physical crosslinked PVA membrane was investigated after thorough studies of electrooxidation of methanol and ethanol and oxygen reduction on the prepared anode and cathode through half-cell analyses using cyclic voltammetry. The experimental results on direct alcohol fuel cell are presented below. Oxygen was used as oxidant unless it is mentioned specifically about another oxidant (atmospheric air). The direct alcohol fuel cell experiments were performed to determine optimum condition of different parameters, such that maximum power density is obtained. The different parameters studied are the KOH doping in physical crosslinked PVA membrane, concentrations of alcohol, electrolyte concentrations, electrocatalyst loading at anode and cathode, electrocatalyst types, oxidant types, cell temperature and membrane types.

4.1.4.1 Effect of KOH doping in physical crosslinked PVA membrane

Fig 4.14a and Fig 4.14b show the polarization curves and power density curves for physical crosslinked PVA membranes doped with the different concentration of KOH ranging from 4 M to 8 M at a temperature of 30 ^{o}C. The anode and cathode were made of Pt-Ru/C and Pt/C_{HSA}, respectively. The electrocatalyst loading at anode and cathode were 1 mg/cm^2. The anode feed consisting of 2 M methanol mixed with optimum concentration of 6 M KOH and 2 M ethanol mixed with optimum concentration of 1 M KOH electrolyte were fed at the anode. The humidified oxygen was used as oxidant at the cathode. It is seen from the single cell study that the cell voltage and power density for a given current density increases with the increase in KOH doping concentration up to 6 M for both methanol (Fig 4.14a) and ethanol (Fig 4.14b). However, further increase in KOH doping

concentration beyond 6 M, the cell performance decreases irrespective of alcohol types used in DAFC.

It is observed in the Fig (4.14a) that the 6 M KOH doped PVA membrane results in an OCV of 0.656 V, maximum power density of 2.59 mW/cm^2 at a current density of 9.06 mA/cm^2 for methanol as anode feed. Whereas, 7 M and 8 M KOH doped PVA membrane generated maximum power density of 2.33 mW/cm^2 at a current density of 8.69 mA/cm^2 and maximum power density of 2.22 mW/cm^2 at a current density of 8.48 mA/cm^2, respectively. The OCV of 0.653 V and 0.651 V were obtained for KOH doping of 7 M and 8 M, respectively.

Similarly, ethanol as anode feed, 6 M KOH doped PVA membrane results in an OCV of 0.73 V and maximum power density of 1.93 mW/cm^2 at a current density of 8.06 mA/cm^2 (Fig 4.14b). Whereas, 7 M and 8 M KOH doped membrane generated maximum power density of 1.79 mW/cm^2 at a current density of 7.89 mA/cm^2 and maximum power density of 1.66 mW/cm^2 at a current density of 7.57 mA/cm^2, respectively. The OCV of 0.731 V and 0.732 V were obtained for KOH doping of 7 M and 8 M, respectively.

The KOH doping concentration dependence of cell performance may be due to the increased KOH uptake within the membrane when impregnated with 6 M KOH. The conductivity of PVA membrane increases which reduces ohmic loss. Moreover, the membrane with the highest ionic conductivity also reduces the electroosmotic drag on OH^- conduction within the synthesized PVA membrane electrolyte (Karimi and Li et al., 2005 and Basu et al., 2008). It is clearly seen that the KOH doping of 6 M gives highest cell performance in terms of power density for both fuels. Thus, 6 M KOH is considered as optimum doping concentration for physical crosslinked PVA membrane. It should also be noted that the PVA based physical crosslinked membrane resulted in highest ionic conductivity of 5.6×10^{-3} S/cm when doped with 6 M KOH (page no. 73).

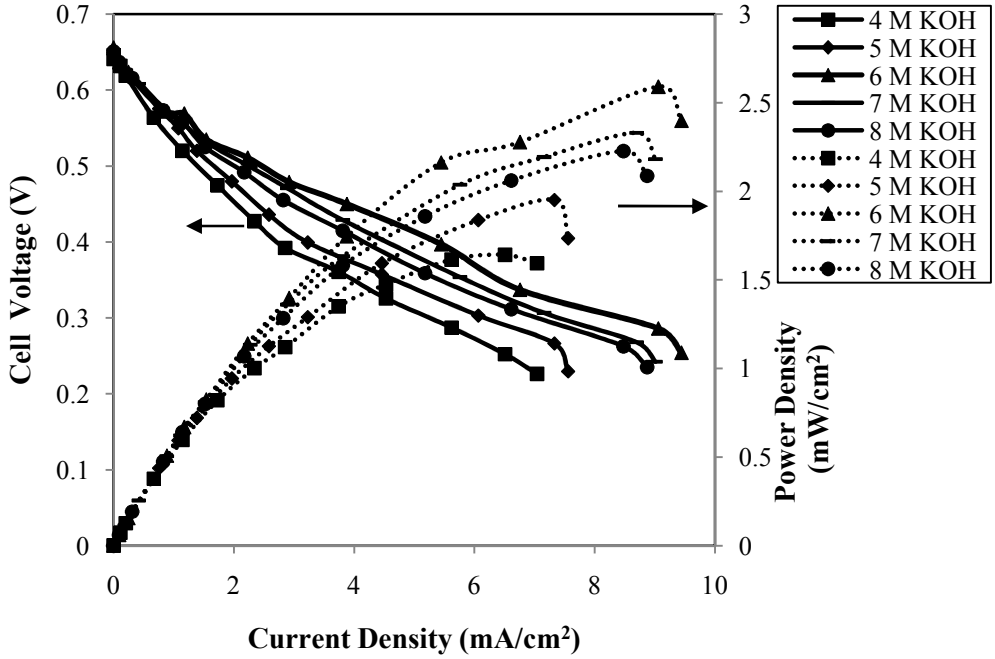

Figure 4.14a Current density vs. cell voltage and current density vs. power density characteristics for physical crosslinked PVA membrane doped with different molar KOH solution using 2 M methanol mixed with 6 M KOH at a temperature of 30 ^{o}C; Dotted line -power density curves; Solid line-polarization curves.

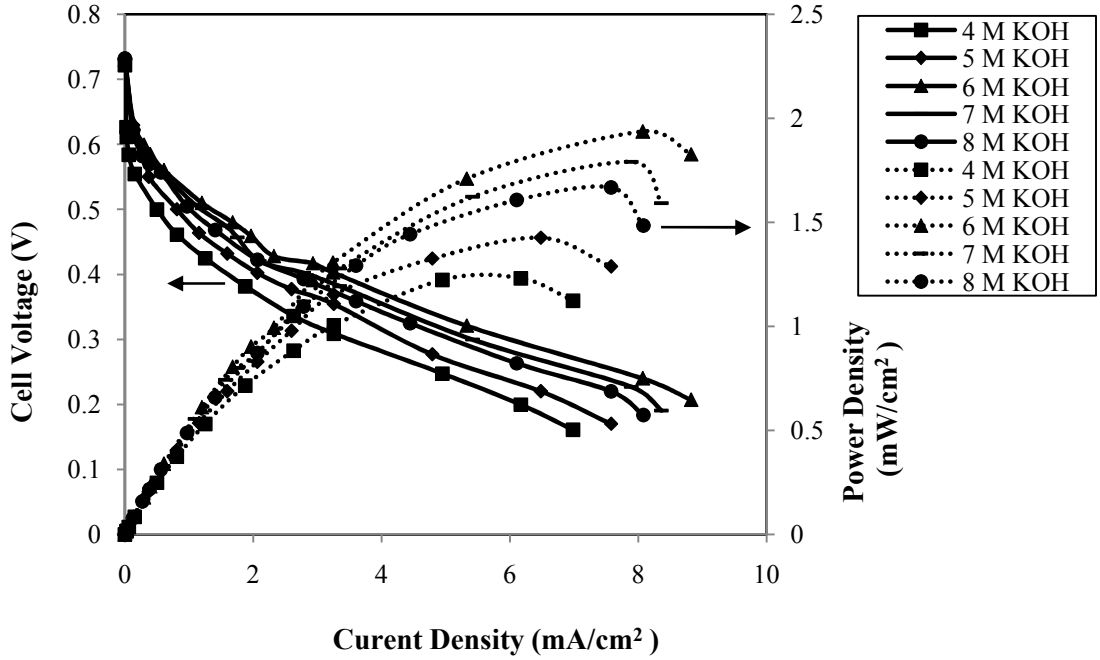

Figure 4.14b Current density vs. cell voltage and current density vs. power density characteristics for physical crosslinked PVA membranes doped with different molar KOH solution using 2 M ethanol mixed with 1 M KOH at a temperature of 30 ^{o}C; Dotted line - power density curves; Solid line-polarization curves.

4.1.4.2 Effect of alcohol concentration

Fig (4.15a) to Fig (4.15b) show the effect of methanol and ethanol concentration mixed with the fixed electrolyte concentration of 1 M KOH on the polarization and power density curves at the temperature of 30 ^{o}C. The anode and cathode electrocatalysts were Pt-Ru/C and Pt/C_{HSA}, respectively. The fixed electrocatalyst loading of 1 mg/cm^2 was taken at both electrodes. The cathode oxidant used was humidified oxygen. It is seen from Fig (4.15a) that the polarization and power density curves shifted upward with the increase in methanol concentration from 1 M to 2 M, while further increase in concentration to 3 M, the curves shift downward. The reason may be the replacement of OH^- ions from the electrocatalyst surface by the methanol considered for the study (Manoharan and Prabhuram 1992). As, OH^- plays an important role in completion of electrooxidation reaction at anode (Equation (4.1), page no. 86).

The maximum open circuit voltage (OCV) of 0.6 V and maximum power density of 1.12 mW/cm^2 at a current density of 5.38 mA/cm^2 were obtained for the methanol of 2 M. However, the methanol of 3 M produced maximum OCV of 0.56 V and maximum power density of 1.07 mW/cm^2 at a current density of 7.63 mA/cm^2 which is lower than 2 M methanol (1.12 mW/cm^2). The methanol of 1 M produced very low power density of 0.73 mW/cm^2 at a current density of 4.28 mA/cm^2.

The similar trend was also observed for ethanol fuel when the concentration of ethanol was increased. It is seen from the Fig (4.15b), the maximum OCV of 0.73 V and maximum power density 1.93 mW/cm^2 at a current density of 8.06 mA/cm^2 were obtained for the ethanol of 2 M. Whereas, the ethanol of 1 M and 3 M produced the maximum power density of 1.09 mW/cm^2 at a current density of 5.44 mA/cm^2 and maximum power density of 1.85 mW/cm^2 at a current density of 6.72 mA/cm^2, respectively. The OCV of

0.70 V and 0.679 V were obtained for 1 M and 3 M ethanol, respectively. The methanol and ethanol concentration of 2 M was found to be the optimum fuel concentration as the DAFC produced highest power density at this concentration. The similar trend were also observed for the electrooxidation of methanol (Fig 4.10a) and ethanol (Fig 4.10b) in cyclic voltammetry experiments, as explained in the section 4.1.3.1.3 (page no. 90).

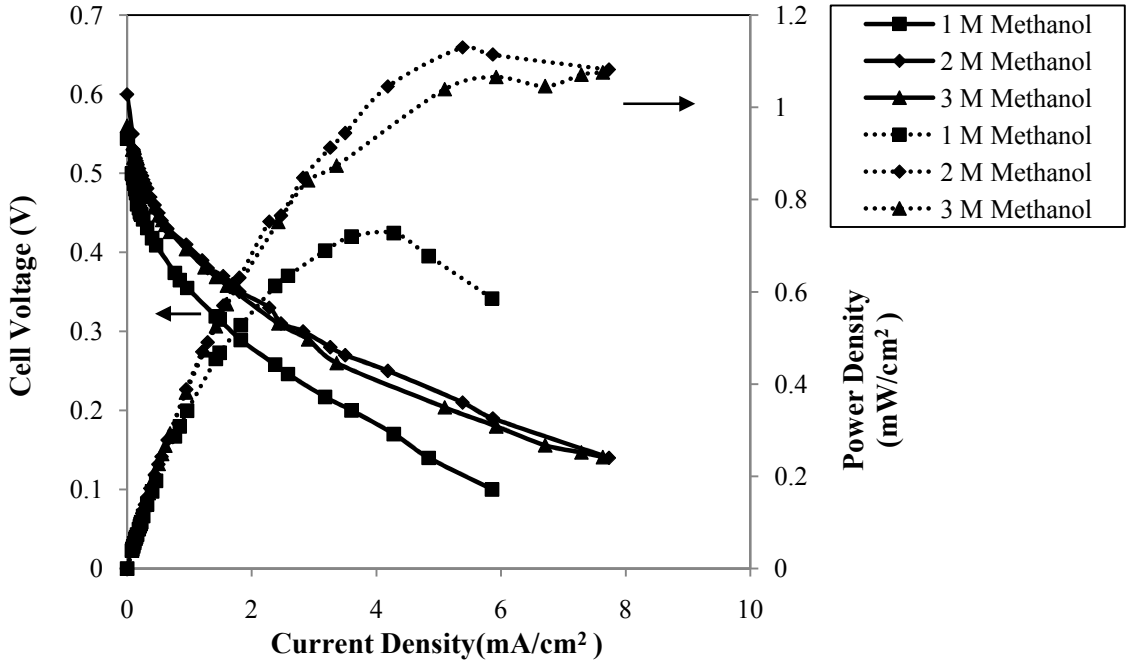

Figure 4.15a Current density vs. cell voltage and current density vs. power density characteristics using fixed 1 M KOH and different methanol concentration using O_2 as oxidant at a temperature of 30 ^oC; Dotted line-power density curves; Solid line-polarization curves.

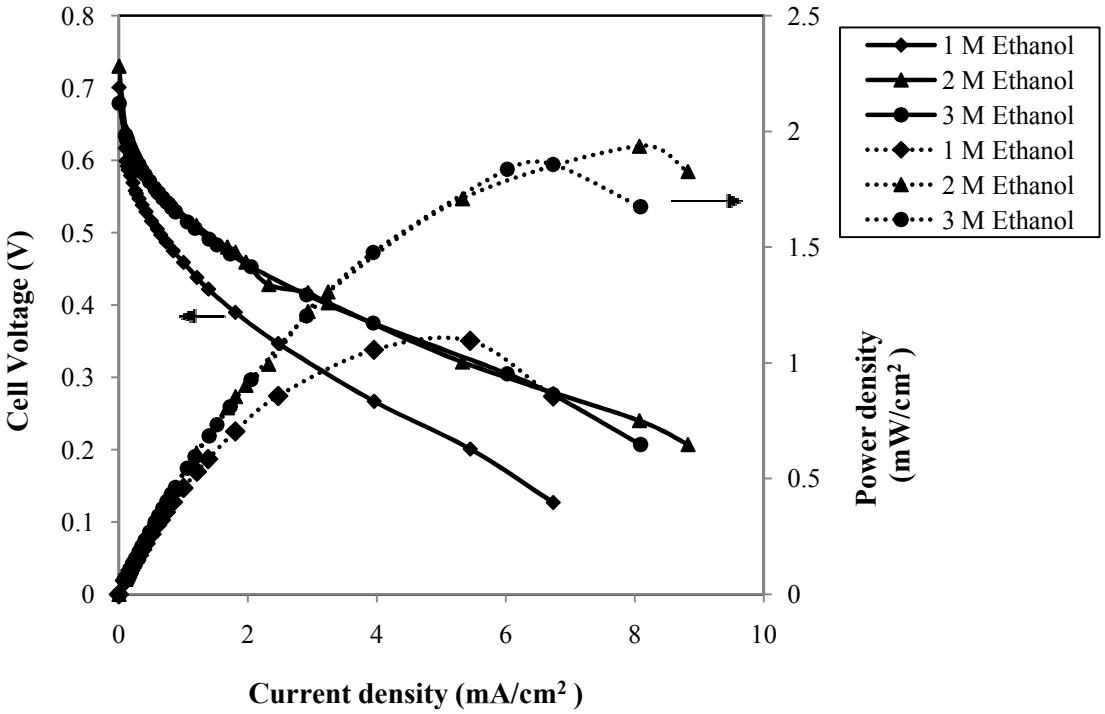

Figure 4.15b Current density vs. cell voltage and current density vs. power density characteristics using fixed 1 M KOH and different ethanol concentration using O_2 as oxidant at a temperature of 30 ^{o}C; Dotted line-power density curves; Solid line-polarization curves.

4.1.4.3 Effect of electrolyte concentration

Fig (4.16a) and Fig (4.16b) show the polarization and power density curves for different electrolyte concentration using fixed anode and cathode loading of 1 mg/cm^2. The anode and cathode electrocatalysts were Pt-Ru/C and Pt/C_{HSA}, respectively. The anode fuels were optimum concentration of methanol (2 M) mixed with various concentration of electrolyte KOH and optimum concentration of ethanol (2 M) mixed with various concentration of KOH electrolyte. The cell temperature was maintained at 30 ^{o}C. The cathode oxidant used was humidified oxygen. It is seen from Fig (4.16a) that the polarization and power density curves shifted upward for methanol fuel with the increase in KOH concentration from 2 M to 6 M. While, further increase in KOH concentration to 8 M, the curve shift downward. The maximum open circuit voltage (OCV) of 0.656 V,

and maximum power density of 2.59 mW/cm^2 at a current density of 9.06 mA/cm^2 were obtained for the 2 M methanol mixed with 6 M KOH concentration. Whereas, maximum power density of 1.36 mW/cm^2 at a current density of 7.27 mA/cm^2, maximum power density of 1.90 mW/cm^2 at a current density of 6.60 mA/cm^2 and maximum power density of 2.22 mW/cm^2 at a current density of 8.23 mA/cm^2, were obtained for 2 M methanol fuel mixed with 2 M, 4 M and 8 M KOH , respectively. The OCV of 0.65 V, 0.60 V and 0.62 V were obtained for 2 M methanol fuel mixed with 2 M, 4 M and 8 M KOH , respectively. Thus, the optimum electrolyte concentration for methanol fuel was 6 M KOH.

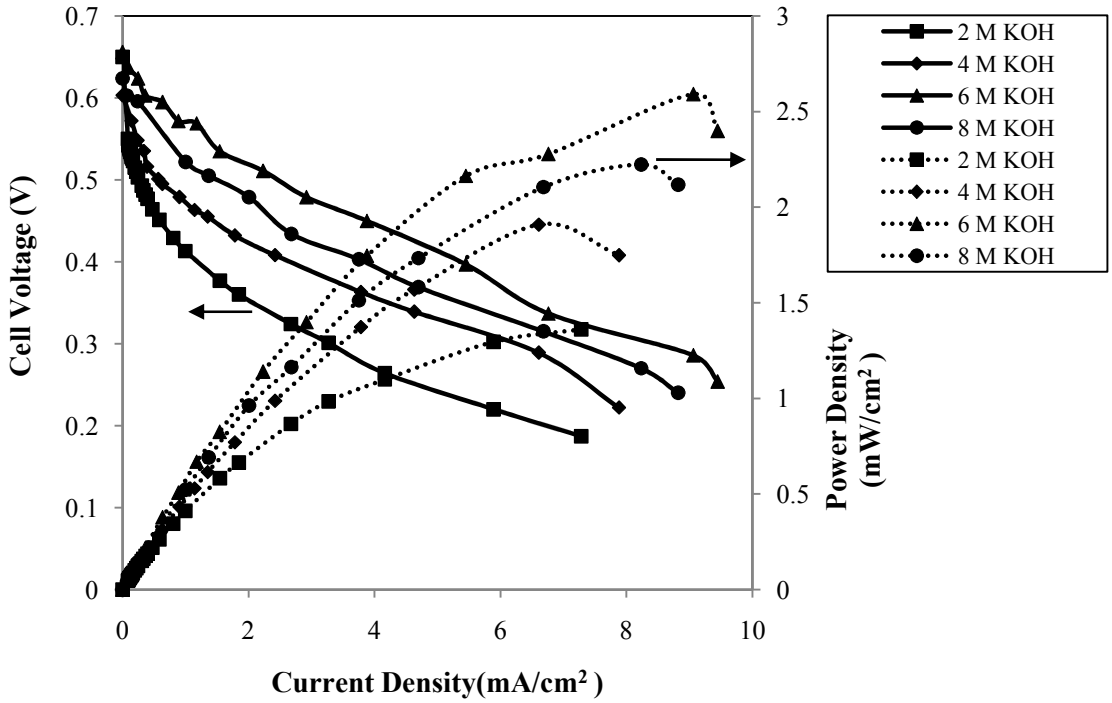

Figure 4.16a Current density vs. cell voltage and current density vs. power density characteristics for fixed 2 M methanol and different KOH using O_2 as oxidant at a temperature of 30 ^oC; Dotted line-power density curves; Solid line-polarization curves.

Similarly, it is seen from Fig (4.16b) that the polarization and power density curves shifted upward for ethanol fuel with the increase in KOH concentration from 0.5 M to 1 M. While, further increase in KOH concentration to 2 M, the curve shifts downward.

The maximum open circuit voltage (OCV) of 0.73 V, and maximum power density of 1.93 mW/cm^2 at a current density of 8.06 mA/cm^2 were obtained for the 2 M ethanol mixed with 1 M KOH concentration. However, maximum power density of 1.43 mW/cm^2 at a current density of 6.39 mA/cm^2, maximum power density of 1.71 mW/cm^2 at a current density of 8.84 mA/cm^2 and maximum power density of 1.70 mW/cm^2 at a current density of 7.67 mA/cm^2, were obtained for 2 M ethanol fuel mixed with 0.5 M, 2 M and 3 M KOH, respectively. The OCV of 0.66 V, 0.658 V and 0.673 V were obtained for 2 M ethanol fuel mixed with 0.5 M, 2 M and 3 M KOH , respectively. Thus, for ethanol fuel the optimum electrolyte concentration was 1 M KOH. In the cyclic voltammetry study similar trend was found for methanol and ethanol both (page no. 93).

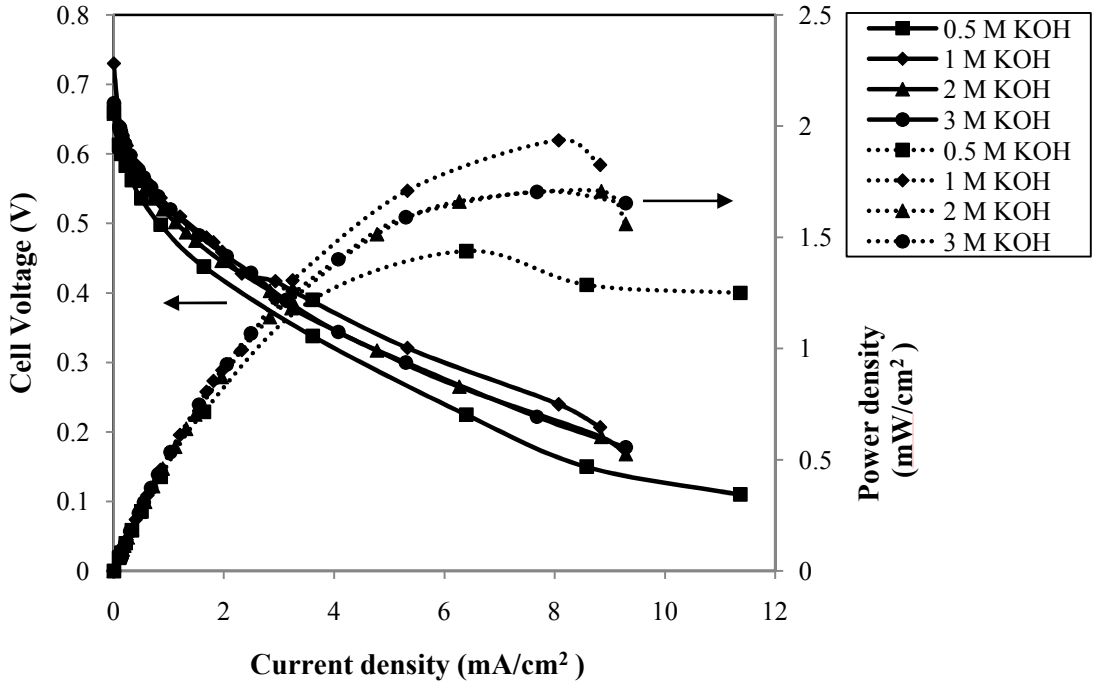

Figure 4.16b Current density vs. cell voltage and current density vs. power density characteristics for fixed 2 M ethanol and different KOH using O_2 as oxidant at a temperature of 30 ^oC; Dotted line-power density curves; Solid line-polarization curves.

4.1.4.4 Effect of anode electrocatalyst loading

Fig (4.17a) and Fig (4.17b) show the polarization curves and power density curves for methanol and ethanol using different anode loadings i.e., 0.5 mg/cm^2, 1 mg/cm^2 and 1.5 mg/cm^2 of Pt–Ru/C, respectively. The cathode was of 1 mg/cm^2 of Pt/C_{HSA}. The anode fuel were 2 M methanol (optimum) mixed with 6 M KOH (optimum) and 2 M ethanol (optimum) mixed with 1 M KOH (optimum), respectively. The cell was operated at a temperature of 30 ^oC. It is seen in the Fig (4.17a) and Fig (4.17b) that the power density and current density increases with the increase in anode electrocatalyst loading from 0.5 mg/cm^2 to 1 mg/cm^2 irrespective of fuel used. While, further increase in electrocatalyst loading beyond 1 mg/cm^2, the cell performance decreases. The reason for this decrease may be electrocatalyst agglomeration at high loading (1.5 mg/cm^2) of Pt-Ru/C electrocatalyst (Pramanik et al., 2008 and Basu et al., 2008). Agglomeration results in a decrease in porosity of the electrocatalyst layer leading to increased diffusional resistance to mass transport of alcohol from bulk phase to the active electrocatalyst layer and this has already been discussed in CV studies (page no. 89). The SEM image of 1.5 mg/cm^2 also shows the electrocatalyst agglomeration (Fig 4.6d, page no. 82). Whereas, well and uniform distribution of electrocatalysts is observed for 1 mg/cm^2 (Fig 4.6c). The above dependence of electrocatalyst loading is also observed in cyclic voltammograms (page no. 88).

It is seen in Fig (4.17a) that the maximum OCV of 0.656 V and maximum power density of 2.59 mW/cm^2 at a current density of 9.06 mA/cm^2 were obtained for 1 mg/cm^2 of Pt-Ru/C anode using methanol as fuel. The electrocatalyst loading of 0.5 mg/cm^2 and 1.5 mg/cm^2 produced maximum power density of 1.94 mW/cm^2 at a current density of 7.19 mA/cm^2 and maximum power density 2.28 mW/cm^2 at a current density of

8.35 mA/cm^2, respectively. The OCV of 0.654 V and 0.653 V were obtained for 0.5 mg/cm^2 and 1.5 mg/cm^2, respectively.

Similarly, it is seen from Fig (4.17b) that the maximum OCV of 0.73 V and maximum power density of 1.93 mW/cm^2 at a current density of 8.06 mA/cm^2 were obtained for 1 mg/cm^2 of Pt-Ru/C anode using ethanol as anode fuel. While, the electrocatalyst loading of 0.5 mg/cm^2 and 1.5 mg/cm^2 Pt-Ru/C produced maximum power density of 1.45 mW/cm^2 at a current density of 6.95 mA/cm^2 and maximum power density of 1.69 mW/cm^2 at a current density of 7.60 mA/cm^2, respectively. The OCV of 0.725 V and 0.734 V were obtained for 0.5 mg/cm^2 and 1.5 mg/cm^2, respectively. Although, not shown here the detailed single cell studies for three different anode Pt-Ru/C electrocatalyst loading viz, 0.5 mg/cm^2, 1 mg/cm^2 and 1.5 mg/cm^2 using other concentrations of methanol and ethanol are presented in Appendix B (page no.197)

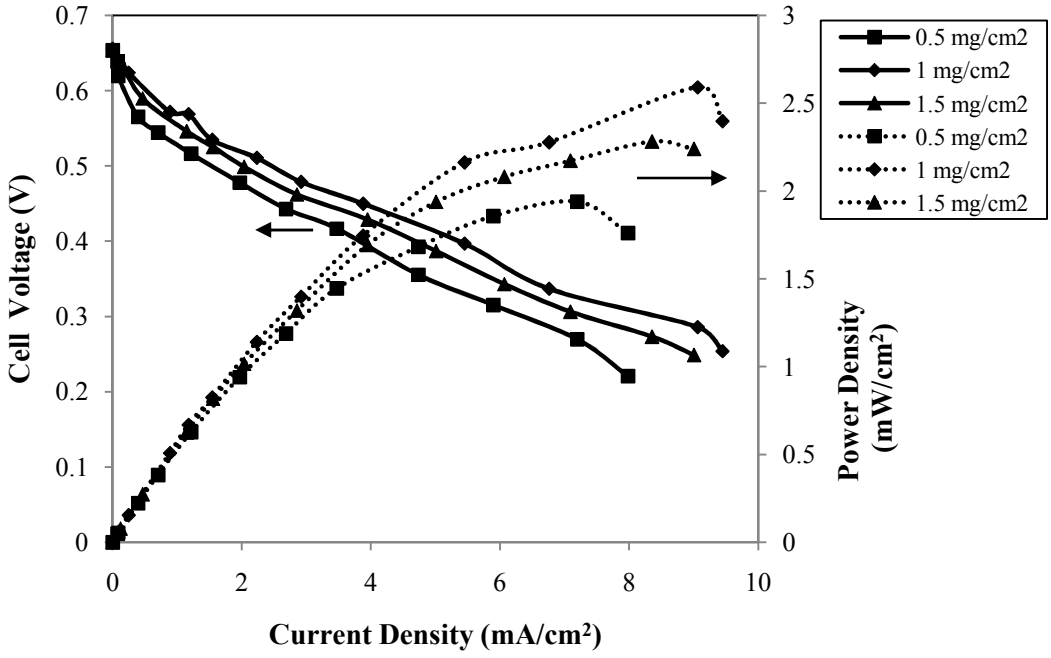

Figure 4.17a Current density vs. cell voltage and current density vs. power density characteristics for different anode loading using 2 M methanol mixed with 6 M KOH at a temperature of 30 ^{o}C; Dotted line-power density curves; Solid line-polarization curves.

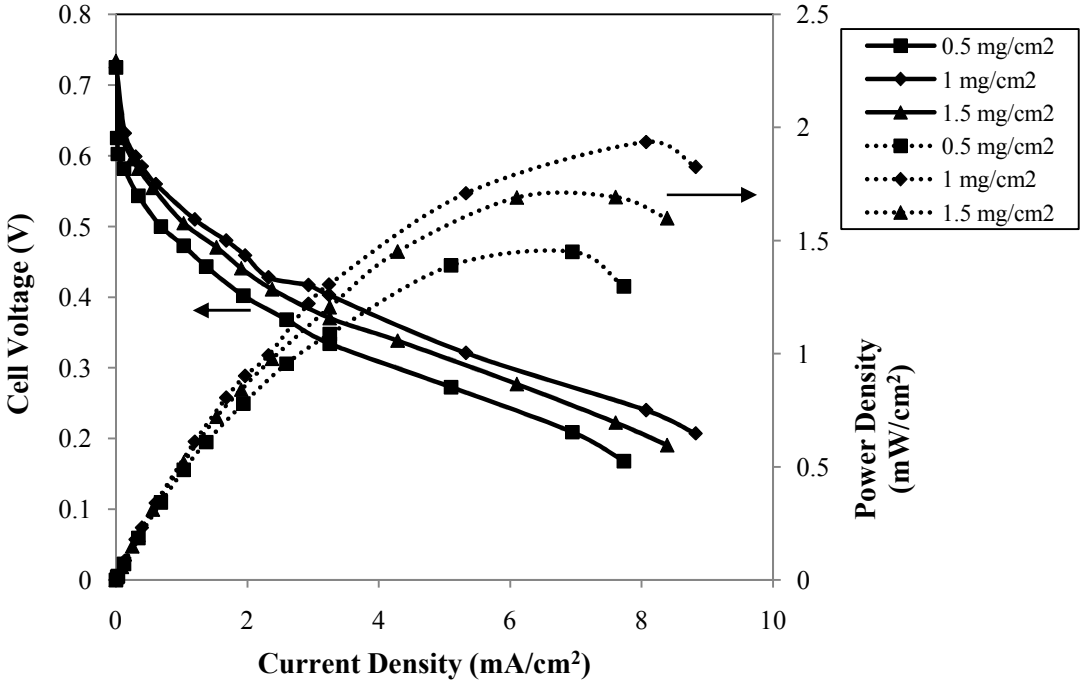

Figure 4.17b Current density vs. cell voltage and current density vs. power density characteristics for different anode loading using 2 M ethanol mixed with 1 M KOH at a temperature of 30 ^{o}C; Dotted line-power density curves; Solid line-polarization curves.

4.1.4.5 Effect of cathode electrocatalyst loading

Fig (4.18a) and Fig (4.18b) show the current density vs. voltage and current density vs. power density for different loading at cathode varying from 0.5 mg/cm^2 to 1.5 mg/cm^2 of Pt/C_{HSA} and optimum anode loading of 1 mg/cm^2 of anode Pt-Ru/C. It is seen in the Fig (4.18a) to Fig (4.18b) that the current density and power density both increases with the increase in cathode electrocatalyst loading from 0.5 mg/cm^2 to 1 mg/cm^2 irrespective of fuel used. While, further increase in electrocatalyst loading beyond 1 mg/cm^2, the cell performance decreases. The reason has already been discussed in the previous section for the varying anode loading (page no. 107). The trend as it was seen with the varying anode loading (Fig 4.19a and Fig 4.18b), the similar trend of polarization and power density curves were also observed for both methanol and ethanol when the cathode (Pt/C_{HSA}) loading was varied from 0.5 mg/cm^2 to 1.5 mg/cm^2.

It is seen in Fig (4.18a) that the maximum OCV of 0.656 V and maximum power density of 2.59 mW/ cm^2 at a current density of 9.06 mA/cm^2 were obtained for 1 mg/cm^2 of Pt/C_{HSA} cathode using methanol as fuel. Whereas, the electrocatalyst loading of 0.5 mg/cm^2 and 1.5 mg/cm^2 produced maximum power density of 1.82 mW/cm^2 at a current density of 7.12 mA/cm^2 and maximum power density of 2.15 mW/cm^2 at a current density of 8.15 mA/cm^2, respectively. The OCV of 0.652 V and 0.654 V were obtained for 0.5 mg/cm^2 and 1.5 mg/cm^2, respectively.

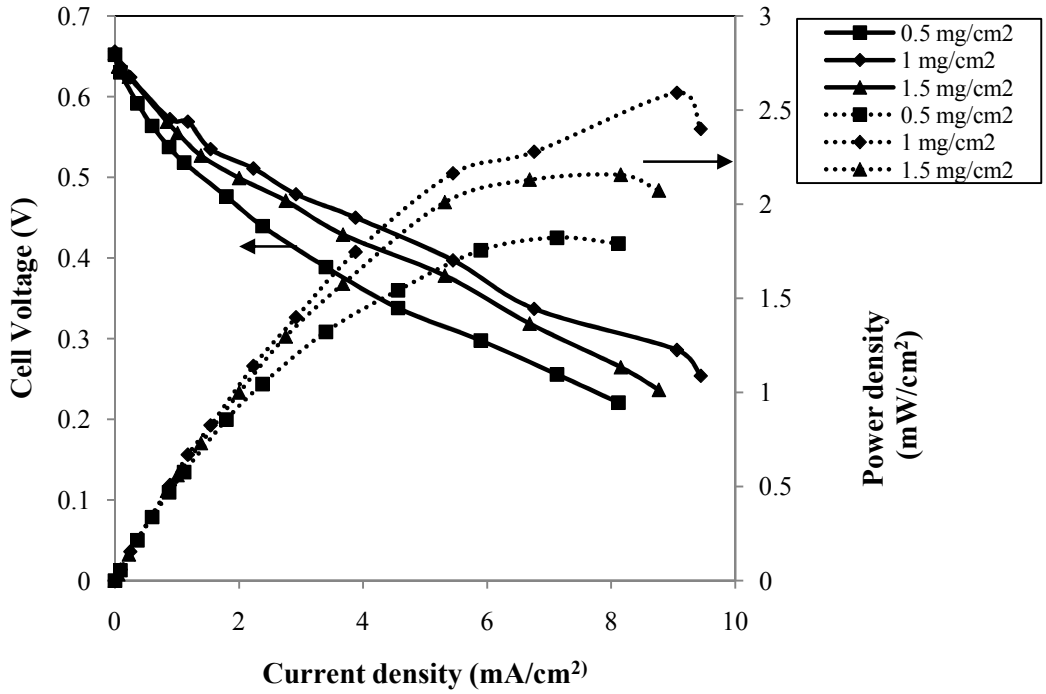

Figure 4.18a Current density vs. cell voltage and current density vs. power density characteristics for different cathode loading using 2 M methanol mixed with 6 M KOH at a temperature of 30 ^oC; Dotted line-power density curves; Solid line-polarization curves.

Similarly, it is seen from Fig (4.18b) that the maximum OCV of 0.73 V and maximum power density of 1.93 mW/cm^2 at a current density of 8.06 mA/cm^2 were obtained for 1 mg/cm^2 of Pt/C_{HSA} cathode using ethanol as anode fuel. While, the electrocatalyst loading of 0.5 mg/cm^2 and 1.5 mg/cm^2 Pt/C_{HSA} produced maximum power density of 1.34 mW/cm^2 at a current density of 6.73 mA/cm^2 and maximum power density of

1.63 mW/cm^2 at a current density of 8.48 mA/cm^2, respectively. The OCV of 0.729 V and 0.731 V were obtained for 0.5 mg/cm^2 and 1.5 mg/cm^2, respectively. From the cathode study it is clear that the optimum cathode loading for methanol and ethanol was 1 mg/cm^2 Pt/C_{HSA}.

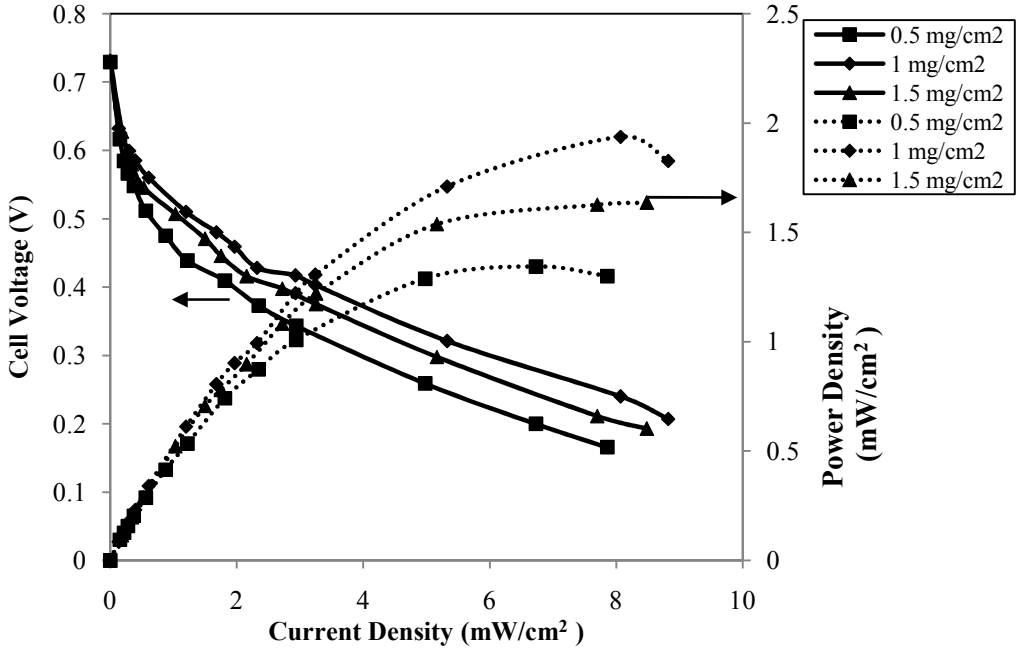

Figure 4.18b Current density vs. cell voltage and current density vs. power density characteristics for different cathode loading using 2 M ethanol mixed with 1 M KOH at a temperature of 30 ^oC; Dotted line-power density curves; Solid line-polarization curves.

4.1.4.6 Effect of electrocatalyst type

Fig (4.19a) and Fig (4.19b) show the polarization curves and power density curves for different types of anode electrocatalyst using methanol and ethanol, respectively. The different anode electrocatalyst evaluated were Pt-Ru/C and Pt/C_{HSA} at an optimum loading of 1 mg/cm^2. The cathode for both the fuel methanol and ethanol were 1 mg/cm^2 Pt/C_{HSA}. The anode electrocatalysts Pt-Ru/C (1 mg/cm^2) resulted in highest cell performance in terms of current density and power density in comparison to Pt/C_{HSA} anode for methanol (Fig 4.19a) and ethanol (Fig 4.19b) both. It is well established that bimetallic Pt-Ru/C alloy electrodes perform as best electrocatalyst for methanol and

ethanol electrooxidation due to its bi-functional mechanism (Lamy et al., 2001 Tripkovic et al., 2002 and Roth et al., 2005). Ruthenium is a good CO^- tolerant catalyst but inactive for methanol or ethanol electrooxidation. Moreover, Ru plays an important role in water dissociation to supply OH_{ad} species to aid the oxidation of adsorbed CO to CO_2 at low overpotential during methanol and ethanol electrooxidation. Nevertheless, the CO formed as a side reaction is oxidized and the poisoning effect is reduced (Tripkovic et al., 2002). Thus, enhance the electrocatalytic activity of Pt-Ru/C for methanol and ethanol both (Gasteiger et al, 1993).

It is observed in the Fig (4.19a) that the maximum OCV of 0.656 V and 0.643 V were produced for fuel methanol using Pt-Ru/C and Pt/C_{HSA}, respectively. Similarly, the OCV of 0.73 V and 0.72 V were obtained for ethanol using Pt-Ru/C and Pt/C_{HSA}, respectively (Fig 4.19b). It is clearly seen, OCV is higher for Pt-Ru/C anode irrespective of fuel used. The maximum power density of 2.59 mW/cm^2 at a current density of 9.06 mA/cm^2 and maximum power density of 1.99 mW/cm^2 at a current density of 7.50 mA/cm^2 were obtained for methanol using Pt-Ru/C and Pt/C_{HSA}, respectively (Fig 4.19a). Whereas, the maximum power density of 1.93 mW/cm^2 at a current density of 8.06 mA/cm^2 and maximum power density of 1.43 mW/cm^2 at a current density of 6.75 mA/cm^2 were obtained for ethanol using Pt-Ru/C and Pt/C_{HSA}, respectively (Fig 4.19b)

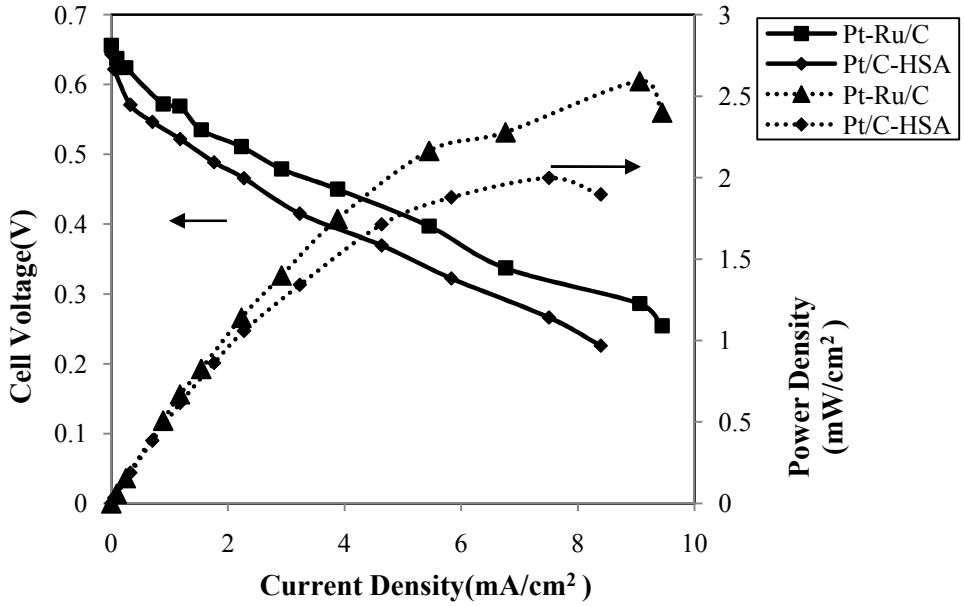

Figure 4.19a Current density versus cell voltage and current density versus power density characteristics using different anode electrocatalyst for 2 M methanol mixed with 6 M KOH at a temperature of 30 ^{o}C; Dotted line-power density curves; Solid line-polarization curves.

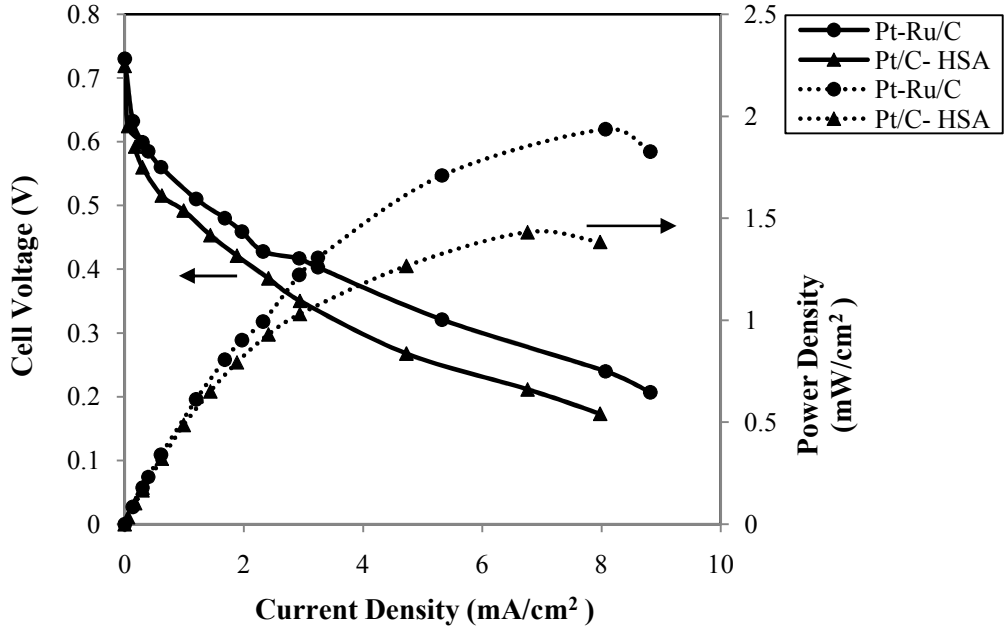

Figure 4.19b Current density versus cell voltage and current density versus power density characteristics using different anode electrocatalyst for 2 M ethanol mixed with 1 M KOH at a temperature of 30 ^{o}C; Dotted line-power density curves; Solid line-polarization curves.

4.1.4.7 Effect of temperature

Fig (4.20a) and Fig (4.20b) show the polarization curves and power density curves at different temperatures for methanol and ethanol fuels, respectively. The anode and cathode were made of Pt-Ru/C and Pt/C_{HSA} of optimum loading (1 mg/cm^2) for both electrodes. The anode feed consisting of optimum 2 M methanol mixed with optimum concentration of 6 M KOH or 2 M ethanol (optimum) fuel mixed with optimum concentration of 1 M KOH electrolyte was fed at the anode and humidified oxygen was used as oxidant at the cathode. The cell performance increases with the increase in cell temperature and the maximum power density increases up to 50 ^oC for both methanol and ethanol fuels and then decreases with the further increase in temperature to 60 ^oC. The initial increase in performance may due to increase in temperature up to 50 ^oC. The increased temperature decreases the viscosity and thus ionic mobility is increased (An et al., 2012 and Schalenbach et al., 2018) and the kinetics of the reaction is also improved. However, at higher temperature (60 ^oC) the membrane might start to get deteriorate causing crossover problem resulting in mixed potential (Gupta and Pramanik 2019b). Thus, the overall cell performance decreases at high temperature of 60 ^oC.

It is observed in Fig (4.20a) that the OCV of 0.656 V, 0.679 V, 0.683 V and 0.692 V were obtained at temperatures of 30 ^oC, 40 ^oC, 50 ^oC, and 60 ^oC, respectively. The maximum OCV of 0.683 V and maximum power density of 3.90 mW/cm^2 at a current density of 11.17 mA/cm^2 were observed at temperature of 50 ^oC for methanol fuel. Whereas, the maximum power density of 2.59 mW/cm^2 at a current density of 9.06 mA/cm^2, maximum power density of 3.10 mW/cm^2 at a current density of 9.89 mA/cm^2 and maximum power density of 3.53 mW/cm^2 at a current density of 10.50 mA/cm^2 were observed for methanol at the temperature of 30 ^oC, 40 ^oC and 60 ^oC, respectively (Fig 4.20a).

Similarly, it is seen from the Fig (4.20b) that the OCV of 0.73 V, 0.734 V, 0.735 V and 0.737 V were obtained at the temperature of 30 ^{o}C, 40 ^{o}C , 50 ^{o}C, and 60 ^{o}C, respectively. The maximum OCV of 0.735 V and maximum power density of 2.99 mW/cm^2 at a current density of 9.08 mA/cm^2 were obtained at a temperature of 50 ^{o}C for ethanol fuel. However, maximum power density of 1.93 mW/cm^2 at a current density of 8.06 mA/cm^2 , maximum power density of 2.57 mW/cm^2 at a current density of 8.58 mA/cm^2 and maximum power density of 2.77 mW/cm^2 at a current density of 8.79 mA/cm^2 were observed for ethanol at the temperature of 30 ^{o}C 40 ^{o}C and 60 ^{o}C, respectively.

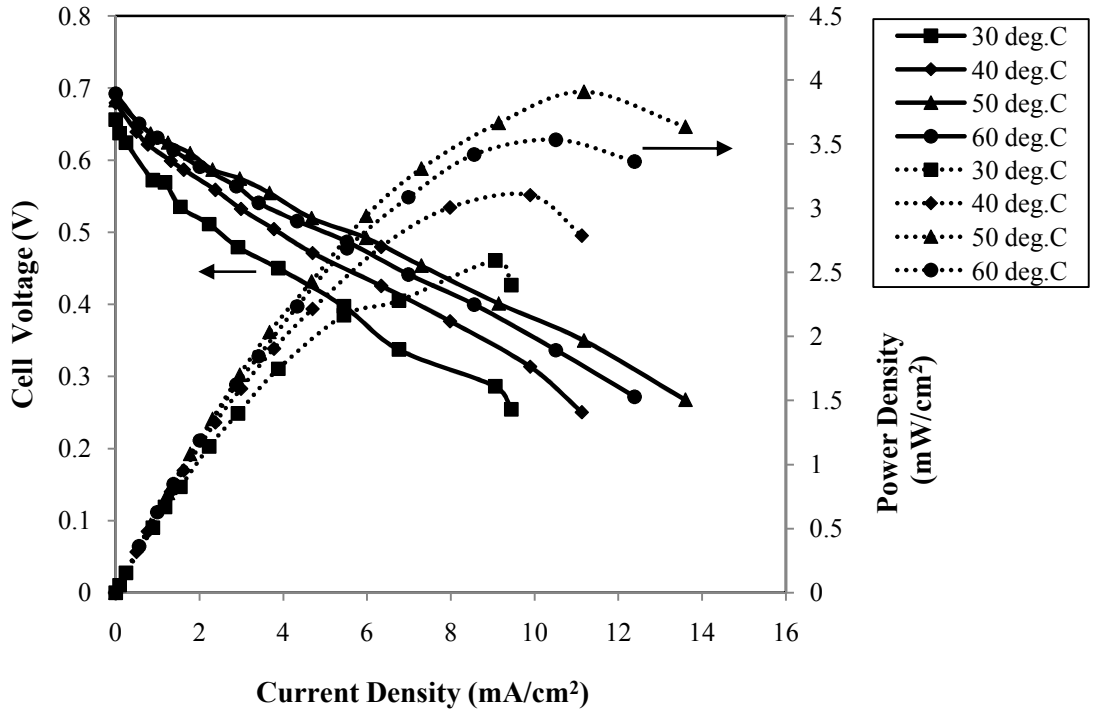

Figure 4.20a Current density vs. cell voltage and current density vs. power density characteristics for 2 M methanol mixed with 6 M KOH at various temperatures; Dotted line -power density curves; Solid line-polarization curves.

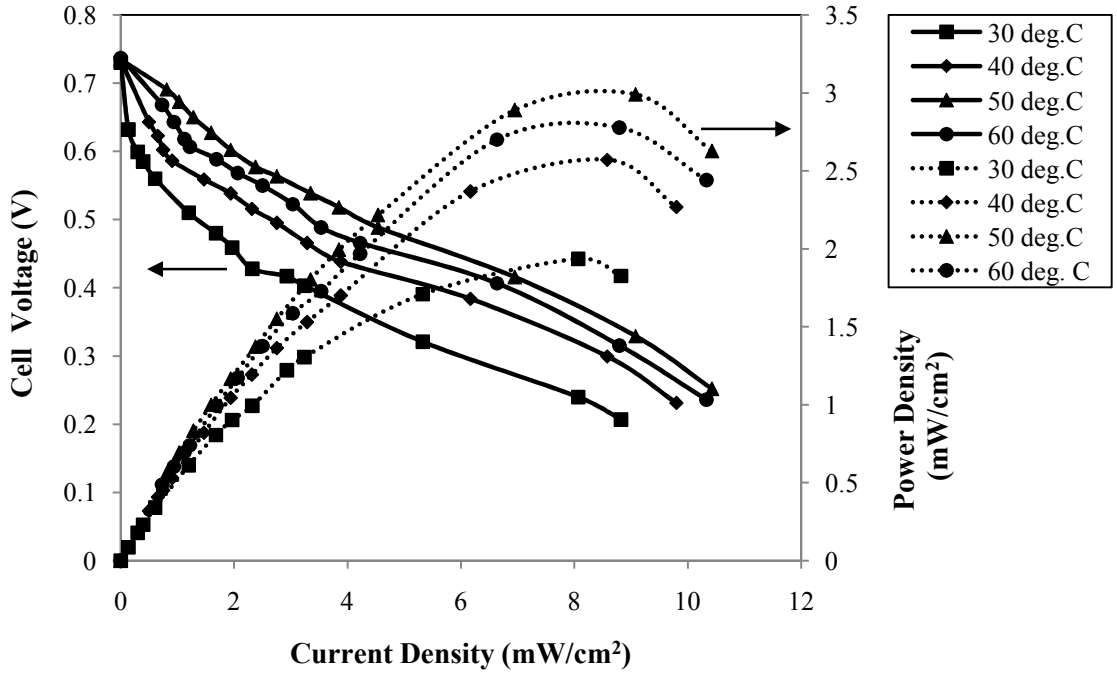

Figure 4.20b Current density vs. cell voltage and current density vs power density characteristics for 2 M ethanol mixed with 1 M KOH at various temperatures; Dotted line -power density curves; Solid line-polarization curves.

4.1.4.8 Effect of oxidant at cathode

Fig (4.21a) and Fig (4.21b) show the polarization curves and power density curves using oxygen and air as oxidant at cathode for methanol and ethanol, respectively. The anode and cathode were made of Pt-Ru/C and Pt/C_{HSA} of 1 mg/cm^2 for both electrodes. The anode feed consisting of 2 M methanol mixed with optimum concentration of 6 M KOH or 2 M ethanol mixed with optimum concentration of 1 M KOH electrolyte was fed at the anode. The operating temperature of DAFC was maintained at 30 ^oC. It is seen in the Fig (4.21a) and Fig (4.21b) that the cell performance using oxygen as oxidant is better than the air as oxidant for methanol (Fig 4.21a) and ethanol (Fig 4.21b) both fuels. The better performance of cell for oxygen as oxidant could be explained using Nernst equation. The Nernst equation shows that the increase in purity or concentration of reactants reduce the voltage loss. Moreover, the electrocatalytic sites are more effectively occupied by oxygen molecules at higher concentration (Larminie and Dicks 2003).

It is observed in the Fig (4.21a) that the maximum OCV of 0.656 V and maximum power density of 2.59 mW/cm^2 at a current density of 9.06 mA/cm^2 were obtained for oxygen as oxidant and methanol as fuel. Whereas, maximum OCV of 0.636 V and maximum power density of 1.92 mW/cm^2 at a current density of 7.36 mA/cm^2 were observed for air as oxidant and methanol as fuel. It is clearly seen that the OCV and current densities are always higher for oxygen as oxidant at cathode.

Similarly, it seen from Fig (4.21b) that the maximum OCV of 0.73 V and maximum power density of 1.93 mW/cm^2 at a current density of 8.06 mA/cm^2 were obtained for oxygen used as oxidant and ethanol as fuel. Whereas, maximum OCV of 0.71 V and maximum power density of 1.4 mW/cm^2 at a current density of 5.73 mA/cm^2 were observed for air used as oxidant and ethanol as fuel.

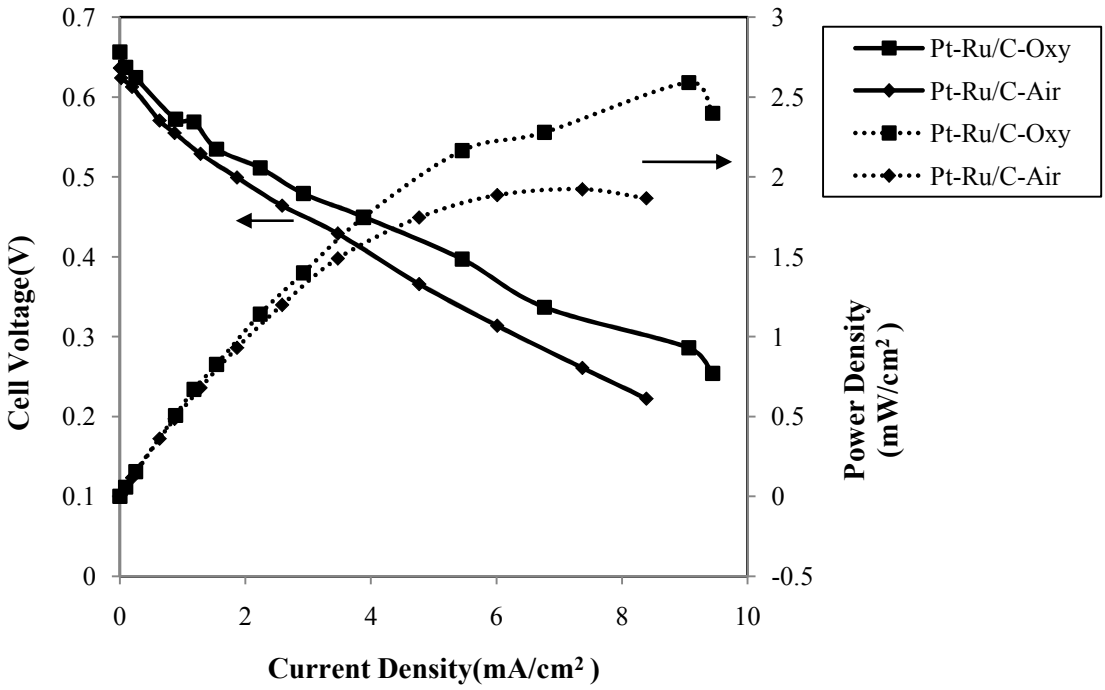

Figure 4.21a Current density versus cell voltage and current density versus power density characteristics using oxygen and air for 2 M methanol mixed with 6 M KOH at a temperature of 30 ^{o}C; Dotted line -power density curves; Solid line-polarization curves.

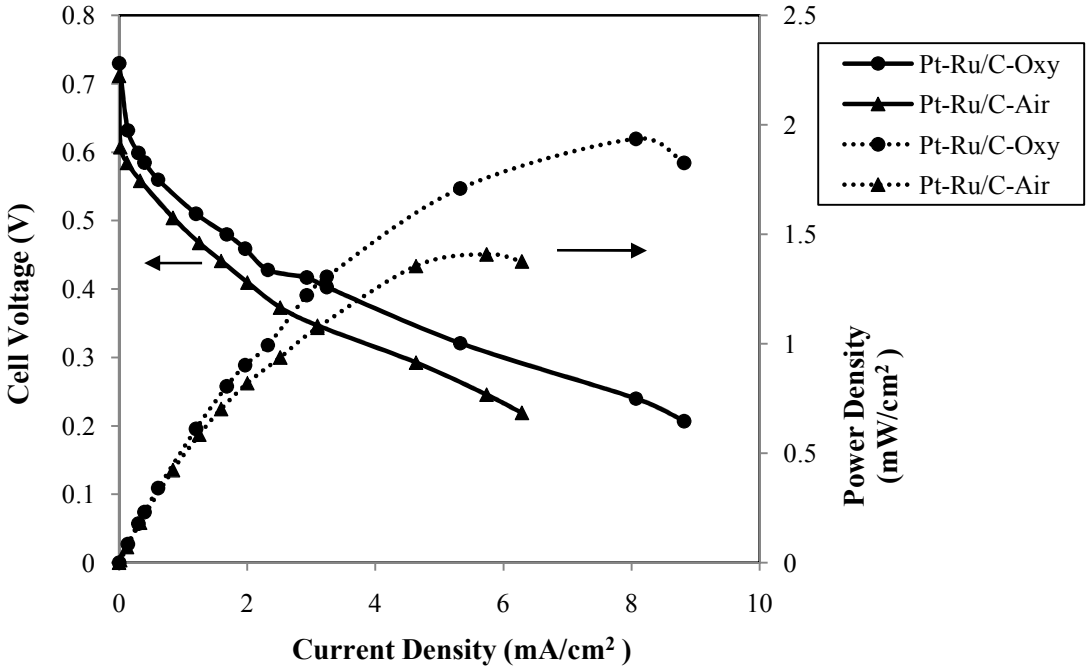

Figure 4.21b Current density versus cell voltage and current density versus power density using characteristics oxygen and air for 2 M ethanol mixed with 1 M KOH at a temperature of 30 ^{o}C; Dotted line -power density curves; Solid line-polarization curves.

4.1.4.9 Effect of membrane types

Fig (4.22a) and Fig (4.22b) show the polarization and power density curves for different membrane types for methanol and ethanol, respectively. The anode and cathode electrocatalysts were Pt-Ru/C and Pt/C_{HSA}, respectively. The fixed electrocatalyst loading of 1 mg/cm^2 was taken at both electrodes. The anode fuel were 2 M methanol (optimum) mixed with 6 M KOH (optimum) and 2 M ethanol (optimum) mixed with 1 M KOH (optimum), respectively. The cell temperature was maintained at 30 ^{o}C. The cathode oxidant used was humidified oxygen. The physical crosslinked PVA membrane resulted in highest cell performance in terms of current density and power density in comparison to the pristine PVA membrane for methanol (Fig 4.22a) and ethanol (Fig 22b) both. The reason may be due to the very low ionic conductivity of pristine PVA membrane (0.89 x

10^{-3} S/cm) in comparison to physical crosslinked PVA membrane (5.6 x 10^{-3} S/cm) as the cell performance is directly related to ionic conductivity (Gupta and Pramanik 2019b).

It is observed in the Fig (4.22a) that the maximum OCV of 0.577 V and 0.656 V were produced for fuel methanol using pristine and physical crosslinked PVA membrane, respectively. Similarly, the OCV of 0.582 V and 0.73 V were obtained for ethanol using pristine and physical crosslinked PVA membrane, respectively (Fig 4.22b). It is clearly seen that the OCV is higher for the physical crosslinked PVA membrane irrespective of fuel used. The maximum power density of 1.39 mW/cm^2 at a current density of 8.8 mA/cm^2 and maximum power density of 2.59 mW/cm^2 at a current density of 9.06 mA/cm^2 were obtained for methanol using pristine and physical crosslinked PVA membrane, respectively (Fig 4.22a). Whereas, the maximum power density of 1.17 mW/cm^2 at a current density of 4.8 mA/cm^2 and maximum power density of 1.93 mW/cm^2 at a current density of 8.06 mA/cm^2 were obtained for ethanol using pristine and physical crosslinked PVA membrane, respectively (Fig 4.22b).

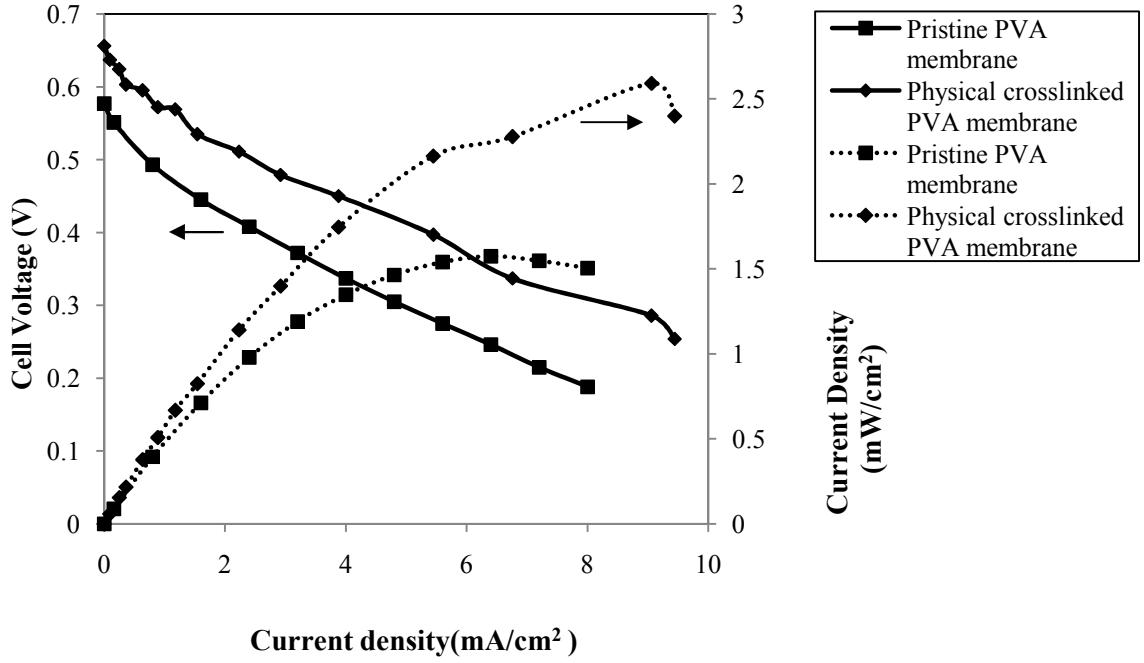

Figure 4.22a Current density vs. cell voltage and current density vs. power density characteristics for pristine and physical crosslinked PVA membrane using 2 M methanol mixed with 6 M KOH at a temperature of 30 ^{o}C; Dotted line-power density curves; Solid line-polarization curves.

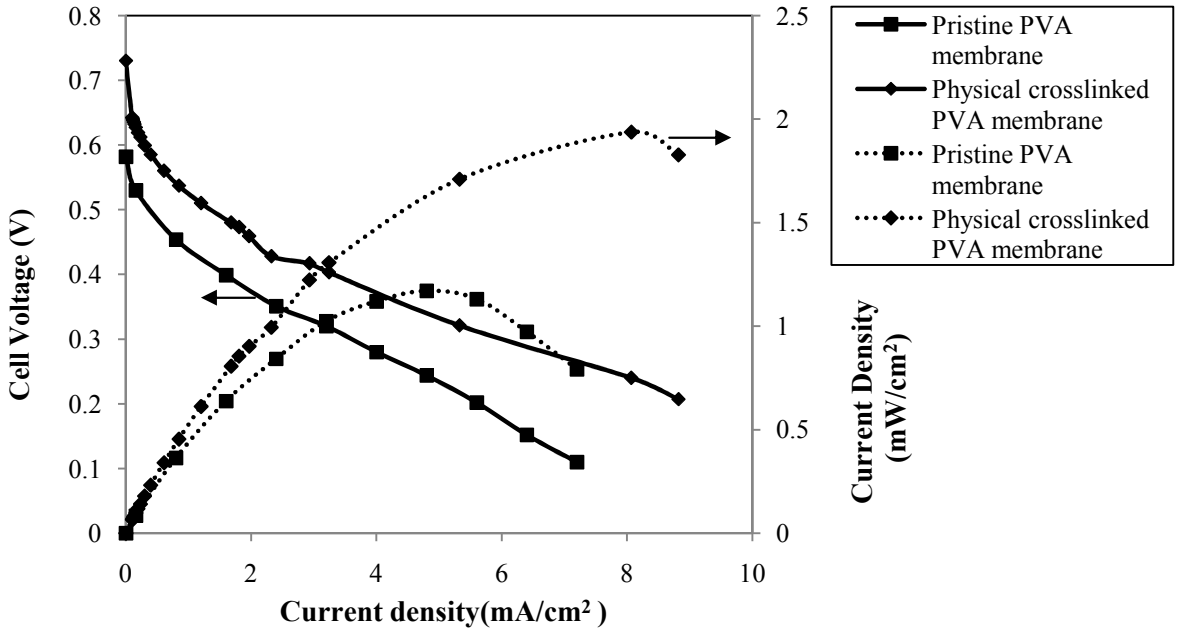

Figure 4.22b Current density vs. cell voltage and current density vs. power density characteristics for pristine and physical crosslinked PVA membrane using 2 M ethanol mixed with 1 M KOH at a temperature of 30 ^{o}C; Dotted line-power density curves; Solid line-polarization curves.

4.1.4.10 Effect of methanol and ethanol fuel mixture

Fig (4.23) shows the electrooxidation of methanol and ethanol mixture of various molar ratios. The anode and cathode were made of Pt-Ru/C and Pt/C_{HSA} of optimum loading (1 mg/cm^2) for both electrodes. The humidified oxygen was used as oxidant at the cathode. The electrolyte was physical crosslinked PVA membrane doped with 6 M KOH. Fig (4.23) shows that the polarization and power density curves shifted upwards with the increase in methanol to ethanol molar ratio for 1:1 to 1:3. However, further increase in molar ratio to 1:4 the current density decreases. The maximum OCV of 0.64 V and maximum power density of 1.14 mW/cm^2 at a current density of 4.31 mA/cm^2 was obtained for the molar ratio of 1:3.

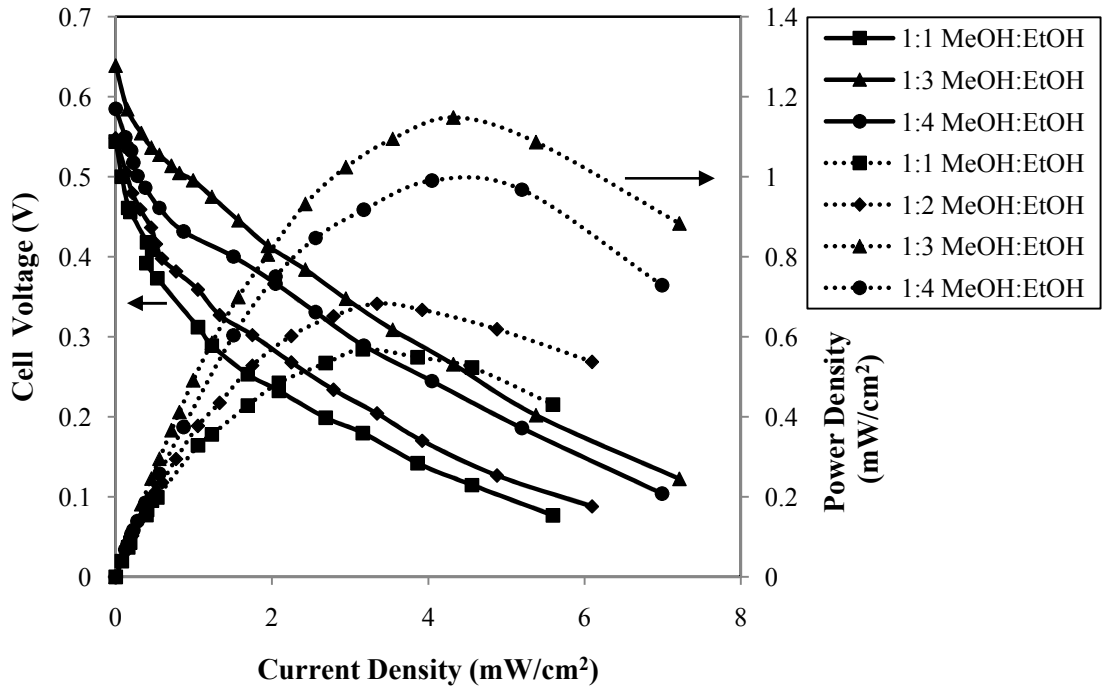

Figure 4.23 Current density vs. cell voltage and current density vs. power density characteristics for different molar ratios of methanol to ethanol using O_2 as oxidant at a temperature of 30 ^oC; MeOH-Methanol, EtOH-Ethanol; Dotted line-power density curves; Solid line-polarization curves.

It is obvious that the maximum current density of the mixture is lower than the pure solutions of methanol and ethanol as discussed earlier (Fig 4.15a and Fig 4.15b, page no. 103-104) and it has already been discussed in the CV study (page no. 95). As explained

by Morin et.al, the molecular structure of electroactive species has a great influence on its electro activity particularly on a platinum based electrode (Morin et al., 1990). As per anode reaction (Equation (2.5) (page no. 21)), the presence of OH^- ions are very much essential for completion of anode reactions and release of electrons. The increase in ethanol concentration in the mixture beyond the optimum ratio of methanol to ethanol (1:3), the electrocatalyst occupied by the OH^- ions is replaced by the ethanol molecules. Thus, the electrooxidation reaction of ethanol molecule gets inhibited due to lack of OH^- ions at the electrocatalyst sites, which resulting in lower peak current density (Gupta and Pramanik 2019a, Wongyao et al., 2011 and Leo et al., 2013)." Thus, the peak current density for the fuel mixture beyond (1: 3) decreases.

4.1.4.11 Stability test

Stability test is very important for studying the long term performance of the developed fuel cell. The Fig (4.24) shows the stability test data performed for 15 h at a constant load. Table (4.3) also shows the variation of operating cell potential (OCP) with time at a constant load. The anode and cathode were made of Pt-Ru/C and Pt/C_{HSA} of optimum loading (1 mg/cm^2) for both electrodes. The humidified oxygen was used as oxidant at the cathode. The electrolyte was physical crosslinked PVA membrane doped with 6 M KOH. The physical crosslinked membrane showed a significant decreasing trend for ethanol or methanol or their mixture. The OCP deteriorated from 0.513 V to 0.267 V for methanol, 0.540 V to 0.310 V for ethanol and 0.484 V to 0.218 V for their mixture after 15 hrs of DAFC operation. The considerable decrease in OCP may due to poor crosslinking by physical crosslinking method.

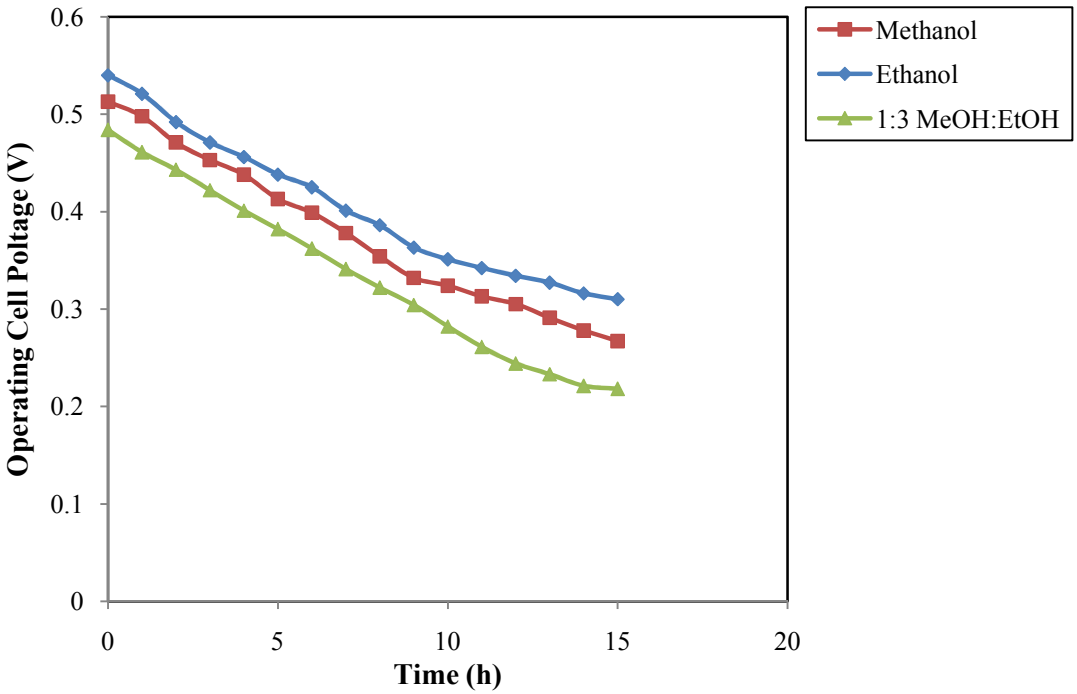

Figure 4.24 Stability test of the DAFC using methanol or ethanol or their mixture as fuel at constant load at a temperature of 30 ^{o}C; MeOH-Methanol, EtOH-Ethanol;

Table 4.3 Variation of operating cell potential with time at a constant load.

Fuel	**Operating Time (h)**	**Operating Cell Potential (V)**
Methanol	0	0.513
	5	0.413
	10	0.324
	15	0.267
Ethanol	0	0.540
	5	0.438
	10	0.351
	15	0.310
MeOH: EtOH (1:3)	0	0.484
	5	0.382
	10	0.282
	15	0.218

4.2 Performance of alkaline membrane synthesized by chemical crosslinking: Part II

4.2.1 Membrane characterization

The chemical crosslinked PVA membranes of approximately 180 ± 10 μm uniform thickness were obtained at the end of the process as described in section 3.3.1 (page no.57) The obtained membranes were clear and homogenous, with a good mechanical flexibility. The important properties and indicators of the synthesized chemical crosslinked PVA membrane like water uptake (W_U), KOH uptake (Q_U), ionic conductivity, high resolution scanning electron microscopy/energy dispersive X-ray spectroscopy (HR-SEM/EDX), fourier transform infrared spectroscopy (FTIR), X-ray diffraction (XRD) and mechanical testing are discussed below in detail.

4.2.1.1 Water uptake

The presence of water molecule within the membrane structure is very much essential for the use of PVA membrane in fuel cell as already discussed in **Part I** (page no. 68). The values for water uptake and KOH uptake of the membranes crosslinked by different concentrations of GA were evaluated after immersing in 0 M KOH/water and KOH solution of different concentration which are shown in Table (4.4). The amount of crosslinking agent effect the water uptake and KOH uptake both. The water uptake for 1 wt %, 2 wt %, 2.5 wt % and 3 wt % glutaraldehyde (GA) crosslinked membrane immersed in 0 M KOH/water were 60.2 wt %, 41.1 wt %, 29.3 wt % and 15.4 wt %, respectively. The recorded water uptake of the pristine membrane and physical crosslinked membrane for the same condition were 131.8 wt % and 70 wt %, respectively. The water uptake of pristine and physical crosslinked PVA membranes were more than double as compared to the glutaraldehyde crosslinked membrane. Moreover, it is observed from Table (4.4) that the water uptake of the PVA membrane decreases with

Table 4.4 Water uptake (W_U) and KOH uptake (Q_U) of pristine and chemical crosslinked PVA membrane with different glutaraldehyde concentration as a function of KOH concentration at a temperature of 30 ^oC.

Membrane Types	GA Concentration (wt %)	0 M KOH		4 M KOH		5 M KOH		6 M KOH		7 M KOH		8 M KOH	
		W_U (wt %)	Q_U (wt %)	W_U (wt %)	Q_U (wt %)	W_U (wt %)	Q_U (wt %)	W_U (wt %)	Q_U (wt %)	W_U (wt %)	Q_U (wt %)	W_U (wt %)	Q_U (wt %)
Pristine PVA	0	131.8 ± 3.8	0	51.5 ± 2.4	23.1 ± 2.1	39.2 ± 2.4	29.1 ± 2.2	33.0 ± 2.6	37.8 ± 2.1	29.5 ± 1.9	33.7 ± 2.4	25.6 ± 2.3	31.6 ± 1.7
Crosslinked PVA	1	60.2 ± 3.4	0	45.7 ± 2.3	25.4 ± 2.3	40.6 ± 2.5	31.8 ± 2.1	39.9 ± 2.5	38.3 ± 2.2	35.5 ± 1.9	34.1 ± 2.6	32.6 ± 2.4	32.9 ± 1.7
Crosslinked PVA	2	41.1 ± 3.2	0	35.9 ± 2.3	29.0 ± 2.5	28.2 ± 2.4	35.3 ± 2.1	24.7 ± 2.3	46.3 ± 2.3	21.3 ± 1.8	42.9 ± 2.3	19.3 ± 2.4	37.4 ± 1.9
Crosslinked PVA	2.5	29.3 ± 3.1	0	19.1 ± 2.3	29.1 ± 2.5	17.6 ± 2.1	41.6 ± 2.7	14.5 ± 2.2	**59.4** ± 2.7	13.7 ± 1.9	51.1 ± 2.1	12.5 ± 2.5	55.2 ± 2.0
Crosslinked PVA	3	15.4 ± 2.6	0	19.0 ± 2.2	27.5 ± 2.1	17.3 ± 2.5	38.9 ± 2.3	15.7 ± 2.3	50.8 ± 2.3	14.5 ± 1.9	47.7 ± 2.1	12.7 ± 2.6	42.4 ± 2.3

the increase in GA concentration when immersed in 0 M KOH/water. This decreased trend may be due to the presence of the GA crosslinker (Gupta and Pramanik 2019b). The crosslinker GA increases the interactions of the polymer chains in the matrix which hinders expansion of the polymer network. Thus, chain mobility is hindered and a reduction in void volume occurs resulting in low water uptake in comparison to pristine PVA membrane (Zhou et al., 2010 and Tripathi et al., 2010). It is also seen from the Table (4.4), the water uptake decreases with increase in KOH concentration up to 8 M irrespective of membrane types. The crosslinked membrane with 1 wt % GA results in water uptake of 60.2 wt %, 45.7 wt %, 40.6 wt %, 39.9 wt %, 35.5 wt % and 32.6 wt % when immersed in 0 M KOH/ water, 4 M, 5 M, 6 M, 7 M and 8 M, respectively. Similar trend of water uptake was found for other types of membrane also (Table 4.4) It may be due to the increase in solution viscosity at higher concentration of KOH and decrease in water molecules in the solution at higher KOH concentration (Gupta and Pramanik 2019b, Merle et al., 2012 and An et al., 2012).

As discussed earlier with the increase in KOH concentration similar effect was also observed in case of the pristine and physical crosslinked PVA membrane (page no. 70). It should be noted that higher water uptake results in too much swelling of the membrane and a loss in mechanical strength. However, membranes may become brittle with low levels of water uptake (Merle et al., 2012). Thus, PVA membrane crosslinked with 2.5 wt % of GA could give better results in terms of KOH uptake and ionic conductivity as it contains a moderate amount of water uptake i.e., 29.3 wt % which is in between too high (60.2 wt %) and too low (15.4 wt %) water uptake.

4.2.1.2 KOH uptake

The values for KOH uptake as a function of KOH concentration is shown in Table (4.4). It is clearly seen in the Table (4.4) that the KOH uptake is low for the pristine PVA membrane as compared to that of the crosslinked PVA membrane. It may be concluded from Table (4.4) that with the increase in KOH concentration up to 6 M, the KOH uptake of pristine and chemical crosslinked PVA membrane increases irrespective of GA crosslinker concentration. However, with the increase in KOH concentration beyond 6 M, a decrease in KOH uptake is observed. The highest KOH uptake of 59.4 wt % was found for the PVA membrane crosslinked with 2.5 wt % GA when doped with 6 M KOH solution. Whereas, the KOH uptake of GA crosslinked membrane decreased to 51.1 wt % with the further increase in KOH concentration to 7 M. The KOH uptake for the same membrane doped with 4 M and 5 M KOH concentrations were 29.2 wt % and 41.6 wt %, respectively. Similarly, the maximum KOH uptake of 37.8 wt % was obtained for pristine PVA membrane doped with 6 M KOH solution. Whereas, the KOH uptake values of 23.1 wt %, 29.1 wt % and 33.7 wt % were found for the pristine membrane doped with KOH concentration of 4 M, 5 M and 7 M, respectively. Initial increase in KOH uptake is due to the increase in KOH concentration. However, with the subsequent increase in KOH concentration, the ionic mobility decreases due to increased solution viscosity. Due to this, additional ions could not be taken into the polymer matrix (Fu et al., 2010 and An et al., 2012). Thus, the maximum amount of KOH uptake is observed for PVA membrane doped with 6 M KOH concentration as the membrane gets saturated at this concentration (Table 4.4).

It is also observed from Table (4.4) that the KOH uptake increases with GA crosslinker concentration up to 2.5 wt % irrespective of KOH doping concentration. However, the KOH uptake decreases at 3 wt % GA concentration. It may be due to the water molecule

entrapped in the GA crosslinked membrane do not allow further water to enter, however they may permit the entry of KOH molecule due to concentration difference. With the increase in GA concentration up to 2.5 wt % the pores increase and thus, the KOH uptake increase. However, with higher GA concentration (3 wt %) the pores may collapse and cause a reduction in KOH uptake (Rudra et al., 2015).

4.2.1.3 Ionic conductivity

The membrane samples for ionic conductivity measurement were prepared in similar way as that of adopted in KOH uptake. Fig (4.25a) to Fig (4.25d) show the electrochemical impedance spectra (EIS) for the PVA membrane crosslinked with 1 wt % , 2 wt % , 2.5 wt % and 3 wt % GA doped with 4 M, 5 M, 6 M, 7 M and 8 M KOH solution, respectively. The EIS of pristine membrane has already been reported in **Part I** (page no. 72).

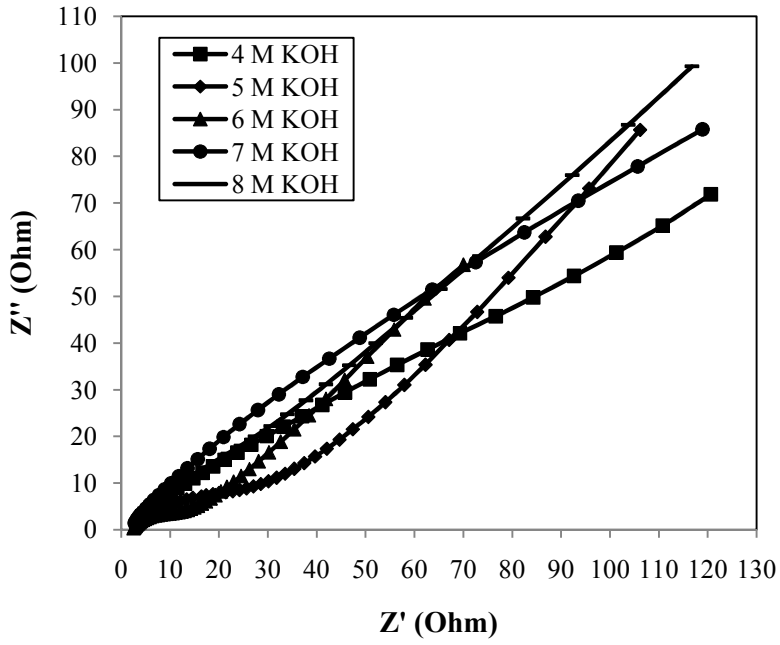

Figure 4.25a Electrochemical impedance spectra (EIS), for PVA membrane crosslinked with 1 wt % GA and doped with various molar KOH solution at a temperature of 30 ^{o}C.

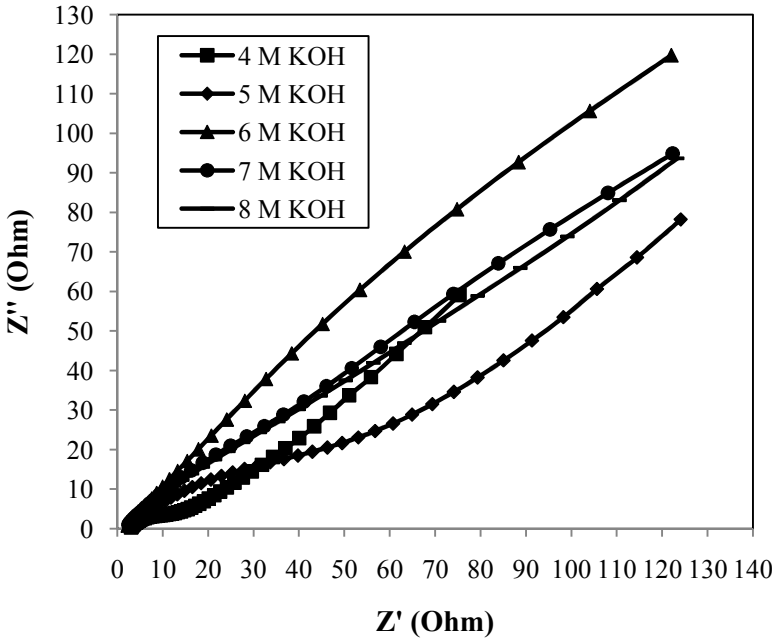

Figure 4.25b Electrochemical impedance spectra (EIS), for PVA membrane crosslinked with 2 wt % GA and doped with various molar KOH solution at a temperature of 30 ^{o}C.

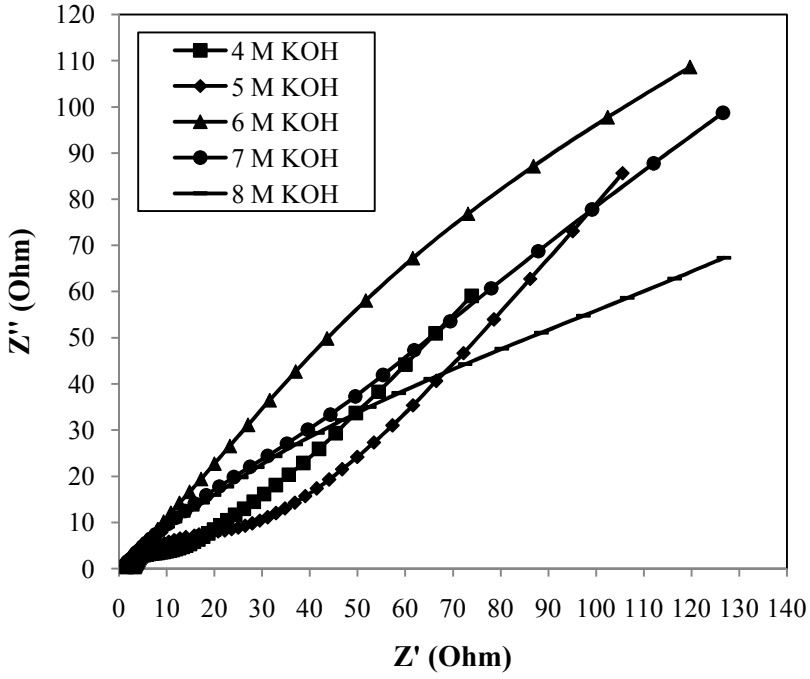

Figure 4.25c Electrochemical impedance spectra (EIS), for PVA membrane crosslinked with 2.5 wt % GA and doped with various molar KOH solution at a temperature of 30 ^{o}C.

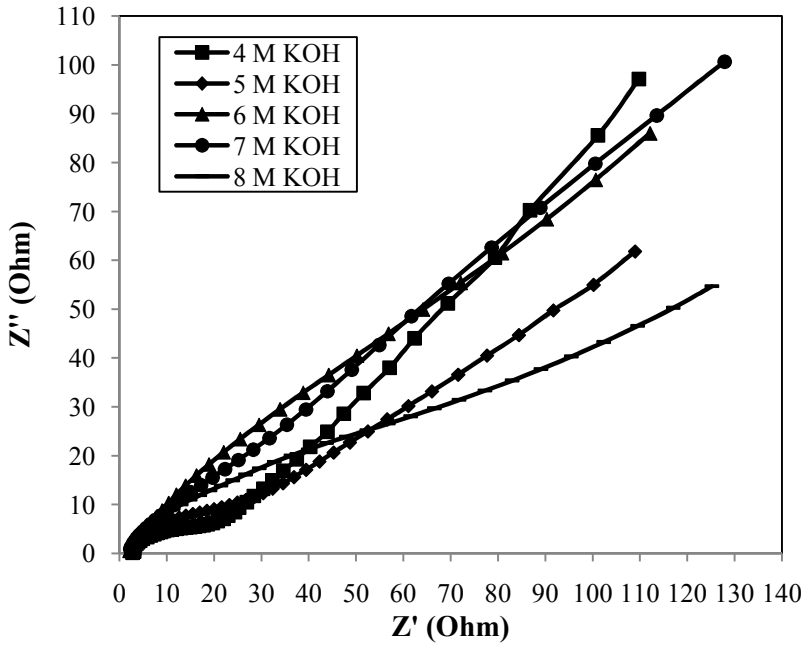

Figure 4.25d Electrochemical impedance spectra (EIS), for PVA membrane crosslinked with 3 wt % GA and doped with various molar KOH solution at a temperature of 30 ^{o}C.

The ionic conductivity of pristine and chemical crosslinked PVA membrane is shown in Table (4.5). A good correlation is observed between ionic conductivity and KOH uptake of the PVA membranes as seen from Table (4.4) and Table (4.5). The ionic conductivity increases with the increase in KOH concentrations up to 6 M and further increase in concentration beyond 6 M it decreases, irrespective of glutaraldehyde crosslinker concentration. The ionic conductivity of pristine also follows a similar trend as discussed in **Part I** (page no. 72). The maximum ionic conductivity of 9×10^{-3} S/cm was obtained for 6 M of KOH crosslinked with 2.5 wt % GA. However, ionic conductivity for 7 M of KOH doping was 8.5×10^{-3} S/cm which is lower than that of membrane doped with 6 M KOH. The ionic conductivity of the same membrane doped with 4 M and 5 M KOH were 7×10^{-3} S/cm and 8×10^{-3} S/cm, respectively. There is a decrease in ionic mobility and increase in solution viscosity at higher KOH concentration which results in decreased ionic conductivity (An et al., 2012 and Fu et al., 2010).

Table 4.5 Ionic conductivity of chemical crosslinked PVA membrane with different glutaraldehyde concentration as a function of KOH concentration at a temperature of 30 ^{o}C.

Membrane Types	**Glutaraldehyde (GA) Concentration (wt %)**	**Ionic Conductivity (x 10^{-3} S/cm)**				
		4 M KOH	**5 M KOH**	**6 M KOH**	**7 M KOH**	**8 M KOH**
Pristine PVA	0	0.42 ± 0.02	0.46 ± 0.03	0.89 ± 0.04	0.58 ± 0.02	0.51 ±0.02
Crosslinked PVA	1	5 ± 0.6	6 ± 0.5	7 ± 0.5	6.5 ± 0.5	6 ± 0.5
Crosslinked PVA	2	6 ± 0.5	7 ± 0.5	8 ± 0.6	7.5 ± 0.6	7 ± 0.5
Crosslinked PVA	**2.5**	7 ± 0.4	8 ± 0.4	**9** ± 0.5	8.5 ± 0.5	8 ± 0.5
Crosslinked PVA	3	6.5 ± 0.5	7.5 ± 0.4	8.5 ± 0.6	8 ± 0.5	7 ±0.49

Similarly, the maximum ionic conductivity of 0.89 × 10^{-3} S/cm was observed for pristine PVA membrane doped with 6 M KOH solution. Although the KOH uptake of the pristine PVA membrane is high at optimum concentration of KOH doping (6 M), the ionic conductivity is very low (0.89 x 10^{-3} S/cm) than the 2.5 wt % GA crosslinked PVA membrane (9 x 10^{-3} S/cm) and physical crosslinked membrane (5.6 x 10^{-3} S/cm). The reason has already been explained in the section 4.1.1.3 (page no. 71). It may be due to the high crystallinity of pristine PVA membrane. The high crystalline nature increases the energy barrier for ion movement and thereby impedes the ion transport (Hema et al., 2009).

Table (4.4) and Table (4.5) show a consistent trend for KOH uptake and ionic conductivity increase up to KOH concentration of 6 M and water uptake and KOH uptake decreases beyond KOH concentration of 6 M. It may be attributed to the high viscosity of KOH solution at higher concentration resulting in low KOH uptake and low

conductivity (An et al., 2012). It is concluded that 6 M KOH is the optimum doping concentration giving a superior quality membrane with highest conductivity which could be used in a DAFC single cell set up for maximum power output.

4.2.1.4 Morphology

The surface morphology of five synthesized membranes viz. the pristine PVA, PVA crosslinked with 1 wt %, 2 wt %, 2.5 wt % and 3 wt % GA, and PVA crosslinked with optimum GA (2.5 wt %), doped with optimum 6 M KOH at the uniform SEM resolution of 500 nm are shown in Fig (4.26a), Fig (4.26b), Fig (4.26c), Fig (4.26d) and Fig (4.26e), respectively. The cross sectional SEM morphology of PVA crosslinked with 2.5 wt % GA (Fig 4.26f) and PVA crosslinked with 2.5 wt % GA doped with 6 M KOH (Fig 4.26g) along with their EDX elemental composition were also investigated. It is seen from Fig (4.26a), pristine PVA membrane consisting of larger cracks which are uniformly distributed over the pristine membrane. Whereas, little hair line cracks are observed with rough surface morphology in the polymer matrix of crosslinked PVA membranes (Fig 4.26b to Fig 4.26d). The membrane surface becomes compact and dense as the crosslinker concentration increases thus, preventing the leaching of KOH out of the membrane. The SEM image of cross-sectional plane for 2.5 wt % GA crosslinked PVA membrane without KOH doping shows uniform pores distribution throughout the cross-sectional plane (Fig 4.26f). The EDX analysis in Fig 4.26f shows the peak of oxygen and carbon showing the characteristics constituents of PVA. When the chemical crosslinked PVA membrane (2.5 wt % GA) is doped with 6 M KOH, the surface roughness of the cast membrane increased drastically with uniform distribution of prominent pores on the surface (Fig 4.26e) and cross-sectional plane of the same membrane shows spike like structures of adsorbed KOH within the membrane matrix (Fig 4.26g). It helps to keep the membrane conductivity consistent during DAFC operations. In the Fig 4.26g additional

peak of potassium (K) is observed indicating incorporation of KOH in the membrane matrix. The presence of Au peak in the EDX image is due to the sputtering of PVA membranes with Au particles.

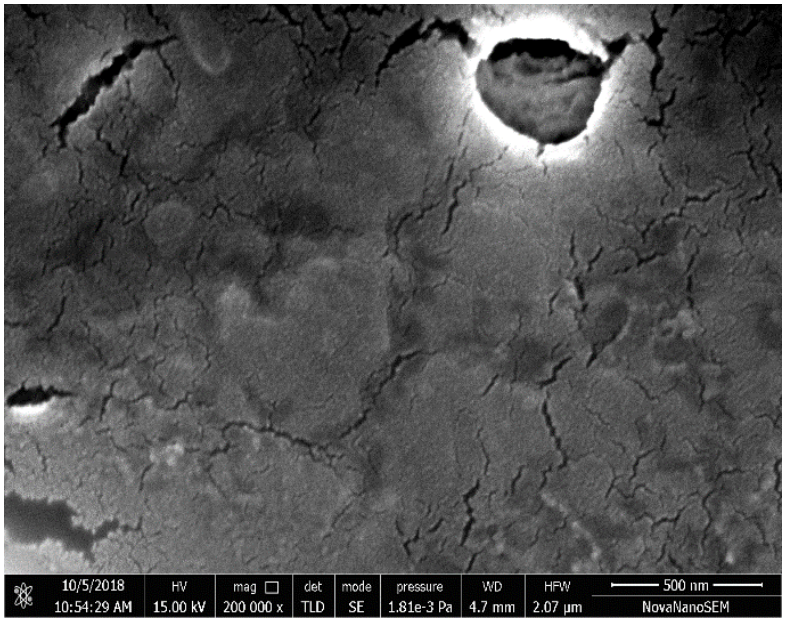

Figure 4.26a SEM image of the surface of pristine PVA.

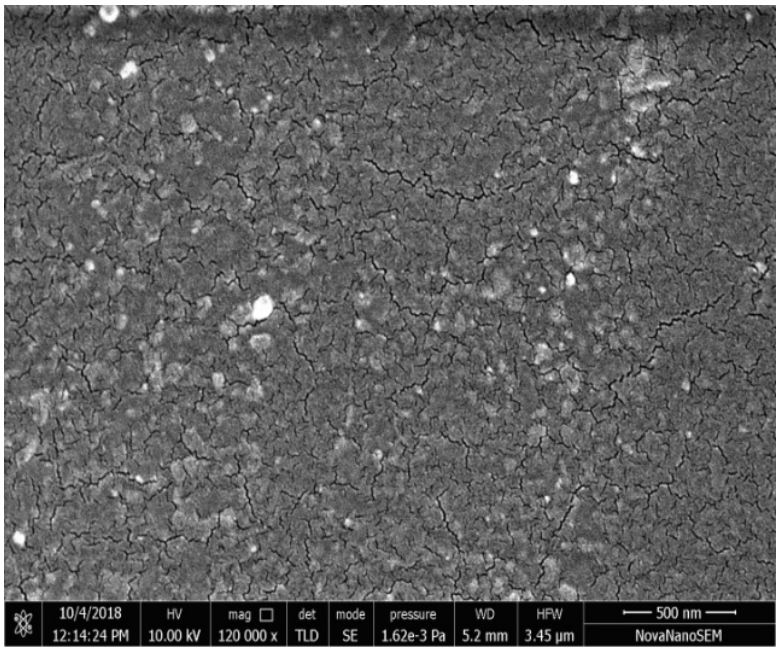

Figure 4.26b SEM image of the surface of crosslinked with 2 wt % GA PVA membrane

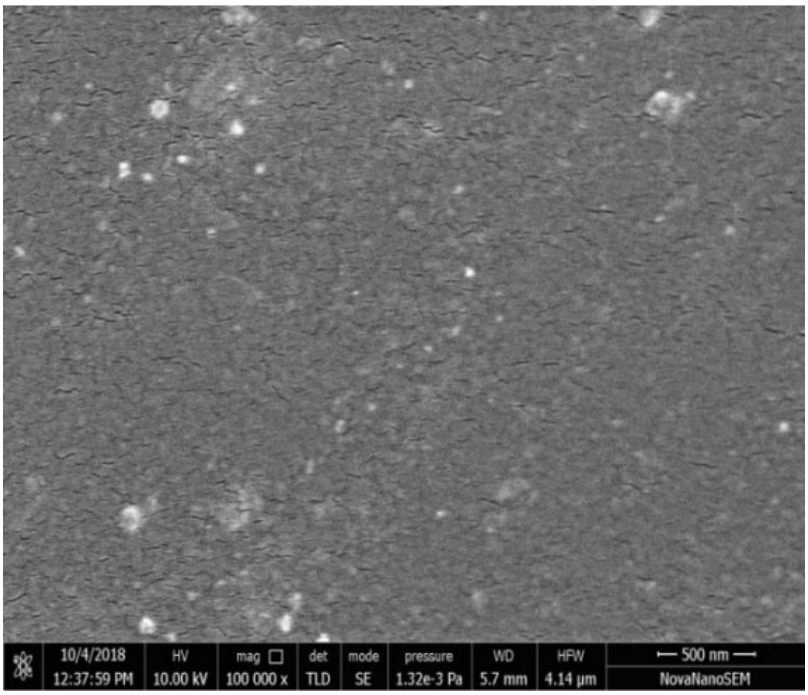

Figure 4.26c SEM images of the surface of crosslinked with 2.5 wt % GA PVA membrane.

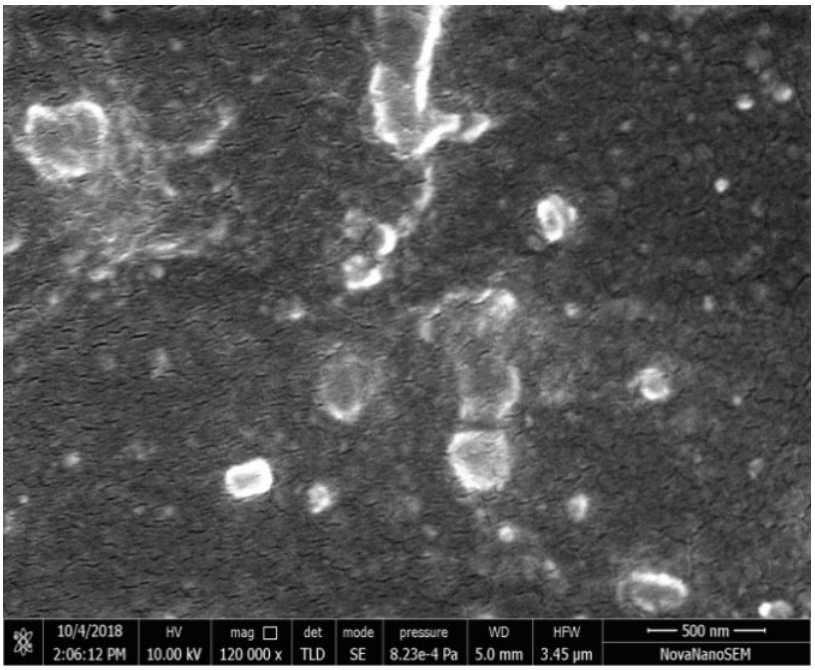

Figure 4.26d SEM images of the surface of crosslinked with 3 wt % GA PVA membrane.

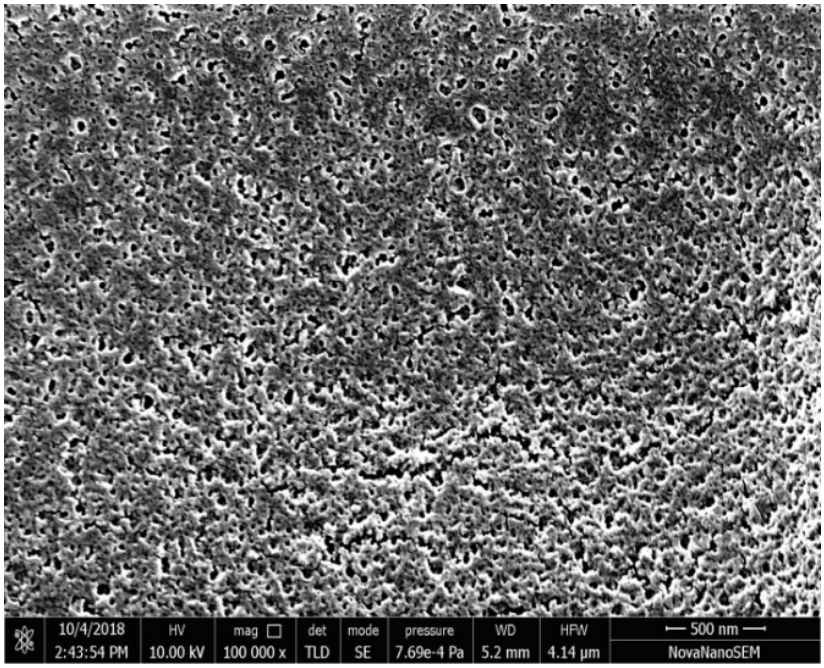

Figure 4.26e SEM images of the surface of crosslinked with 2.5 wt % GA, doped with 6 M KOH PVA membrane.

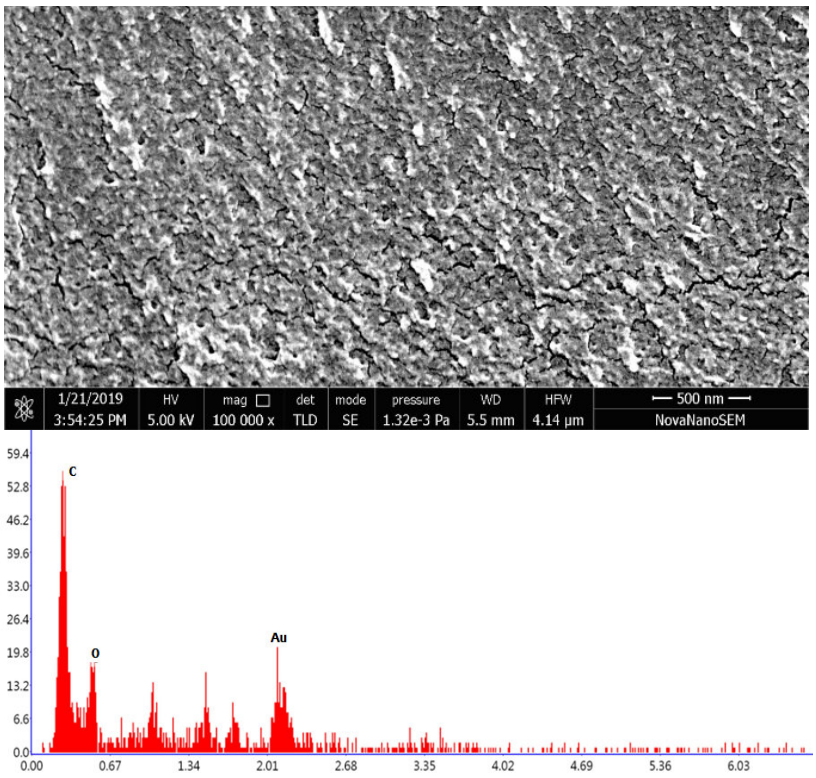

Figure 4.26f SEM-EDX image of cross section of PVA membrane crosslinked with 2.5 wt % GA without KOH.

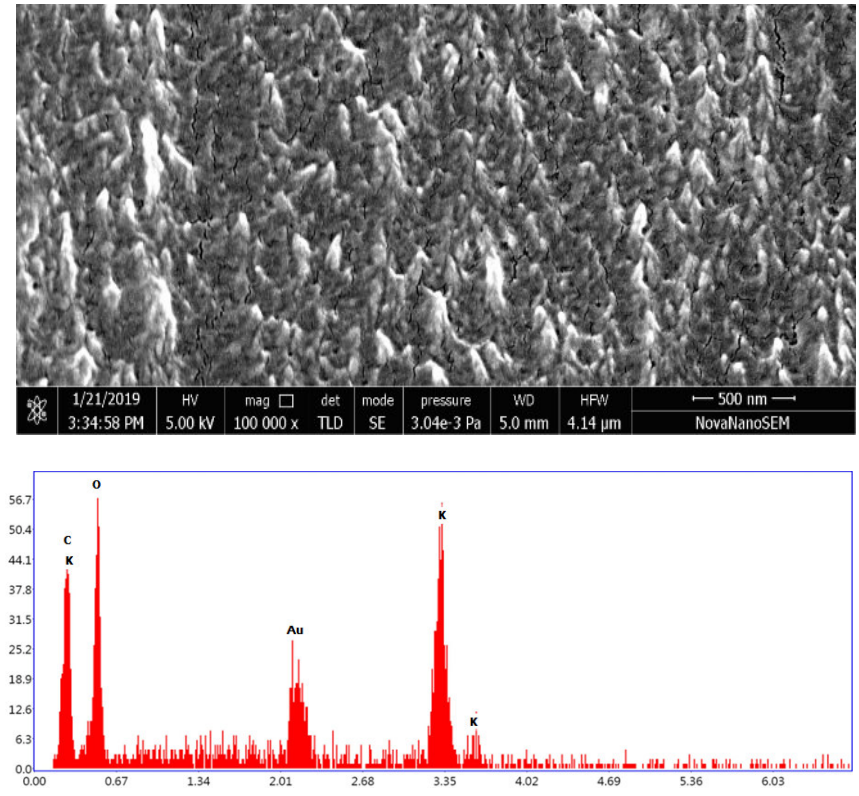

Figure 4.26g SEM-EDX image of cross section of PVA membrane crosslinked with 2.5 wt % GA, doped with 6 M KOH.

4.2.1.5 Crystal structure

The X-ray diffraction (XRD) analysis was performed to examine the crystallinity of the chemical crosslinked PVA polymer membrane. Fig (4.27) shows the diffraction pattern of the pristine PVA membrane, PVA membranes crosslinking with GA concentration of 2 wt %, 2.5 wt % and 3 wt %, without any KOH doping and PVA membrane crosslinking with GA 2.5 wt % doped with optimum 6 M KOH. It is well known that the PVA polymer exhibits a semi-crystalline structure with a large peak at a 2θ angle of 19^{o}–20^{o} (101) and a small peak of 39^{o}–40^{o} (111) (Wu et al., 2008, Herranz et al., 2018, Merle et al., 2012 and Fu et al., 2010).

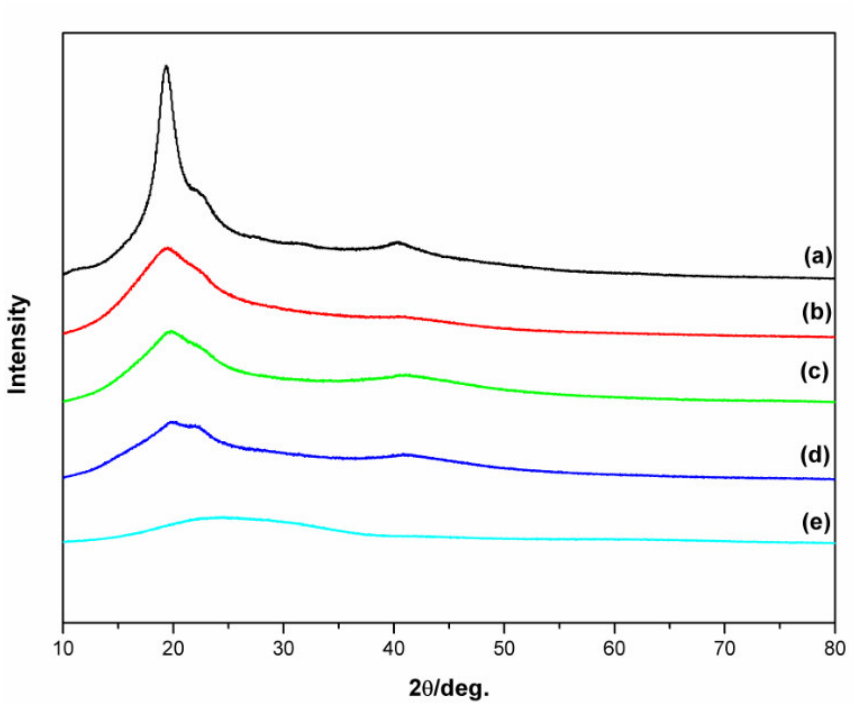

Figure 4.27 XRD spectra of the (a) pristine PVA membrane (b) 2 wt % GA crosslinked PVA membrane (c) 2.5 wt % GA crosslinked PVA membrane (d) 2.5 wt % GA crosslinked, 6 M KOH doped PVA membrane and (e) 3 wt % GA crosslinked PVA membrane.

It is clearly seen in the Fig 4.27 that a large peak appears at 2θ of 20^{o} for the pristine PVA membrane. However, the peak intensity for the glutaraldehyde crosslinked PVA membrane gradually reduced with the increase in concentration of glutaraldehyde concentration. It may be due to the decline in crystallinity and at very high concentration of glutaraldehyde (3 wt %), PVA membrane becomes brittle (Rudra et al., 2015). Moreover, the peak intensity at 2θ of 20^{o} for the 2.5 wt % GA crosslinked PVA membrane doped with 6 M KOH further reduced. It may be due to the plasticizing effect of KOH molecules. The KOH molecules entangle the PVA polymer chains and thus reduce the crystalline domain as explained in **Part I** (page no. 77) (Hirankumar and Mehta 2018).

4.2.1.6 Functional groups

Functional groups of the PVA based membranes were evaluated by FTIR analysis. Fig 4.28 shows the FTIR of the pristine PVA membrane, PVA membranes that were prepared by chemical crosslinking with GA concentration of 2 wt %, 2.5 wt % and 3 wt %, without any KOH doping and PVA membrane prepared by crosslinking with GA 2.5 wt % doped with optimum KOH concentration of 6 M. In the Fig 4.28, the absorption peaks of different PVA membranes are observed at different wave length spectra like –OH stretching of the bound water at about 3228-3431 cm^{-1} (region-i), CH stretching at about 2858- 2984 cm^{-1} (region-ii) and at about 1659-1665 cm^{-1} (region-iii) and 1433-1445 cm^{-1} (region-iv) for the –C–O group. The band at 1096-1105 cm^{-1} (region-v) is due to deformation vibration of the absorbed water molecules.

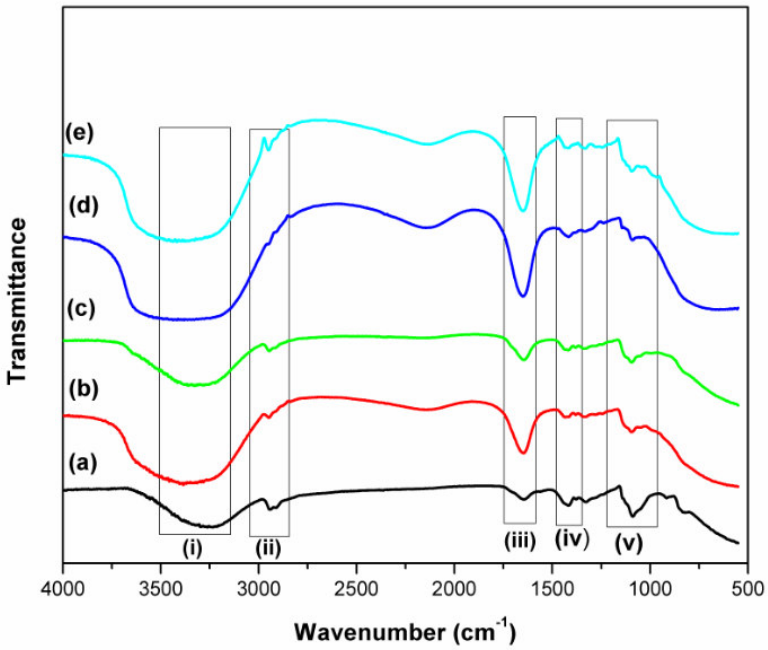

Figure 4.28 FTIR spectrum of the (a) pristine PVA membrane (b) 2 wt % GA crosslinked PVA membrane (c) 2.5 wt % GA crosslinked PVA membrane (d) 2.5 wt % GA crosslinked, 6 M KOH doped PVA membrane and (e) 3 wt % GA crosslinked PVA membrane.

4.2.1.7 Mechanical property

The PVA membrane crosslinked with 2.5 wt % glutaraldehyde showed excellent electrolytic properties like water uptake, KOH uptake and ionic conductivity etc. performance in single cell. Thus, mechanical stability of the pristine PVA and crosslinked PVA with (2.5 wt % GA) membranes were tested and compared. The stress-strain curve of pristine and crosslinked PVA membrane (2.5 wt % GA) are shown in Fig (4.29). The stress-strain curves demonstrate that the crosslinking of PVA with 2.5 wt % glutaraldehyde enhances the mechanical properties of the membrane. The crosslinked PVA membrane (2.5 wt % GA) exhibits a tensile stress of 44 MPa which is higher than that of pristine PVA membrane (37 MPa). It may be due to the more ordered structure of the 2.5 wt % GA crosslinked PVA membrane (Rudra et al., 2015).

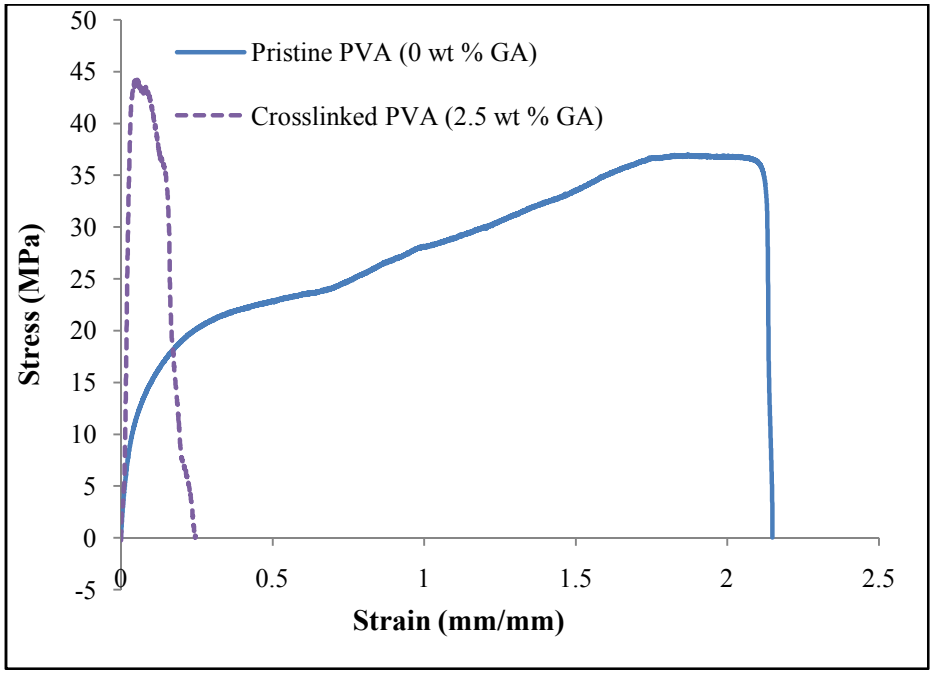

Figure 4.29 The stress-strain curves of pristine PVA membrane and the crosslinked PVA membrane (2.5 wt % GA).

4.2.2 Electrode characterization

The electrode characterization mainly surface morphology by SEM and half cell studies have already been discussed in **Part I** (page no. 80-99). To avoid repetition, the above studies are not presented here in this section.

4.2.3 Single cell studies

The experimental results on direct alcohol fuel cell are presented below. Oxygen was used as oxidant unless it is mentioned specifically about another oxidant (atmospheric air). The direct alcohol fuel cell experiments were performed to determine optimum condition of different parameters, such that maximum power density is obtained. The different parameters studied are the glutaraldehyde concentration, KOH doping in PVA membrane, concentration of alcohols, electrolyte concentrations, electrocatalyst loading at anode and cathode, electrocatalyst type, oxidant types, cell temperature and membrane types.

4.2.3.1 Effect of glutaraldehyde concentration

Fig 4.30a and Fig 4.30b show the polarization curves and power density curves for the PVA membranes crosslinked with different concentration of glutaraldehyde varying from 1 wt % to 3 wt % and impregnated with fixed KOH concentration of 6 M at a temperature of 30 ^{o}C. The anode and cathode were made of Pt-Ru/C and Pt/$C_{HSA,}$ respectively. The electrocatalyst loading at anode and cathode were 1 mg/cm^2. The anode feed consisting of 3 M methanol mixed with 6 M KOH and 2 M ethanol mixed with 1 M KOH were used as fuel and humidified oxygen was used as oxidant at the cathode. It is seen from Fig (4.30a) and Fig (4.30b) that the maximum power density for a given current density increases with increase in glutaraldehyde concentration from 1 to 2.5 wt % for both methanol and

ethanol fuels. However, the performance of the cell decreases when the glutaraldehyde concentration is increased beyond 2.5 wt % i.e., from 2.5 wt % to 3 wt %.

Fig (4.30a) shows that the maximum OCV of 0.63 V and maximum power density of 7.10 mW/cm^2 at a current density of 23.53 mA/cm^2 were observed for 2.5 wt % GA crosslinked PVA membrane using methanol as anode feed. Whereas, 1 wt %, 2 wt % and 3 wt % GA crosslinked PVA membrane produced maximum power density of 5.64 mW/cm^2 at a current density of 20.07 mA/cm^2, maximum power density of 6.15 mW/cm^2 at a current density of 21.22 mA/cm^2 and maximum power density of 6.46 mW/cm^2 at a current density of 22.20 mA/cm^2, respectively. The OCV of 0.622 V, 0.621 V and 0.624 V were obtained for 1 wt %, 2 wt % and 3 wt % GA crosslinked membrane, respectively.

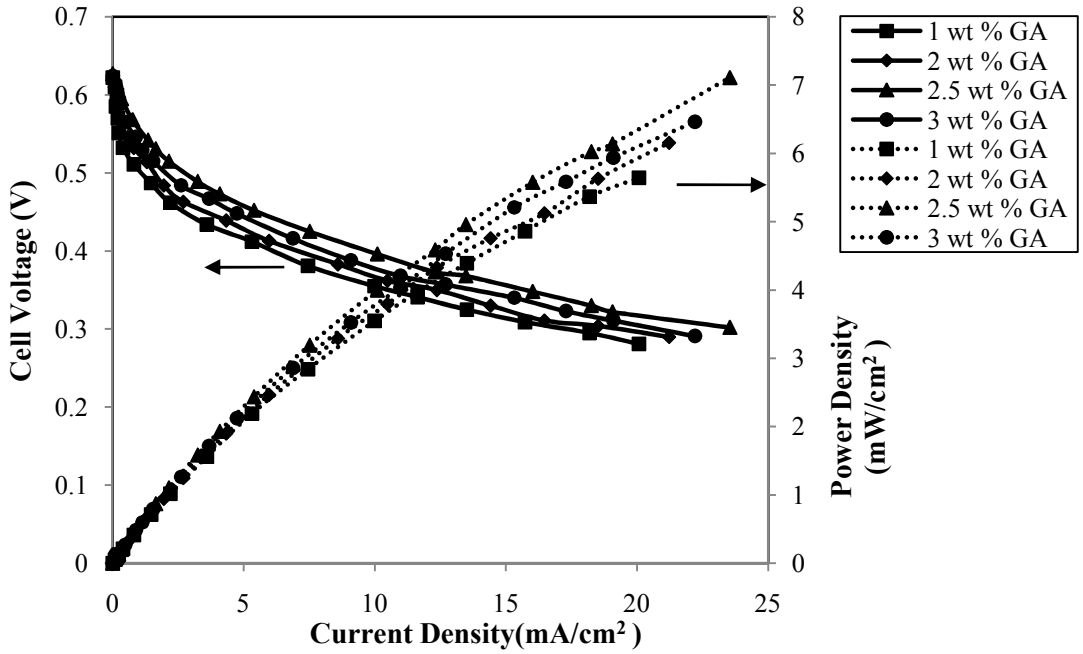

Figure 4.30a Current density vs. cell voltage and current density vs. power density characteristics for PVA membranes crosslinked with different glutaraldehyde (GA) concentration using 3 M methanol mixed with 6 M KOH at a temperature of 30 ^{o}C; Dotted line-power density curves; Solid line-polarization curves.

Similar trend was observed when ethanol was used as fuel (Fig 4.30b). The 2.5 wt % GA crosslinked membrane doped with 6 M KOH results in a maximum OCV of 0.75 V and maximum power density of 3.57 mW/cm^2 at a current density of 17.76 mA/cm^2. Whereas, 1 wt %, 2 wt % and 3 wt % GA crosslinked membrane produced maximum power density of 2.48 mW/cm^2 at a current density of 14.17 mA/cm^2, maximum power density of 2.7 mW/cm^2 at a current density of 15.21 mA/cm^2 and maximum power density of 3.2 mW/cm^2 at a current density of 19.09 mA/cm^2, respectively. The OCV of 0.72 V, 0.73 V and 0.74 V were obtained for 1 wt %, 2 wt % and 3 wt % GA crosslinked membrane, respectively.

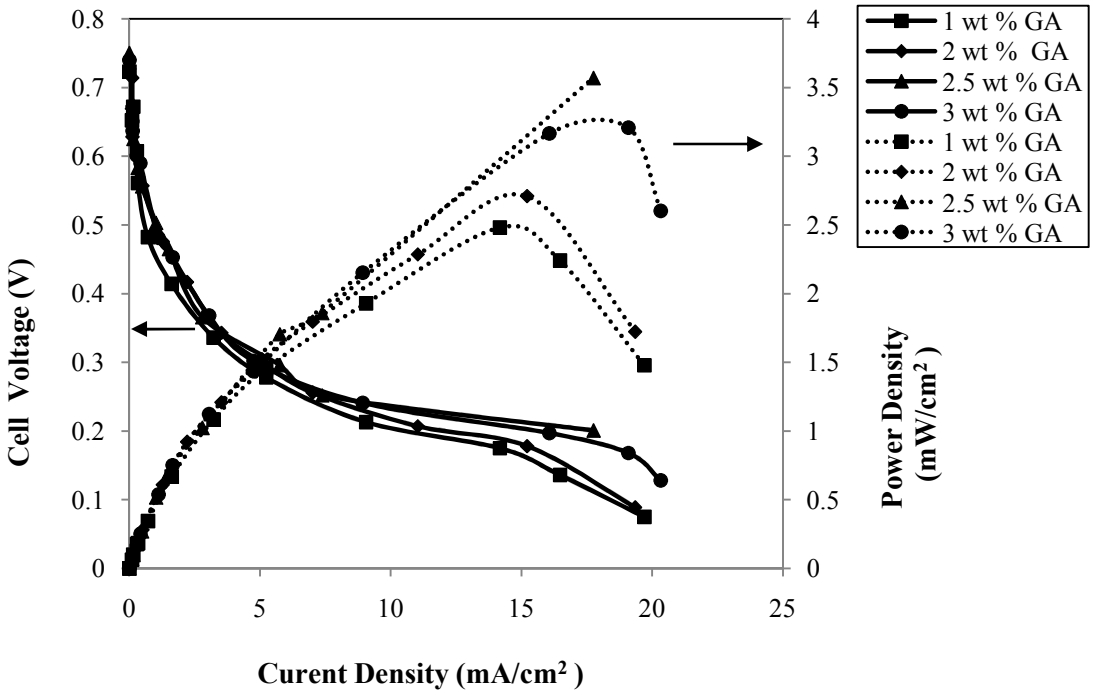

Figure 4.30b Current density vs. cell voltage and current density vs. power density characteristics for PVA membranes crosslinked with different glutaraldehyde (GA) concentration using 2 M ethanol mixed with 1 M KOH at a temperature of 30 ^oC; Dotted line-power density curves; Solid line-polarization curves.

It is seen in Table (4.3) that the KOH (6 M) uptake is highest for the PVA membrane crosslinked by GA of 2.5 wt %. Water uptake is also moderate for 2.5 wt % GA

crosslinked membrane. Due to these key factors, the ionic conductivity of the synthesized membrane crosslinked by 2.5 wt % GA and doped with 6 M KOH reaches at maximum in the order of 9×10^{-3} S/cm (Table 4.4). Thus, at all times, highest performance was obtained for this membrane (Fig 4.26e).

4.2.3.2 Effect of KOH doping in chemical crosslinked PVA membrane

Fig 4.31a and Fig 4.31b show the polarization curves and power density curves for 2.5 wt % GA crosslinked PVA membrane doped with the different concentration of KOH ranging from 4 M to 8 M at a temperature of 30 ^{o}C. The anode and cathode were made of Pt-Ru/C and Pt/C_{HSA}, respectively. The electrocatalyst loading at anode and cathode were 1 mg/cm^2.The anode feed consisting of 3 M methanol mixed with 6 M KOH and 2 M ethanol mixed with 1 M KOH electrolyte were fed at the anode. The humidified oxygen was used as oxidant at the cathode. It is seen from the single cell study that the cell voltage and power density for a given current density increases with the increase in KOH doping concentration up to 6 M for both methanol (Fig 4.31a) and ethanol (Fig 4.31b). However, further increase in KOH doping concentration beyond 6 M, the cell performance decreases irrespective of alcohol types used in DAFC. The similar trend was also observed using physical crosslinked PVA membrane (page no. 102).

It is seen in the Fig (4.31a) that the 6 M KOH doped PVA membrane results in a maximum OCV of 0.63 V and maximum power density of 7.10 mW/cm^2 at a current density of 23.53 mA/cm^2 for methanol as anode feed. Whereas, 7 M and 8 M KOH doped PVA membrane generates maximum power density of 6.66 mW/cm^2 at a current density of 23.21 mA/cm^2 maximum power density of 6.26 mW/cm^2 at a current density of 22.07 mA/cm^2, respectively. The OCV of 0.623 V and 0.622 V were obtained for KOH doping of 7 M and 8 M, respectively.

Similarly, ethanol as anode feed, 6 M KOH doped PVA membrane results in a maximum OCV of 0.75 V and maximum power density of 3.57 mW/cm^2 at a current density of 17.76 mA/cm^2 (Fig 4.31b). Whereas, 7 M and 8 M KOH doped PVA membrane generates maximum power density of 2.9 mW/cm^2 at a current density of 16.75 mA/cm^2 and maximum power density of 2.69 mW/cm^2 at a current density of 16.15 mA/cm^2, respectively. The OCV of 0.74 V and 0.745 V were obtained for KOH doping of 7 M and 8 M, respectively.

The KOH concentration dependence of cell performance may be due to the increased KOH uptake within the membrane when impregnated with 6 M KOH. The conductivity of PVA membrane increases which reduces ohmic loss. Moreover, the membrane with the highest ionic conductivity also reduces the electroosmotic drag on OH^- conduction within the synthesized PVA membrane electrolyte (Gupta and Pramanik 2019b, Karimi and Li 2005 and Basu et al., 2008). It is clearly seen that the KOH doping of 6 M gives highest cell performance in terms of power density for both fuels. Thus, 6 M KOH is considered as optimum doping concentration for 2.5 wt % GA crosslinked PVA membrane. It should also be noted that the PVA based chemical crosslinked (2.5 wt % GA) membrane resulted in highest ionic conductivity of 9×10^{-3} S/cm when doped with 6 M KOH (page no.131).

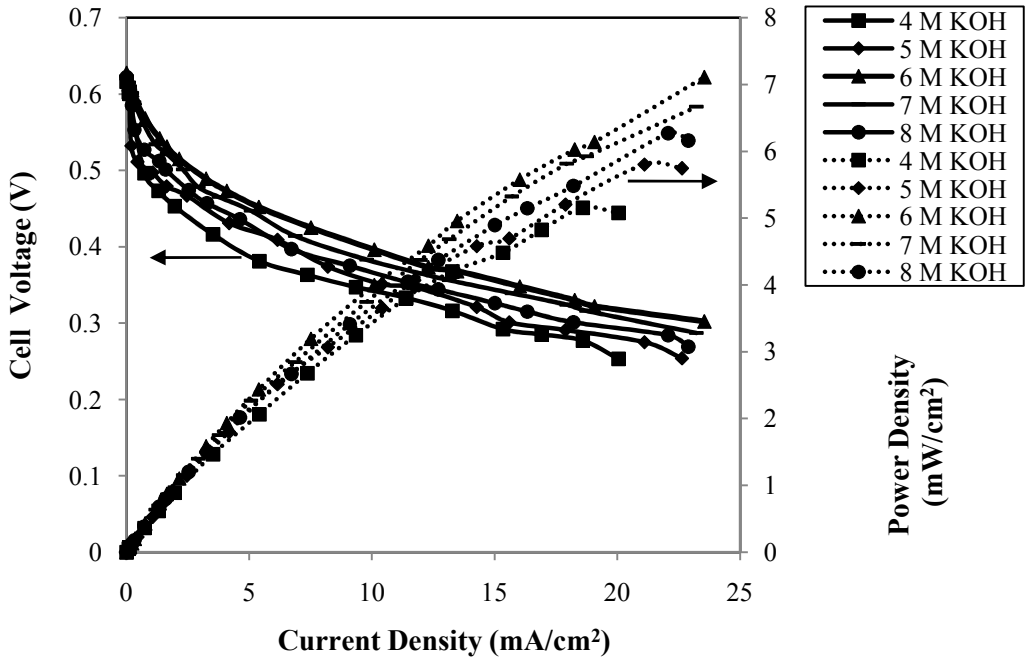

Figure 4.31a Current density vs. cell voltage and current density vs. power density characteristics for PVA membranes doped with different molar KOH solution using 3 M methanol mixed with 6 M KOH at a temperature of 30 ^{o}C; Dotted line-power density curves; Solid line-polarization curves.

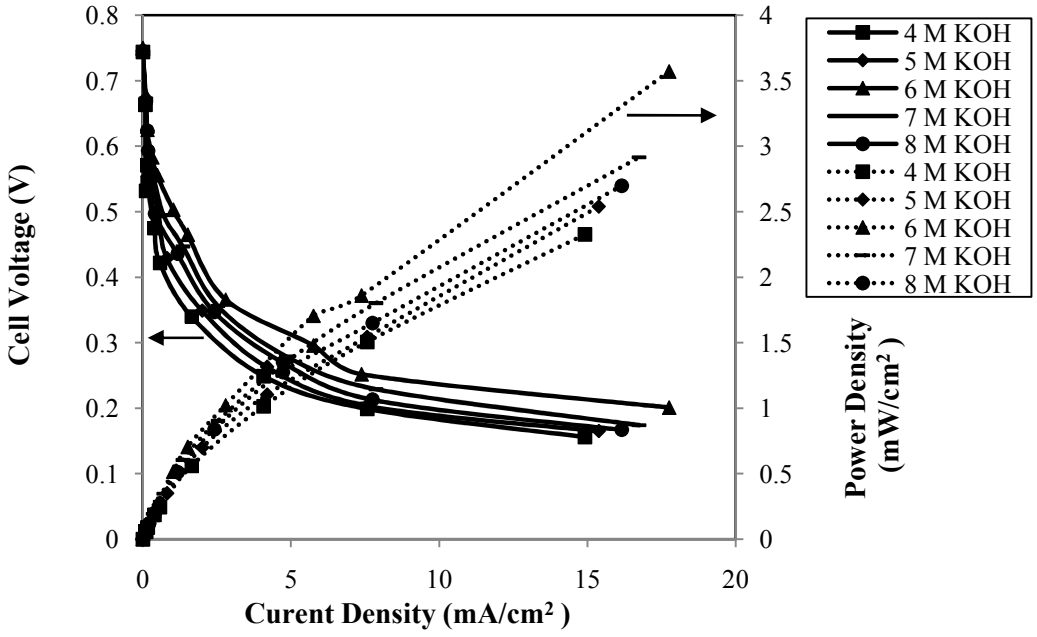

Figure 4.31b Current density vs. cell voltage and current density vs. power density characteristics for PVA membranes doped with different molar KOH solution using 2 M ethanol mixed with 1 M KOH at a temperature of 30 ^{o}C; Dotted line-power density curves; Solid line-polarization curves.

4.2.3.3 Effect of alcohol concentration

Fig (4.32a) and Fig (4.32b) show the effect of methanol and ethanol concentration mixed with the fixed electrolyte (KOH) concentration of 0.5 M on the polarization and power density curves for 2.5 wt % GA crosslinked PVA membrane doped with 6 M KOH solution at a temperature of 30 ^{o}C. The anode and cathode electrocatalysts were Pt-Ru/C and Pt/C_{HSA}, respectively. The fixed electrocatalyst loading of 1 mg/cm^2 was taken at both electrodes. The cathode oxidant used was humidified oxygen. The voltage and power density for a given current density increase with the increase in methanol or ethanol concentration. However, a decreased trend in cell performance is observed beyond 3 M of methanol and 2 M of ethanol, respectively.

It is seen from Fig (4.32a) that the polarization and power density curves shifted upward with the increase in methanol concentration from 1 M to 3 M, while further increase in concentration to 4 M, the curves shift downward. The maximum open circuit voltage (OCV) of 0.58 V and maximum power density of 1.68 mW /cm^2 at a current density of 11.87 mA/cm^2 were obtained for the methanol of 3 M. Whereas, the methanol of 4 M produced an OCV of 0.59 V and maximum power density of 1.45 mW/cm^2 at a current density of 11.04 mA/cm^2 which is lower than 3 M methanol (1.68 mW /cm^2). The methanol of 1 M produced very low power density of 1.18 mW/cm^2 at a current density of 9.76 mA/cm^2.

The similar trend was also observed for ethanol fuel when the concentration of ethanol was increased. It is seen from the Fig (4.32b), the maximum OCV of 0.71 V and maximum power density of 2.48 mW /cm^2 at a current density of 14.43 mA/cm^2 were obtained for the ethanol of 2 M. Whereas, the ethanol of 1 M and 3 M generates maximum power density of 1.99 mW/cm^2 at a current density of 10.08 mA/cm^2 and

maximum power density of 2.29 mW/cm^2 at a current density of 16.17 mA/cm^2, respectively. The OCV of 0.64 V and 0.66 V were obtained for 1 M and 3 M ethanol, respectively. The methanol of 3 M and ethanol of 2 M were found to be the optimum fuel concentration as the DAFC produced highest power density at these concentrations. The similar trend were also observed in cyclic voltammetry experiments (page no. 90) and single cell experiments (page no. 102) using physical crosslinked PVA membrane.

Initially, with the increase in fuel concentration the current density increases because the reaction kinetics improved at higher fuel concentration (Basu et al, 2008, Larminie and Dicks 2003 and Pramanik et al., 2008). The operating cell voltage (at current density i>0) is also improved due to reduction in activation and concentration overpotential (Larminie and Dicks 2003). The OCV (at current density i = 0) also increases with the increase in fuel concentration of methanol up to 3 M and ethanol up to 2 M. The effect of concentration and temperature on OCV could be explained by Nernst equation (Larminie and Dicks 2003). At the higher methanol concentration (4 M) and ethanol concentration (3 M) the cell performance decreases. It may be due to the coverage of the electrocatalyst by fuel increases at very high concentration and, at the same time, the availability of OH^- ion at the electrocatalyst site decreases. It is seen in the anode reaction (Equation (4.1) page no. 86) that the presence of OH^- ions are extremely important to complete the reaction and release electrons which control the anode reaction kinetics. Moreover, excess unreacted fuel may cross the membrane electrolyte and reach to cathode and produce unwanted electrooxidation reaction thereby creating mixed potential problem which reduces cell voltage (Gupta and Pramanik 2019b).

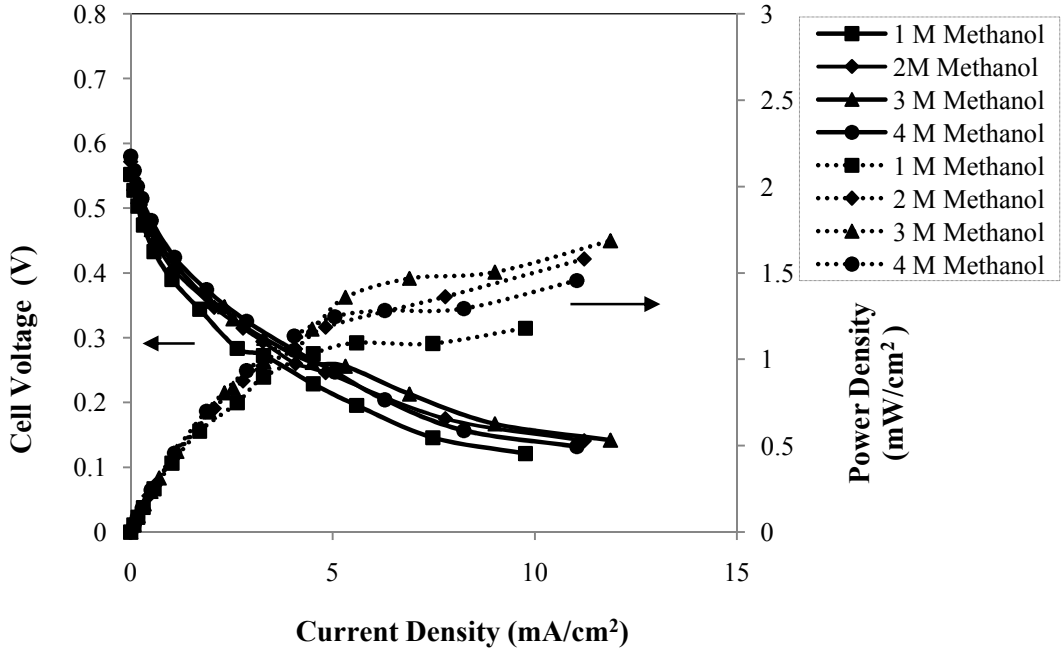

Figure 4.32a Current density vs. cell voltage and current density vs. power density characteristics for different methanol concentration using fixed 0.5 M KOH at a temperature of 30 ^{o}C; Dotted line-power density curves; Solid line-polarization curves.

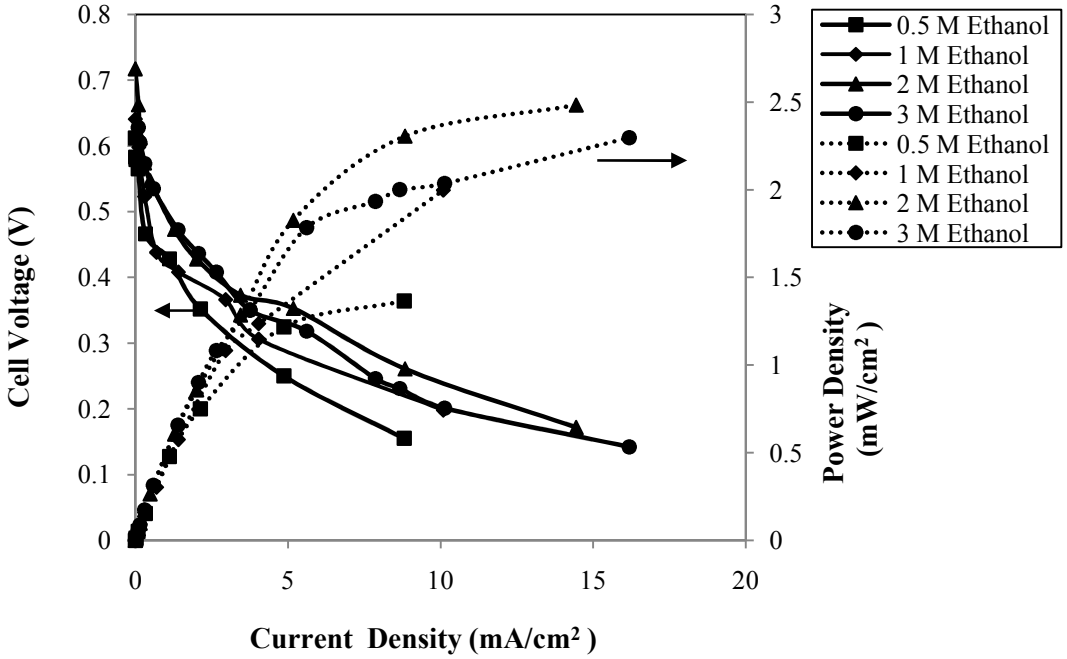

Figure 4.32b Current density vs. cell voltage and current density vs. power density characteristics for different ethanol concentration using fixed 0.5 M KOH at a temperature of 30 ^{o}C; Dotted line-power density curves; Solid line-polarization curves.

4.2.3.4 Effect of electrolyte concentration

Fig (4.33a) and Fig (4.33b) show the polarization and power density curves for different electrolyte concentration using 2.5 wt % GA crosslinked PVA membrane doped with 6 M KOH solution at a temperature of 30 ^{o}C. The anode and cathode electrocatalysts were Pt-Ru/C and Pt/C_{HSA}, respectively. The fixed electrocatalyst loading of 1 mg/cm^2 was taken at both electrodes. The anode fuels were optimum concentration of methanol (3 M) mixed with various concentration of electrolyte KOH and optimum concentration of ethanol (2 M) mixed with various concentration of KOH electrolyte. The cell temperature was maintained at 30 ^{o}C. The cathode oxidant used was humidified oxygen. It is seen from Fig (4.33a) that the polarization and power density curves shifted upward for methanol fuel with the increase in KOH concentration from 2 M to 6 M. While, further increase in KOH concentration to 8 M, the curve shifts downward. The maximum open circuit voltage (OCV) of 0.63 V and maximum power density of 7.10 mW/cm^2 at a current density of 23.53 mA/cm^2 was obtained for the 3 M methanol mixed with 6 M KOH concentration. Whereas, maximum power density of 3 mW/cm^2 at a current density of 16.33 mA/cm^2, maximum power density of 3.8 mW/cm^2 at a current density of 17.28 mA/cm^2 and maximum power density of 5.68 mW/cm^2 at a current density of 16.87 mA/cm^2, were obtained for 3 M methanol fuel mixed with 2 M, 4 M and 8 M KOH , respectively. The OCV of 0.60 V, 0.602 V and 0.64 V were obtained for 3 M methanol fuel mixed with 2 M, 4 M and 6 M KOH, respectively. Thus, the optimum electrolyte concentration for methanol fuel was 6 M KOH.

Similarly, it is seen from Fig (4.33b) that the polarization and power density curves shifted upward for ethanol fuel with the increase in KOH concentration from 0.5 M to 1 M. While, further increase in KOH concentration to 1.5 M, the curve shifts downward. The maximum open circuit voltage (OCV) of 0.75 V and maximum power density of

3.57 mW/cm^2 at a current density of 17.76 mA/cm^2 was obtained for the 2 M ethanol mixed with 1 M KOH concentration. However, maximum power density of 2.48 mW/cm^2 at a current density of 14.43 mA/cm^2, maximum power density of 2.40 mW/cm^2 at a current density of 10.42 mA/cm^2 and maximum power density of 3.29 mW/cm^2 at a current density of 16.28 mA/cm^2 were obtained for 2 M ethanol fuel mixed with 0.5 M, 1.5 M and 2 M KOH, respectively. The OCV of 0.72 V, 0.68 V and 0.63 V were obtained for 2 M ethanol fuel mixed with 0.5 M, 1.5 M and 2 M KOH, respectively. Thus, for ethanol fuel, the optimum electrolyte concentration was 1 M KOH. In the cyclic voltammetry (page no. 93) study and single cell study using physical crosslinked PVA membrane (page no. 104) similar trend was found for methanol and ethanol both.

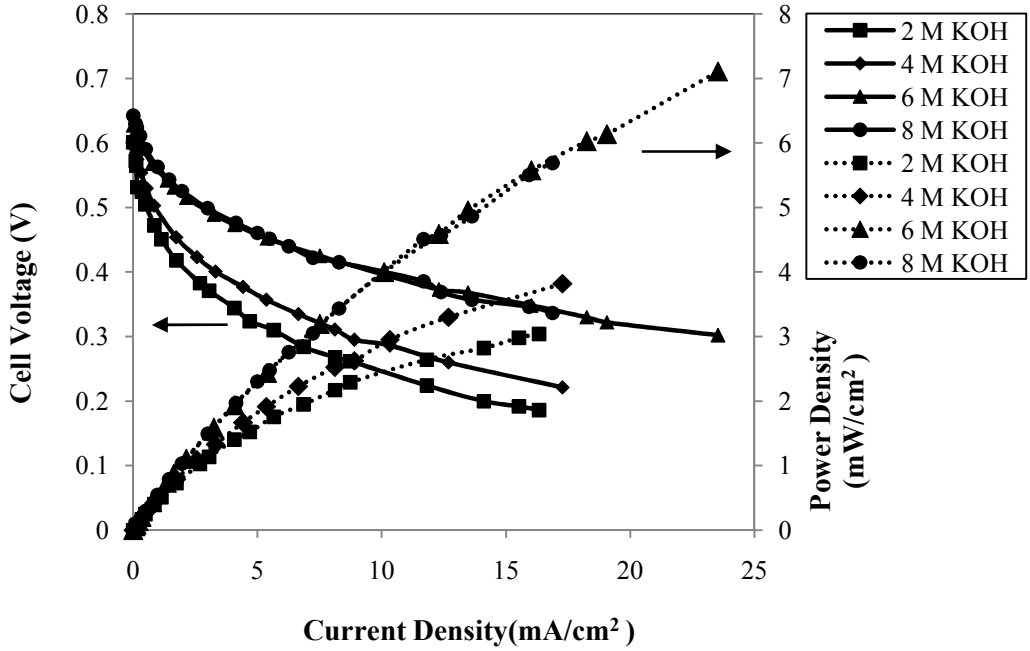

Figure 4.33a Current density vs. cell voltage and current density vs. power density characteristics for different KOH concentration using fixed 3 M methanol at a temperature of 30 ^{o}C; Dotted line-power density curves; Solid line-polarization curves.

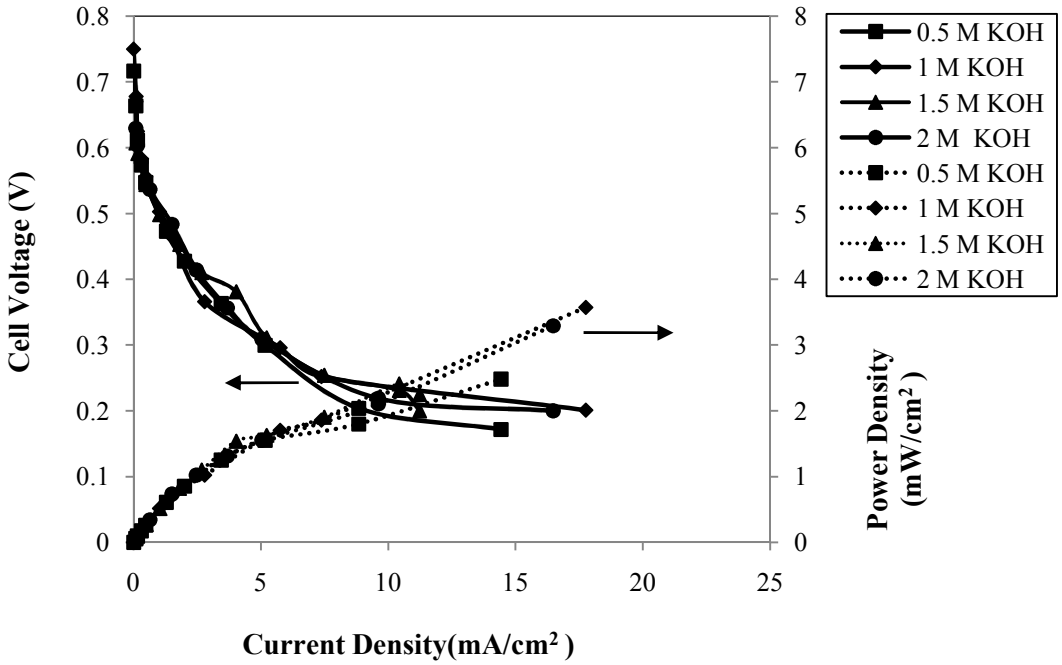

Figure 4.33b Current density vs. cell voltage and current density vs. power density characteristics for different KOH concentration using fixed 2 M ethanol and at a temperature of 30 ^{o}C; Dotted line-power density curves; Solid line-polarization curves.

The increase in KOH concentration enhances the OH_{ads} species on the electrode, which in turn increases the rate of fuel electrooxidation and thus the maximum current density is observed (Rathoure and Pramanik 2016). However, with the further increase in KOH concentration the current density decreases. Higher KOH concentration results in more OH^- ions which competes with the fixed fuel molecule for the adsorption on electrocatalyst site thereby forming PtO layer (Gupta and Pramanik 2018) and thus, reducing the cell performance.

4.2.3.5 Effect of anode electrocatalyst loading

Fig (4.34a) and Fig (4.34b) show the polarization curves and power density curves for methanol and ethanol using different anode loadings i.e., 0.5 mg/cm^2, 1 mg/cm^2 and 1.5 mg/cm^2 of Pt–Ru/C, respectively. The cathode was of 1 mg/cm^2 of Pt/C_{HSA}. The anode fuel were 3 M methanol (optimum) mixed with 6 M KOH (optimum) and 2 M ethanol (optimum) mixed with 1 M KOH (optimum), respectively. The electrolyte was 2.5 wt %

GA crosslinked PVA and doped with 6 M KOH. The cell was operated at a temperature of 30 ^{o}C. It is seen in the Fig (4.34a) and Fig (4.34b) that the power density and current density increases with the increase in anode electrocatalyst loading from 0.5 mg/cm^2 to 1 mg/cm^2 irrespective of fuel used. While, further increase in electrocatalyst loading beyond 1 mg/cm^2, the cell performance decreases. The reason for this decrease may be electrocatalyst agglomeration at high loading (1.5 mg/cm^2) of Pt-Ru/C electrocatalyst (Pramanik et al., 2008). Agglomeration results in a decrease in porosity of the electrocatalyst layer leading to increased diffusional resistance to mass transport of alcohol from bulk phase to the active electrocatalyst layer (Basu et al., 2008) and this has already been discussed in CV studies (page no. 89). The SEM image of 1.5 mg/cm^2 also shows the electrocatalyst agglomeration (Fig 4.6d, page no. 82). Whereas, well and uniform distribution of electrocatalysts is observed for 1 mg/cm^2 (Fig 4.6c). The above dependence of electrocatalyst loading is also observed in cyclic voltammograms (page no. 88) and single cell study using physical crosslinked PVA membrane (page no. 107).

It is seen in Fig (4.34a) that the maximum OCV of 0.63 V and maximum power density of 7.10 mW/ cm^2 at a current density of 23.53 mA/cm^2 were obtained for 1 mg/cm^2 of Pt-Ru/C anode using methanol as fuel. The electrocatalyst loading beyond 1 mg/cm^2 gives poor performance in terms of current density and power density. The electrocatalyst loading of 0.5 mg/cm^2 and 1.5 mg/cm^2 produced maximum power density of 4.59 mW/cm^2 at a current density of 16.90 mA/cm^2 and maximum power density of 5.97 mW/cm^2 at a current density of 20.81 mA/cm^2, respectively. The OCV of 0.628 V and 0.629 V were obtained for 0.5 mg/cm^2 and 1.5 mg/cm^2, respectively.

Similarly, it is seen from (Fig 4.34b) that the maximum OCV of 0.75 V and maximum power density of 3.57 mW/ cm^2 at a current density of 17.76 mA/cm^2 were obtained for

1 mg/cm^2 Pt-Ru/C anode using ethanol as anode fuel. While, the electrocatalyst loading of 0.5 mg/cm^2 and 1.5 mg/cm^2 Pt-Ru/C produced maximum power density of 1.49 mW/cm^2 at a current density of 7.68 mA/cm^2 and maximum power density of 2.98 mW/cm^2 at a current density of 12.77 mA/cm^2, respectively. The OCV of 0.70 V and 0.71 V were obtained for 0.5 mg/cm^2 and 1.5 mg/cm^2, respectively. Although, not shown here the detailed single cell studies for three different anode electrocatalyst loading viz, 0.5 mg/cm^2, 1 mg/cm^2 and 1.5 mg/cm^2 are presented in Appendix C (page no. 211).

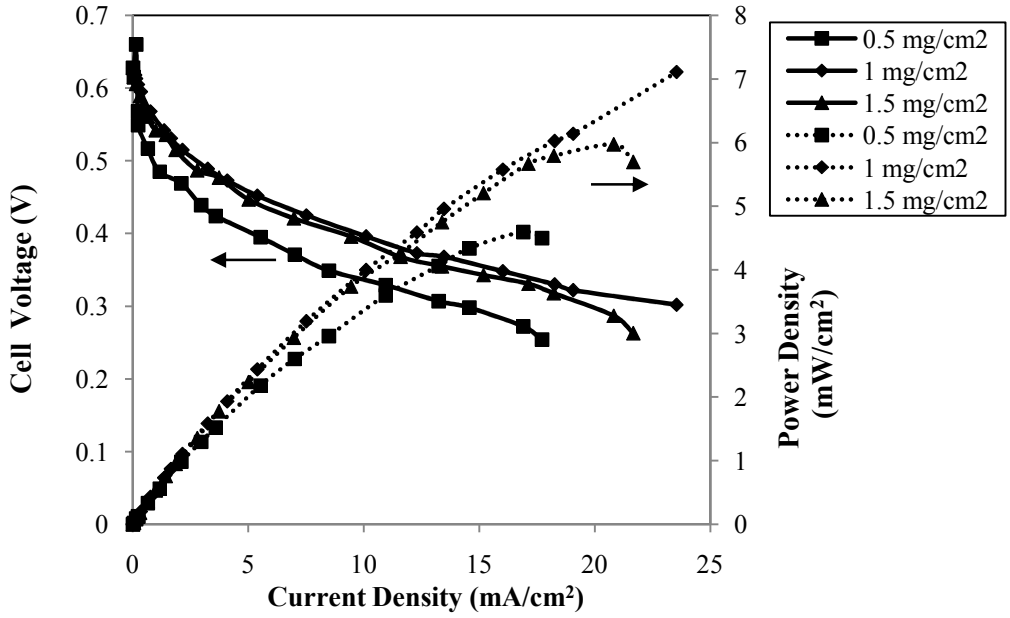

Figure 4.34a Current density vs. cell voltage and current density vs. power density characteristics for different anode loading using 3 M methanol mixed with 6 M KOH at a temperature of 30 ^{o}C; Dotted line-power density curves; Solid line-polarization curves.

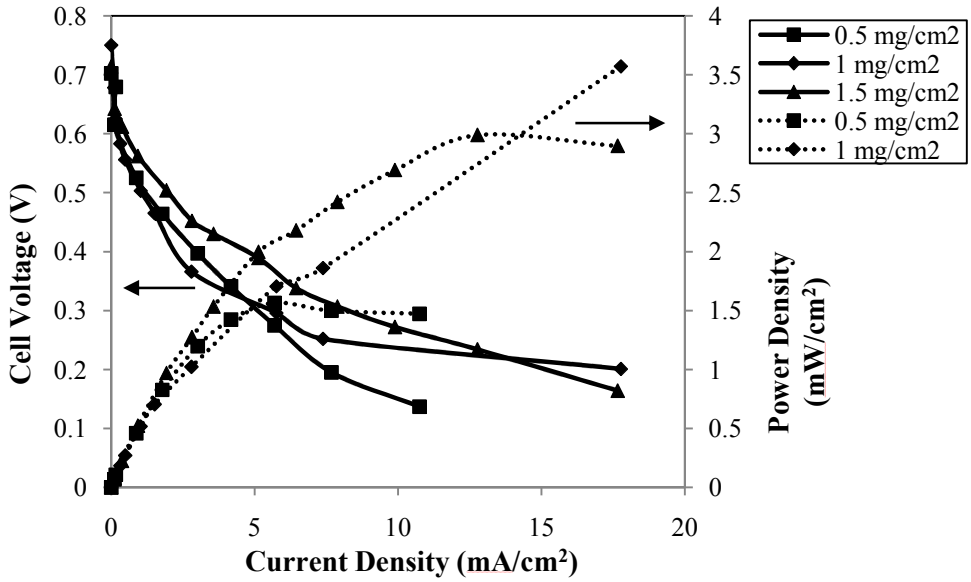

Figure 4.34b Current density vs. cell voltage and current density vs. power density characteristics for different anode loading using 2 M ethanol mixed with 1 M KOH at a temperature of 30 ^{o}C; Dotted line-power density curves; Solid line-polarization curves.

4.2.3.6 Effect of cathode electrocatalyst loading

Fig (4.35a) and Fig (4.35b) show the current density vs. voltage and current density vs. power density for different loading at cathode varying from 0.5 mg/cm^2 to 1.5 mg/cm^2 of Pt/C_{HSA} and optimum anode loading of 1 mg/cm^2 of anode Pt-Ru/C. The electrolyte was 2.5 wt % GA crosslinked PVA membrane doped with 6 M KOH. It is seen in the Fig (4.35a) and Fig (4.35b) that the current density and power density both increases with the increase in cathode electrocatalyst loading from 0.5 mg/cm^2 to 1 mg/cm^2 irrespective of fuel used. While, further increase in electrocatalyst loading beyond 1 mg/cm^2, the cell performance decreases. The reason has already been discussed in the previous section for the varying anode loading (page no. 152). The trend as it was seen with the varying anode loading (Fig 4.34a and Fig 4.34b), the similar trend of polarization and power density curves were also observed for both methanol and ethanol when the cathode (Pt/C_{HSA}) loading was varied from 0.5 mg/cm^2 to 1.5 mg/cm^2.

It is seen in the Fig (4.35a) that the maximum OCV of 0.63 V and maximum power density of 7.10 mW/cm^2 at a current density of 23.53 mA/cm^2 were obtained for 1 mg/cm^2 of Pt/C $_{HSA}$ cathode using methanol as fuel. The electrocatalyst loading of 0.5 mg/cm^2 and 1.5 mg/cm^2 produced maximum power density of 4.77 mW/cm^2 at a current density of 17.61 mA/cm^2 and maximum power density of 6.26 mW/cm^2 at a current density of 21.68 mA/cm^2, respectively. The OCV of 0.61 V and 0.62 V were obtained for 0.5 mg/cm^2 and 1.5 mg/cm^2, respectively.

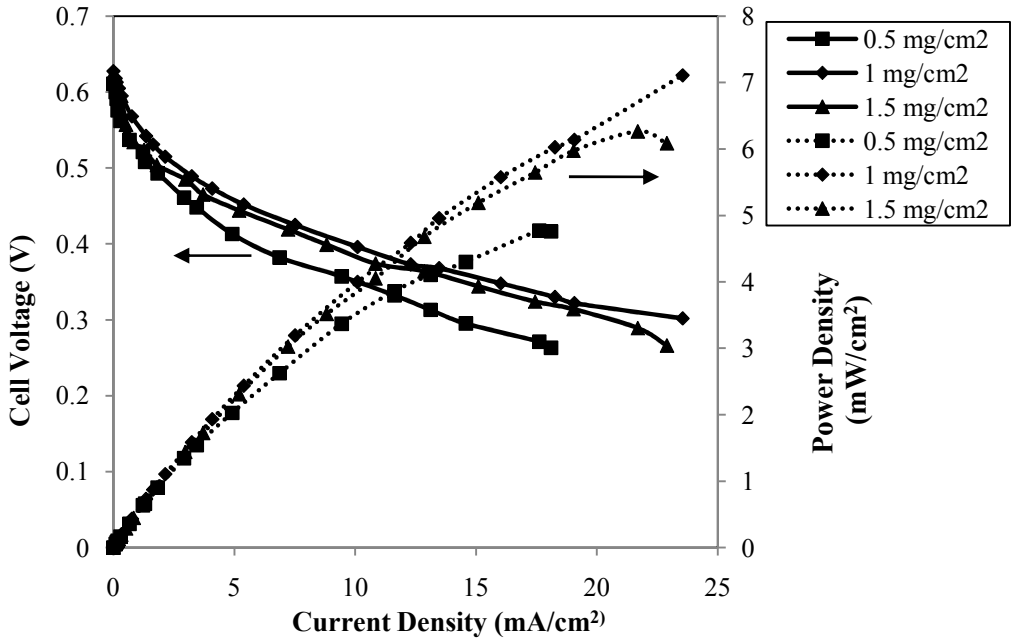

Figure 4.35a Current density vs. cell voltage and current density vs. power density characteristics for different cathode loading using 3 M methanol mixed with 6 M KOH at a temperature of 30 ^{o}C; Dotted line-power density curves; Solid line-polarization curves.

Similarly, it is seen from Fig (4.35b) that the maximum OCV of 0.75 V and maximum power density of 3.57 mW/cm^2 at a current density of 17.76 mA/cm^2 were obtained for 1 mg/cm^2 of Pt/C $_{HSA}$ cathode using ethanol as fuel (Fig 4.35b). While, the electrocatalyst loading of 0.5 mg/cm^2 and 1.5 mg/cm^2 Pt-Ru/C produced maximum power density of 1.06 mW/cm^2 at a current density of 5.31 mA/cm^2 and maximum power density of 2.68 mW/cm^2 at a current density of 15.37 mA/cm^2, respectively. The OCV of 0.73 V and

0.72 V were obtained for 0.5 mg/cm^2 and 1.5 mg/cm^2, respectively. From the cathode study it is clear that the optimum cathode loading for methanol and ethanol was 1 mg/cm^2 Pt/C_{HSA}.

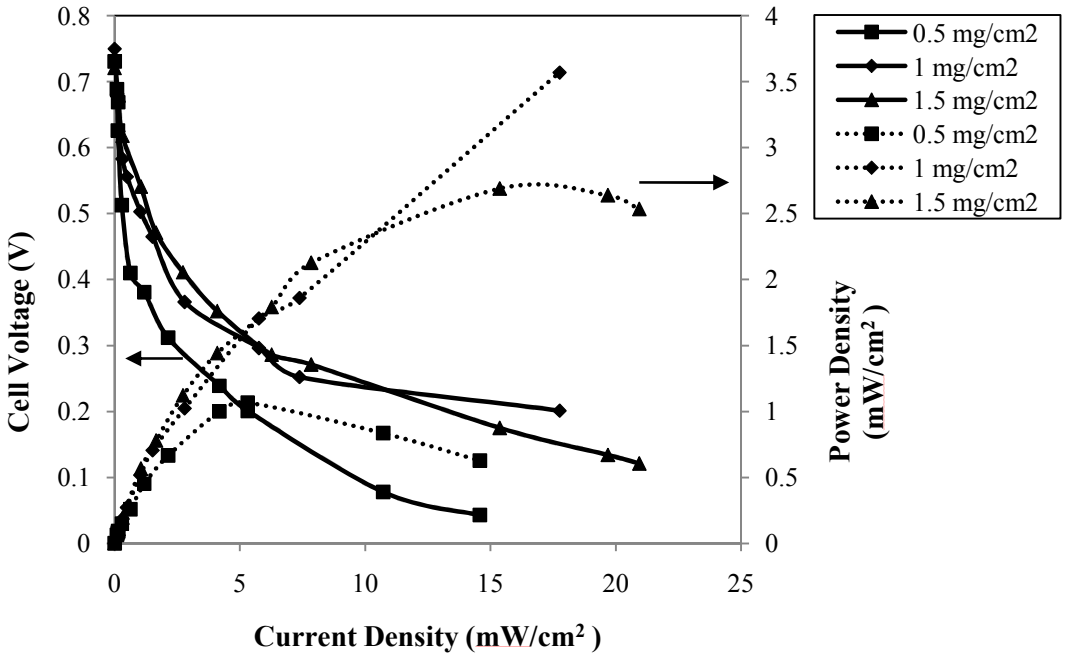

Figure 4.35b Current density vs. cell voltage and current density vs. power density characteristics for different cathode loading using 2 M ethanol mixed with 1 M KOH at a temperature of 30 ^oC; Dotted line-power density curves; Solid line-polarization curves.

4.2.3.7 Effect of electrocatalyst type

Fig (4.36a) and Fig (4.36b) show the polarization curves and power density curves for different types of anode electrocatalyst using methanol and ethanol, respectively. The different anode electrocatalyst evaluated were Pt-Ru/C and Pt/C_{HSA} at an optimum loading of 1 mg/cm^2. The cathode for both the fuel methanol and ethanol were 1 mg/cm^2 Pt/C_{HSA}. The electrolyte was 2.5 wt % GA crosslinked PVA membrane doped with 6 M KOH. The anode electrocatalysts Pt-Ru/C (1 mg/cm^2) resulted in highest cell performance in terms of current density and power density in comparison to Pt/C_{HSA} anode for methanol (Fig 4.36a) and ethanol (Fig 36b) both. It is well established that bimetallic Pt-Ru/C alloy electrodes performs as best electrocatalyst for methanol and

ethanol electrooxidation due to its bi-functional mechanism (Lamy et al., 2001, Tripkovic et al., 2002 and Roth et al., 2005). Ruthenium is a good CO tolerant catalyst but inactive for methanol and ethanol electrooxidation. Moreover, Ru plays an important role in water dissociation to supply OH_{ad} species to aid the oxidation of adsorbed CO to CO_2 at low overpotential during methanol and ethanol electrooxidation. Nevertheless, the CO formed as a side reaction is oxidized and the poisoning effect is reduced (Tripkovic et al., 2002). Thus, enhance the electrocatalytic activity of Pt-Ru/C for methanol and ethanol both (Gasteiger et al, 1993). Similar trend was also observed in single cell study using physical crosslinked PVA membrane (page no. 111).

It is observed in the Fig (4.36a) that the maximum OCV of 0.63 V and 0.60 V were produced methanol using Pt-Ru/C and Pt/C_{HSA}, respectively. Similarly, the OCV of 0.75 V and 0.74 V were obtained for ethanol using Pt-Ru/C and Pt/C_{HSA}, respectively (Fig 4.36b). It is clearly seen, OCV is higher for Pt-Ru/C anode irrespective of fuel used. The maximum power density of 7.10 mW/cm^2 at a current density of 23.53 mA/cm^2 and maximum power density of 5.41 mW/cm^2 at a current density of 19.67 mA/cm^2 were obtained for methanol using Pt-Ru/C and Pt/C_{HSA}, respectively (Fig 4.36a). Whereas, the maximum power density of 3.57 mW/cm^2 at a current density of 17.76 mA/cm^2 and maximum power density of 2.34 mW/cm^2 at a current density of 15.03 mA/cm^2 were obtained for ethanol using Pt-Ru/C and Pt/C_{HSA}, respectively (Fig 4.36b)

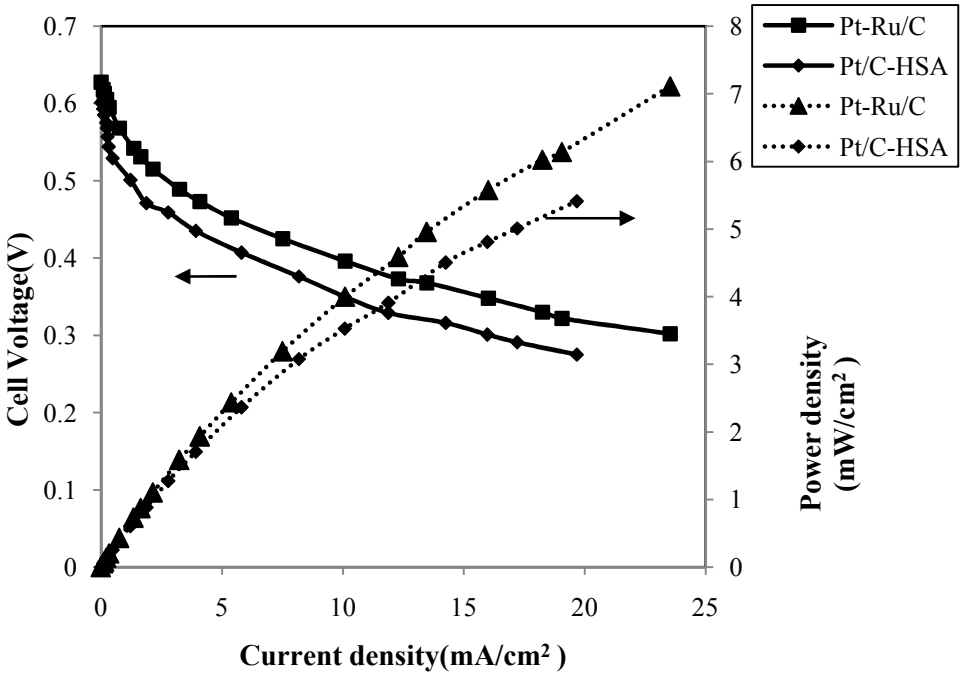

Figure 4.36a Current density vs. cell voltage and current density vs. power density characteristics for different anode electrocatalyst using 3 M methanol mixed with 6 M KOH at a temperature of 30 ^{o}C; Dotted line-power density curves; Solid line-polarization curves.

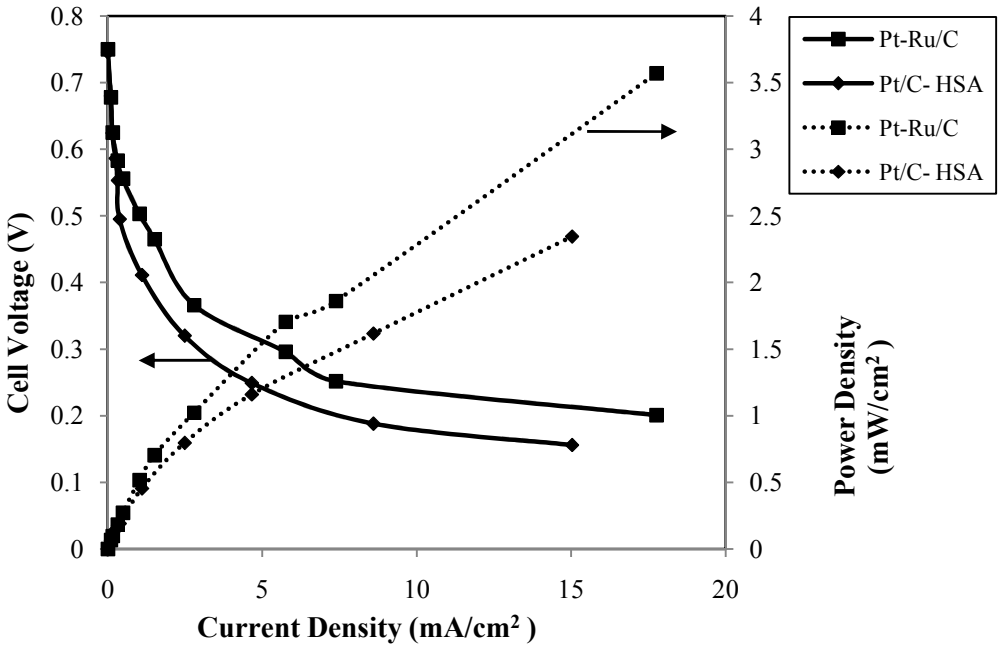

Figure 4.36b Current density vs. cell voltage and current density vs. power density characteristics for different anode electrocatalyst using 2 M ethanol mixed with 1 M KOH at a temperature of 30 ^{o}C; Dotted line-power density curves; Solid line-polarization curves.

4.2.3.8 Effect of temperature

Fig (4.37a) and Fig (4.37b) show the polarization and power density curves for different temperature using methanol and ethanol fuels, respectively. The anode and cathode were made of Pt-Ru/C and Pt/C_{HSA} of optimum loading (1 mg/cm^2) for both electrodes. The electrolyte was 2.5 wt % GA crosslinked PVA membrane doped with 6 M KOH. The anode fuel were 3 M methanol (optimum) mixed with 6 M KOH (optimum) and 2 M ethanol (optimum) mixed with 1 M KOH (optimum), respectively. The humidified oxygen was used as oxidant at the cathode. The maximum operating temperature was maintained at 60 ^oC because of the thermal stability problem of PVA based alkaline membrane beyond the cell temperature 60 ^oC. When, the cell was operated at 70 ^oC, the cell output went down immediately and that was due to the membrane degradation at high temperature. The OCV and power density of DAFC increases progressively with the increase in temperature up to 60 ^oC. It is observed in Fig (4.37a), that the OCV of 0.63 V, 0.634 V, 0.647 V and 0.65 V were obtained at temperatures of 30 ^oC, 40 ^oC, 50 ^oC, and 60 ^oC, respectively. The maximum OCV of 0.65 V and the power density of 11.07 mW/cm^2 at a current density of 31.03 mA/cm^2 was recorded at a cell temperature of 60 ^oC for methanol fuel. Whereas, a maximum power density of 7.10 mW/cm^2 at a current density of 23.53 mA/cm^2, maximum power density of 6.78 mW/cm^2 at a current density of 19.78 mA/cm^2 and maximum power density of 11.07 mW/cm^2 at a current density of 31.03 mA/cm^2 were observed at the temperature of 30 ^oC, 40 ^oC and 50 ^oC, respectively (Fig 4.37b).

Similarly, it is seen from the Fig (4.37b) that the OCV of 0.75 V, 0.76 V, 0.79 V and 0.82 V were obtained at the temperature of 30 ^oC, 40 ^oC , 50 ^oC, and 60 ^oC, respectively. The maximum OCV of 0.82 V and the maximum power density of 6.94 mW/cm^2 at a current density of 22.23 mA/cm^2 were recorded at a cell temperature of 60 ^oC for ethanol

fuel. However, maximum power density of 3.57 mW/cm^2 at a current density of 17.76 mA/cm^2, maximum power density of 4.78 mW/cm^2 at a current density of 20.89 mA/cm^2 and maximum power density of 5.6 mW/cm^2 at a current density of 21.35 mA/cm^2 were observed at the temperature of 30 ^{o}C, 40 ^{o}C and 50 ^{o}C, respectively. As already discussed, the dependency of OCV on temperature could be explained using Nernst equation (Larminie and Dicks 2003). The cell power density also increases with increase in temperature. It is well known that the anode and cathode kinetics improve with the increase in temperature resulting in high current density and power density (Gupta and Pramanik 2019b).

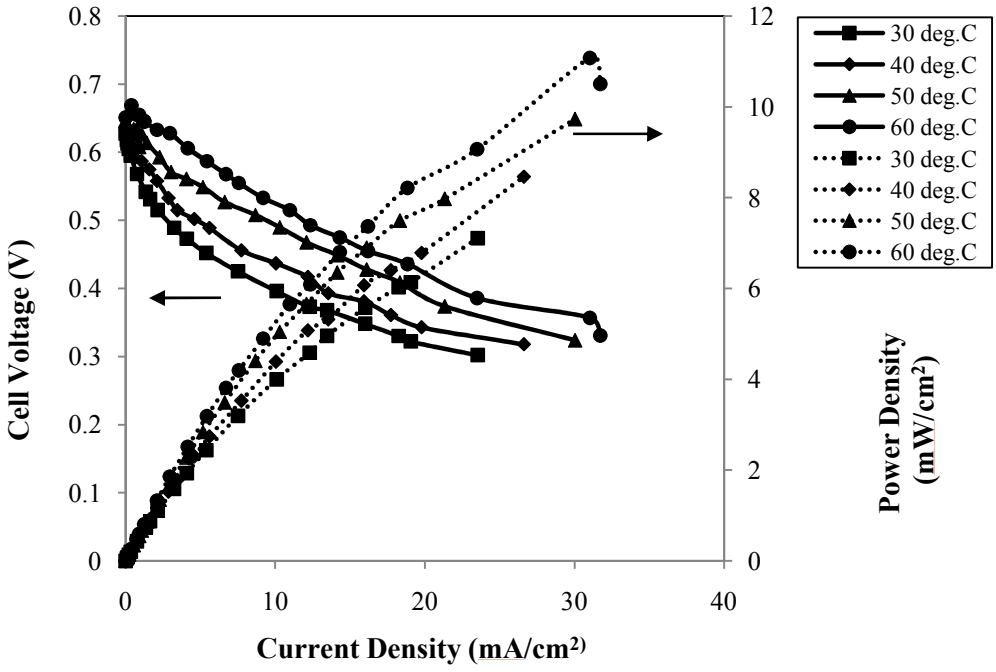

Figure 4.37a Current density vs. cell voltage and current density vs. power density characteristics at various temperatures for 3 M methanol mixed with 6 M KOH; Dotted line-power density curves; Solid line-polarization curves.

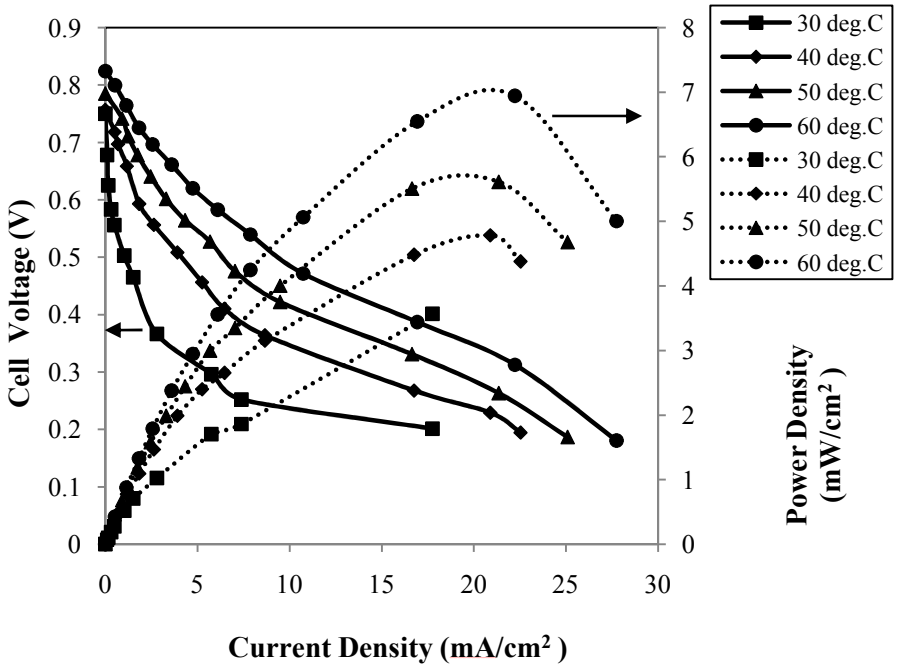

Figure 4.37b Current density vs. cell voltage and current density vs. power density characteristics at various temperatures for 2 M ethanol mixed with 1 M KOH; Dotted line -power density curves; Solid line-polarization curves.

4.2.3.9 Effect of oxidant at cathode

Fig (4.38a) and Fig (4.38a) show the polarization curves and power density curves using oxygen and air as oxidant at cathode for methanol and ethanol, respectively. The anode and cathode were made of Pt-Ru/C and Pt/C_{HSA} of 1 mg/cm^2 for both electrodes. The anode fuel were 3 M methanol (optimum) mixed with 6 M KOH (optimum) and 2 M ethanol (optimum) mixed with 1 M KOH (optimum), respectively. The operating temperature of DAFC was maintained at 30 ^oC. It is seen in the Fig (4.27a) and Fig (4.27b) that the cell performance using oxygen as oxidant is better than the air as oxidant for methanol (Fig 4.27a) and ethanol (Fig 4.27b) both fuels. The better performance of cell for oxygen as oxidant could be explained using Nernst equation. The Nernst equation shows that the increase in purity or concentration of reactants reduces the voltage loss. Moreover, the electrocatalytic sites are more effectively occupied by oxygen molecules at higher concentration (Larminie and Dicks 2003).

It is observed in the Fig (4.38a) that the maximum OCV of 0.63 V and maximum power density of 7.10 mW/cm^2 at a current density of 23.53 mA/cm^2 were observed for oxygen as oxidant and methanol as fuel. Whereas, an OCV of 0.57 V and maximum power density of 4.18 mW/cm^2 at a current density of 17.25 mA/cm^2 were observed for air as oxidant and methanol as fuel. It is clearly seen that the OCV and current densities are always higher for oxygen as oxidant at cathode.

Similarly, it is seen from Fig 4.38b that the maximum OCV of 0.75 V and maximum power density of 3.57 mW/cm^2 at a current density of 17.76 mA/cm^2 were observed for oxygen used as oxidant and ethanol as fuel. Whereas, an OCV of 0.62 V and maximum power density of 1.64 mW/cm^2 at a current density of 11.72 mA/cm^2 were observed for air used as oxidant and ethanol as fuel.

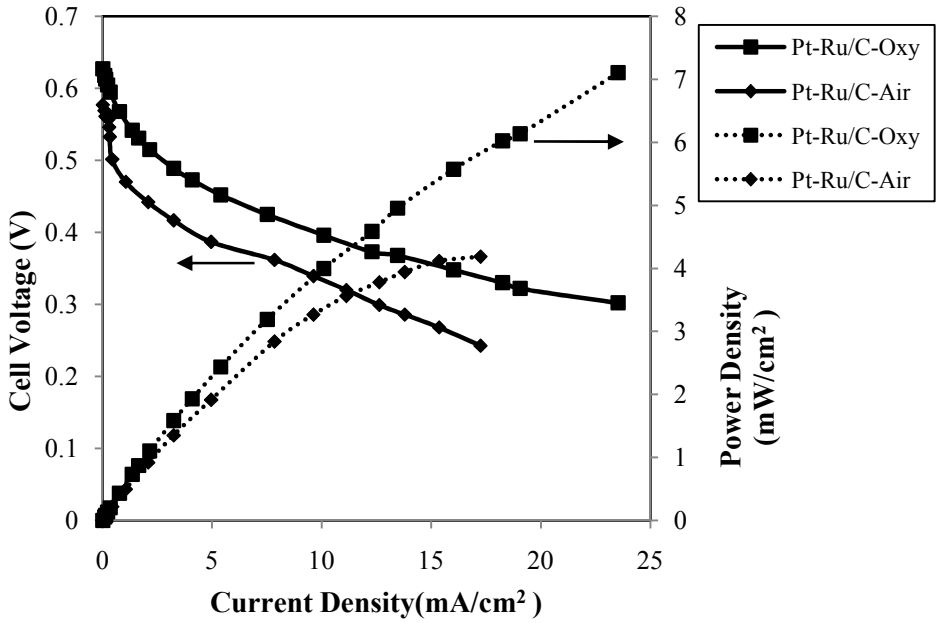

Figure 4.38a Current density vs. cell voltage and current density vs. power density characteristics for oxygen and air using 3 M methanol mixed with 6 M KOH at a temperature of 30 ^{o}C; Dotted line-power density curves; Solid line-polarization curves.

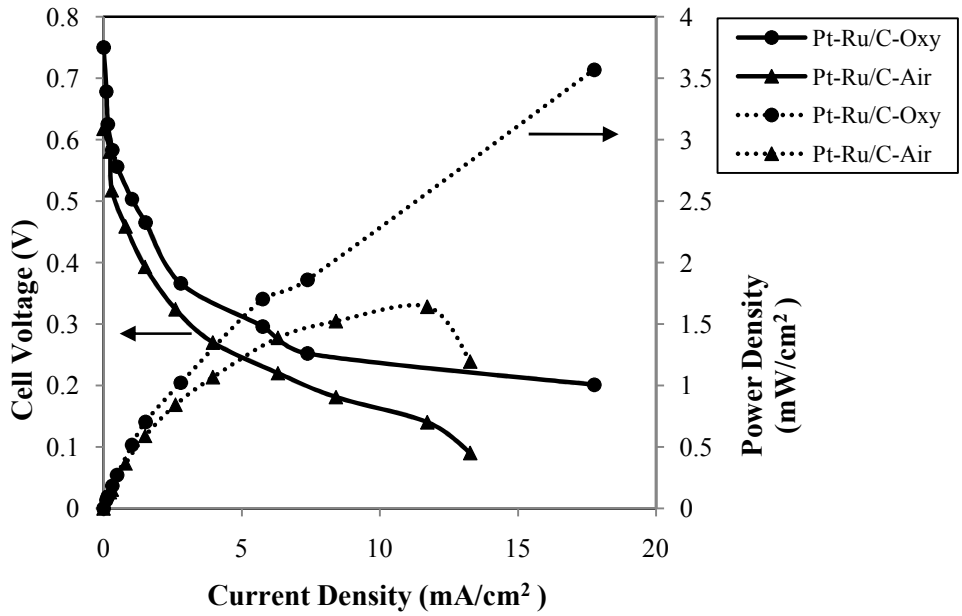

Figure 4.38b Current density vs. cell voltage and current density vs. power density characteristics for oxygen and air using 2 M ethanol mixed with 1 M KOH at a temperature of 30 ^{o}C; Dotted line-power density curves; Solid line-polarization curves.

4.2.3.10 Effect of membrane types

Fig (4.39a) and Fig (4.39b) show the polarization and power density curves for different membrane types for methanol and ethanol, respectively. The anode and cathode electrocatalysts were Pt-Ru/C and Pt/C_{HSA}, respectively. The fixed electrocatalyst loading of 1 mg/cm^2 was taken at both electrodes. The anode fuel were 3 M methanol (optimum) mixed with 6 M KOH (optimum) and 2 M ethanol (optimum) mixed with 1 M KOH (optimum), respectively. The cell temperature was maintained at 30 ^{o}C. The cathode oxidant used was humidified oxygen. The 2.5 wt % GA crosslinked PVA membrane resulted in highest cell performance in terms of current density and power density in comparison to the pristine PVA membrane for methanol (Fig 4.39a) and ethanol (Fig 39b) both. The reason may be due to the very low ionic conductivity of pristine membrane (0.89 x 10^{-3} S/cm) in comparison to 2.5 wt % GA crosslinked PVA membrane (9 x 10^{-3} S/cm) as the cell performance is directly related to ionic conductivity.

It is observed in the Fig (4.39a) that the maximum OCV of 0.577 V and 0.63 V were produced for fuel methanol using pristine and 2.5 wt % GA crosslinked PVA membrane, respectively. Similarly, the OCV of 0.582 V and 0.75 V were obtained for ethanol using pristine and 2.5 wt % GA crosslinked PVA membrane, respectively (Fig 4.39b). It is clearly seen, OCV is higher for 2.5 wt % GA crosslinked PVA membrane irrespective of fuel used. The maximum power density of 1.37 mW/cm^2 at a current density of 5.6 mA/cm^2 and maximum power density of 7.10 mW/cm^2 at a current density of 23.53 mA/cm^2 were obtained for methanol using pristine and 2.5 wt % GA crosslinked PVA membrane, respectively (Fig 4.39a). Whereas, the maximum power density of 1.17 mW/cm^2 at a current density of 4.8 mA/cm^2 and maximum power density of 3.57 mW/cm^2 at a current density of 17.76 mA/cm^2 were obtained for ethanol using pristine and 2.5 wt % GAcrosslinked PVA membrane, respectively (Fig 4.39b).

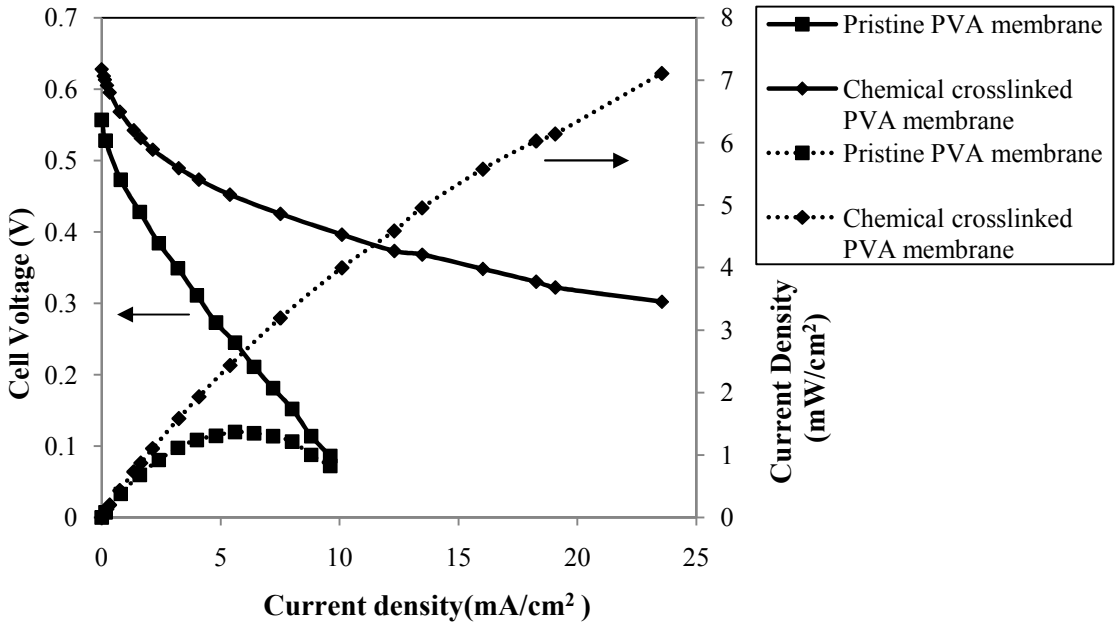

Figure 4.39a Current density vs. cell voltage and current density vs. power density characteristics for pristine and chemical crosslinked (2.5 wt % GA) PVA membrane using 3 M methanol mixed with 6 M KOH at a temperature of 30 ^{o}C; Dotted line-power density curves; Solid line-polarization curves.

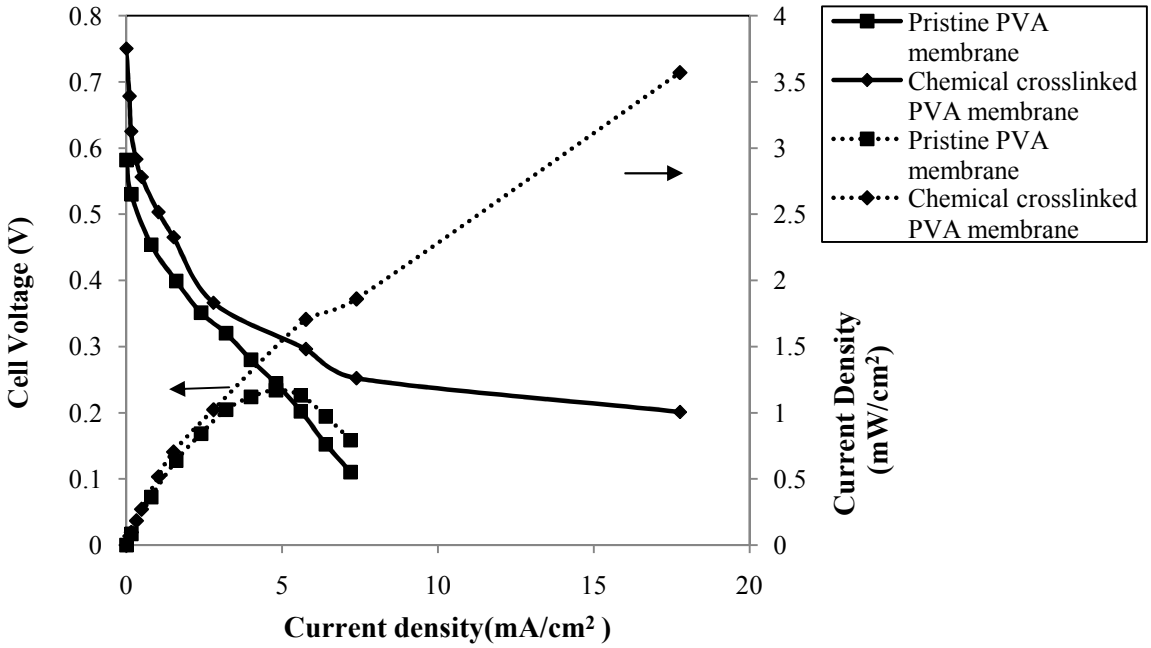

Figure 4.39b Current density vs. cell voltage and current density vs. power density characteristics for pristine and chemical crosslinked (2.5 wt % GA) PVA membrane using 2 M ethanol mixed with 1 M KOH at a temperature of 30 ^{o}C; Dotted line-power density curves; Solid line-polarization curves.

4.2.3.11 Effect of methanol and ethanol mixture

Fig (4.40) shows the electrooxidation of ethanol and methanol mixture of various molar ratios. The anode and cathode were made of Pt-Ru/C and Pt/C_{HSA} of optimum loading (1 mg/cm^2) for both electrodes. The humidified oxygen was used as oxidant at the cathode. The electrolyte was 2.5 wt % GA crosslinked PVA membrane doped with 6 M KOH. Fig (4.40) shows that the polarization and power density curves shifted upwards with the increase in methanol to ethanol molar ratio for 1:1 to 1:3. However, further increase in molar ratio to 1:4 the current density decreases. The maximum OCV of 0.66 V, maximum current density of 11.54 mA/cm^2 and maximum power density of 1.98 mW/cm^2 was obtained for the molar ratio of 1:3. It is obvious that the maximum current density of the mixture is lower than the pure solutions of methanol and ethanol as discussed earlier (Fig 4.32a and Fig 4.32b, page no.148). As explained by Morin et.al, the molecular structure of electroactive species has a great influence on its electro activity

particularly on a platinum based electrode (Morin et al., 1990). As per anode reaction (Equation (2.5) (page no. 21)), the presence of OH^- ions are very much essential for completion of anode reactions and release of electrons. The increase in ethanol concentration in the mixture beyond the optimum ratio of methanol to ethanol (1:3), the electrocatalyst occupied by the OH^- ions is replaced by the ethanol molecules. Thus, the electrooxidation reaction of ethanol molecule gets inhibited due to lack of OH^- ions at the electrocatalyst sites, which resulting in lower peak current density (Gupta and Pramanik 2019a, Wongyao et al., 2011 and Leo et al., 2013)." Thus, the peak current density for the fuel mixture beyond (1: 3) decreases. The same reason for performance decreased using ethanol in the mixture at higher ratio (1:4) has already been discussed in the CV study (Fig 4.12, page no. 96)

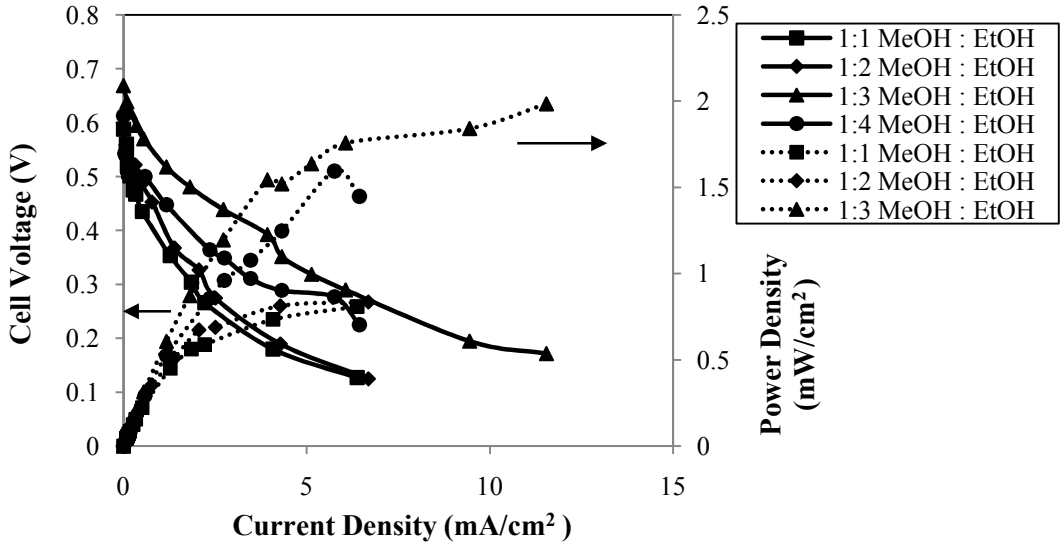

Figure 4.40 Current density vs. cell voltage and current density vs. power density characteristics for different molar ratios of methanol to ethanol at a temperature of 30 ^oC; MeOH-Methanol, EtOH-Ethanol; Dotted line-power density curves; Solid line-polarization curves.

4.2.3.12 Stability test

Stability test is very important for studying the long term performance of the developed fuel cell. The Fig (4.41) shows the stability test data performed for 15 h at a constant load. Table (4.6) shows the variation of operating cell potential (OCP) with time at a constant

load. The anode and cathode were made of Pt-Ru/C and Pt/C_{HSA} of optimum loading (1 mg/cm^2) for both electrodes. The electrolyte was 2.5 wt % GA crosslinked PVA membrane doped with 6 M KOH. The humidified oxygen was used as oxidant at the cathode. The chemical crosslinked membrane showed stable performance in terms of operating cell potential (OCP) for methanol, ethanol and their mixture. The OCP decreased slightly from 0.583 V to 0.563 V for methanol, 0.612 V to 0.595 V for ethanol, and 0.548 V to 0.536 V for their mixture after 15 hrs of DAFC operation. In the case of chemical crosslinked PVA membrane KOH is efficiently trapped within the ordered membrane matrix. Thus, the membrane exhibits constant ionic conductivity for a fairly long duration. Consequently, stable performance is observed over a time period of 15 h.

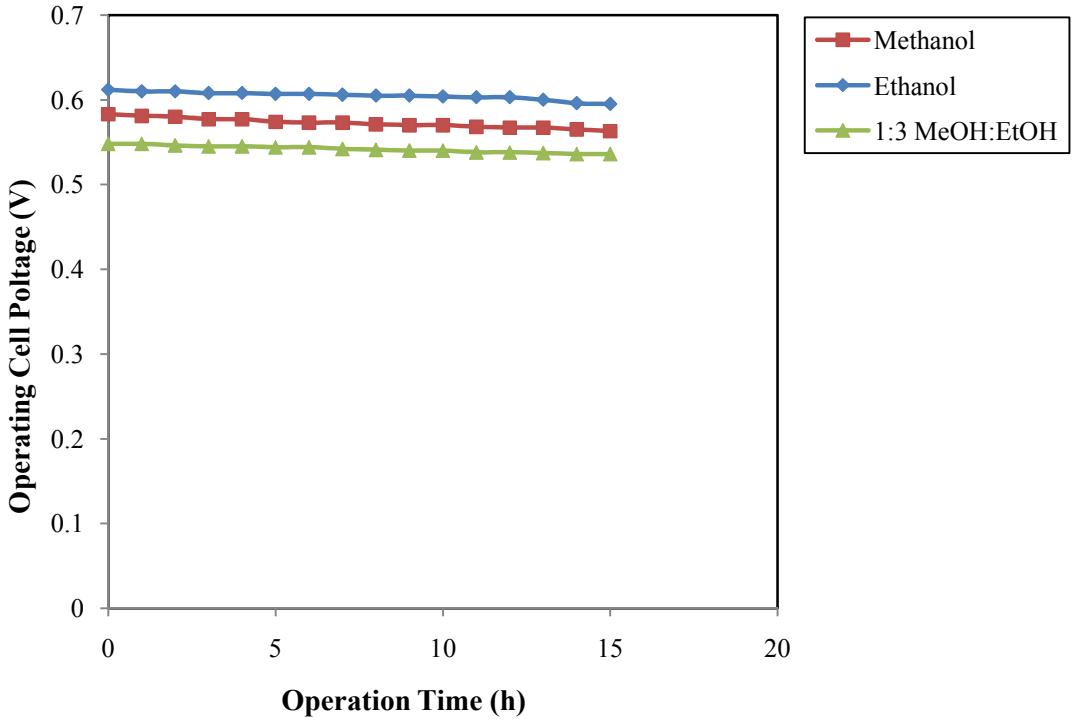

Figure 4.41 Stability test of the DAFC using 3 M methanol mixed with 6 M KOH or 2 M ethanol mixed with 1 M KOH or methanol-ethanol mixture mixed with 0.5 M KOH at constant load at a temperature of 30 ^oC; MeOH-Methanol, EtOH-Ethanol;

Table 4.6 Variation of operating cell potential (OCP) with time at a constant load.

Fuel	**Operating Time (h)**	**Operating Cell Potential (V)**
Methanol	0	0.583
	5	0.574
	10	0.570
	15	0.563
Ethanol	0	0.612
	5	0.607
	10	0.604
	15	0.595
MeOH:EtOH (1 : 3)	0	0.548
	5	0.544
	10	0.540
	15	0.536

4.2.4 Comparison of the performance for physical crosslinked and chemical crosslinked PVA membrane

Table (4.7) shows the performance comparison for physical crosslinked and chemical crosslinked with 2.5 wt % GA PVA membrane in a DAFC using methanol and ethanol as fuel. The optimum doping concentration of 6 M KOH was used for both the membrane types. The anode and cathode electrocatalysts were Pt-Ru/C and Pt/C_{HSA}, respectively. The optimum electrocatalyst loading of 1 mg/cm^2 was taken at both electrodes. The cell temperature was maintained at 30 ^oC. The cathode oxidant used was humidified oxygen. From the Table (4.7) it is clear that the highest cell performance in terms of power

Table 4.7 Performance comparison of physical and chemical crosslinked PVA membrane at a temperature of 30 ^{o}C using optimum conditions.

Membrane Types	**Fuel and Electrolyte**	**Open Circuit Voltage (V)**	**Maximum Power Density (mW/cm^2)**	**Current Density at Maximum Power Density (mA/cm^2)**
Physical Crosslinked PVA	Fuel : 2 M methanol Electrolyte: 6 M KOH	0.65	2.59	9.06
	Fuel : 2 M ethanol Electrolyte: 1 M KOH	0.73	1.93	8.06
Chemical Crosslinked PVA	Fuel : 3 M methanol Electrolyte: 6 M KOH	0.63	**7.10**	23.53
	Fuel : 2 M ethanol Electrolyte: 1 M KOH	0.75	**3.57**	17.76

density and current density is observed for the 2.5 wt % GA crosslinked PVA membrane irrespective of alcohol used in DAFC. Whereas, the maximum power density of physical crosslinked PVA membrane was low for both fuels in comparison to chemical crosslinked membrane. It may be due to the poor crosslinking in physical crosslinked PVA membrane. Due to poor crosslinking in physical crosslinked PVA membrane the alcohol crossover may take place from anode to cathode and result in mixed potential. Thus, reducing the overall cell performance. It should be noted that the ionic conductivity of physical crosslinked PVA membrane (5.6×10^{-3} S/cm) is lower compared to that of 2.5 wt % GA crosslinked PVA membrane (9×10^{-3} S/cm).

The maximum open circuit voltage (OCV) of 0.63 V and maximum power density of 7.1 mW/cm^2 at a current density of 23.53 mA/cm^2 were obtained for the 2.5 wt % GA crosslinked PVA membrane using methanol as fuel. However, an OCV of 0.65 V and maximum power density of 2.59 mW/cm^2 at a current density of 9.06 mA/cm^2 was obtained for physical crosslinked PVA membrane using methanol at optimum conditions. Similarly, the maximum open circuit voltage (OCV) of 0.75 V and maximum power density of 3.57 mW/cm^2 at a current density of 17.76 mA/cm^2 were obtained for the 2.5 wt % GA crosslinked PVA membrane using ethanol as fuel. Whereas, an OCV of 0.73 V and maximum power density of 1.93 mW/cm^2 at a current density of 8.06 mA/cm^2 was obtained for physical crosslinked PVA membrane using ethanol at optimum condition (Table 4.7). Although, it is not discussed here, the performance of pristine PVA membrane in the DAFC using similar condition was very low in comparison to chemical crosslinked and physical crosslinked PVA membrane.

4.2.5. Efficiency of the fuel cell

Fuel cell efficiency or total efficiency was calculated by the product of various individual efficiencies (Carrette et al., 2001). The equation for total efficiency of fuel cell (Equation (4.8)) is given below:

$$\boldsymbol{\eta_{FC,Total}} = \boldsymbol{\eta_r^{cell}} \text{ x } \boldsymbol{\eta_V} \text{ x } \boldsymbol{\eta_F} \text{ x } \boldsymbol{\eta_U} \text{ x } \boldsymbol{\eta_H} \quad (4.8)$$

Where, $\eta_{FC,Total}$ is the total efficiency of the fuel cell, η_r^{cell} is the thermodynamic efficiency, η_V is the electrochemical efficiency, η_F is the Faradaic efficiency, η_U is the fuel utilization efficiency and η_H is the heating value efficiency.

Thermodynamic efficiency is obtained from the enthalpy change (ΔH) and the Gibbs free energy change (ΔG) of the reactions taking place in alkaline direct methanol or ethanol fuel cell. The electrochemical efficiency ($\boldsymbol{\eta_V}$) takes in to account the losses caused due to electrode overpotentials. It is defined as the ratio of operating cell potential to theoretical cell potential. Faradaic efficiency ($\boldsymbol{\eta_F}$) is expressed as the ratio of experimental current to theoretical maximum current. The fuel utilization efficiency ($\boldsymbol{\eta_U}$) is assumed to be 0.95 (Larminie and Dicks 2003) since all the fuel is not consumed in the reaction. Heating value efficiency (η_H) is neglected in the current study as the fuel is in pure form. It is defined as the ratio of heating value of the fuel that is converted electrochemical to heating value of all the fuels component present in the fuel (Carrette et al., 2001). Thus, after considering all the assumptions the final form of the Equation (4.8) is written as:

$$\boldsymbol{\eta_{FC,Total}} = \boldsymbol{\eta_r^{cell}} \text{ x } \boldsymbol{\eta_V} \text{ x } \boldsymbol{\eta_F} \text{ x } \boldsymbol{\eta_U} \quad (4.9)$$

Table (4.8) and Table (4.9) shows the individual and total efficiency of methanol and ethanol fuel using physical and chemical crosslinked PVA membrane, respectively. It is

observed that the total efficiency of fuel cell using methanol as fuel is higher than ethanol. Alkaline direct methanol fuel cell using physical and chemical crosslinked PVA membrane at a temperature of 30 ^{o}C show a total efficiency of 48 % and 46 %, respectively. However, the total efficiency of alkaline direct ethanol fuel cell at the same temperature (30 ^{o}C) using physical crosslinked and chemical crosslinked PVA membrane are 39 % and 40 %, respectively.

Table 4.8 Individual efficiencies for different fuels used in direct alcohol fuel cell for physical crosslinked PVA membrane at a temperature of 30 ^{o}C.

Fuel	η_r^{cell} (%)	η_V(%)	η_F (%)	η_U (%)	Total Efficiency (%)
Methanol (30 ^{o}C)	0.95	0.54	1	0.95	48
Ethanol (30 ^{o}C)	0.96	0.64	0.67	0.95	39

Table 4.9 Individual efficiencies for different fuels used in direct alcohol fuel cell for chemical crosslinked PVA membrane at a temperature of 30 ^{o}C.

Fuel	η_r^{cell} (%)	η_V(%)	η_F (%)	η_U (%)	Total Efficiency (%)
Methanol (30 ^{o}C)	0.95	0.52	1	0.95	46
Ethanol (30 ^{o}C)	0.96	0.66	0.67	0.95	40